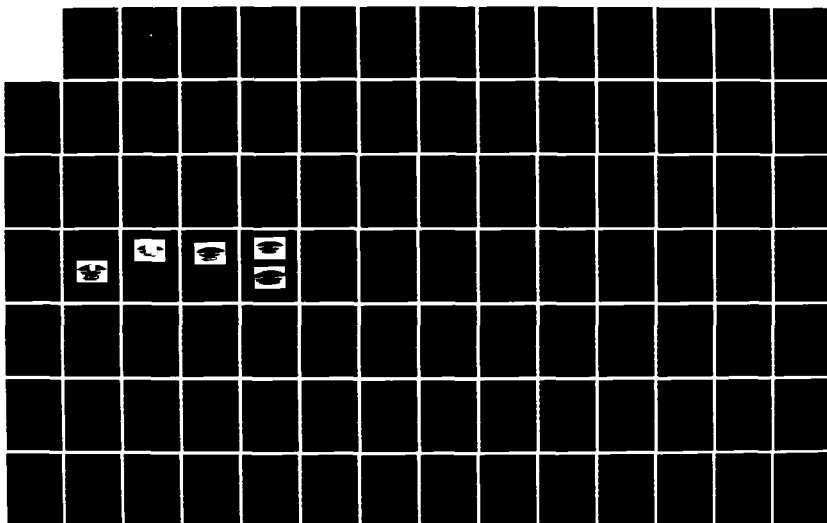AD-A167 806   A FEASIBILITY STUDY OF A SHIPBOARD COMBAT SURVIVABLE HF   1/2
                ANTENNA DESIGN(U) NAVAL POSTGRADUATE SCHOOL MONTEREY CA
                J C TERTOCHA MAR 86 NPS-62-86-003

UNCLASSIFIED   F/G 9/5   NL

MICROCOPY RESOLUTION TEST CHART

NATIONAL BUREAU OF STANDARDS 1963 A

NPS-62-86-003

NAVAL POSTGRADUATE SCHOOL
Monterey, California

DTIC
ELECTE
MAY 2 2 1986
S E D

THESIS

A FEASIBILITY STUDY OF A SHIPBOARD
COMBAT SURVIVABLE HF ANTENNA DESIGN

by

James C. Tertocha

March 1986

Thesis Adsisor: R.W. Adler

86   5   21   081

NAVAL POSTGRADUATE SCHOOL
Monterey, CA 93943

Rear Admiral R. H. Shumaker   D. A. Schrady
Superintendent   Provost

Reproduction of all or part of this report is authorized.

Released By:

JOHN N. DYER
Dean of Science and Engineering

REPORT DOCUMENTATION PAGE

1a. REPORT SECURITY CLASSIFICATION UNCLASSIFIED			1b. RESTRICTIVE MARKINGS			
2a. SECURITY CLASSIFICATION AUTHORITY			3 DISTRIBUTION/AVAILABILITY OF REPORT Approved for public release; distribution is unlimited			
2b. DECLASSIFICATION/DOWNGRADING SCHEDULE						
4 PERFORMING ORGANIZATION REPORT NUMBER(S) NPS-62-86-003			5. MONITORING ORGANIZATION REPORT NUMBER(S)			
6a. NAME OF PERFORMING ORGANIZATION Naval Postgraduate School	6b. OFFICE SYMBOL (If applicable) Code 62		7a. NAME OF MONITORING ORGANIZATION Naval Ocean Systems Center			
6c. ADDRESS (City, State, and ZIP Code) Monterey, California 93943-5000			7b. ADDRESS (City, State, and ZIP Code) San Diego, CA 92152			
8a. NAME OF FUNDING/SPONSORING ORGANIZATION Naval Ocean Systems Center	8b. OFFICE SYMBOL (If applicable) Code 825		9. PROCUREMENT INSTRUMENT IDENTIFICATION NUMBER			
8c. ADDRESS (City, State, and ZIP Code) San Diego, California 92152			10 SOURCE OF FUNDING NUMBERS			
			PROGRAM ELEMENT NO.	PROJECT NO	TASK NO	WORK UNIT ACCESSION NO

11 TITLE (Include Security Classification)

A FEASIBILITY STUDY OF A SHIPBOARD COMBAT SURVIVABLE HF ANTENNA DESIGN

12 PERSONAL AUTHOR(S)
Tertocha, James C.

13a TYPE OF REPORT Master's Thesis	13b TIME COVERED FROM _____ TO _____	14 DATE OF REPORT (Year, Month, Day) 1986, March	15 PAGE COUNT 126

16 SUPPLEMENTARY NOTATION

17	COSATI CODES		18 SUBJECT TERMS (Continue on reverse if necessary and identify by block number)
FIELD	GROUP	SUB-GROUP	Combat Survivable Antenna; Computer Modeling of Antennas

19 ABSTRACT (Continue on reverse if necessary and identify by block number)

This thesis investigates the feasibility of a shipboard combat survivable HF antenna design. The antenna is modeled as a rectangular volume excited by a square patch atop a monopole centered at one of the volume's faces. Several computer models of the driving antenna are modeled with the Numerical Electromagnetics Code (NEC) and compared. Scale models of the driving antennas are made and their impedance measurements compared to NEC computer models. Input impedances and radiation patterns of the survivable antenna are presented which indicate adequate performance given a 3:1 SWR.

20 DISTRIBUTION/AVAILABILITY OF ABSTRACT ☒ UNCLASSIFIED/UNLIMITED ☐ SAME AS RPT ☐ DTIC USERS	21 ABSTRACT SECURITY CLASSIFICATION Unclassified	
22a NAME OF RESPONSIBLE INDIVIDUAL Prof. Richard W. Adler	22b TELEPHONE (Include Area Code) (408) 646-2352	22c OFFICE SYMBOL Code 62Ab

DD FORM 1473, 84 MAR
83 APR edition may be used until exhausted
All other editions are obsolete

1

A Feasibility Study of a Shipboard
Combat Survivable HF Antenna Design

by

James C. Tertocha
Lieutenant, United States Navy
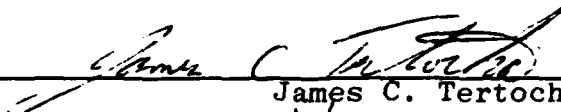B.S., University of Southern California, 1979

Submitted in partial fulfillment of the
requirements for the degree of

MASTER OF SCIENCE IN ELECTRICAL ENGINEERING
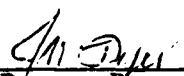

from the

NAVAL POSTGRADUATE SCHOOL
March 1986

Author: _____
                      James C. Tertocha

Approved by: _____
                      R.W. Adler, Thesis Advisor

            _____
                      S. Jauregui, Second Reader

            _____
                 Harriett Rigas, Chairman, Department of
                 Electrical and Computer Engineering

            _____
              John N. Dyer, Dean of Science and Engineering

ABSTRACT

This thesis investigates the feasibility of a shipboard combat survivable HF antenna design. The antenna is modeled as a rectangular volume excited by a square patch atop a monopole centered at one of the volume's faces. Several computer models of the driving antenna are modeled with the Numerical Electromagnetics Code (NEC) and compared. Scale models of the driving antennas are made and their impedance measurements compared to NEC computer models. Input impedances and radiation patterns of the survivable antenna are presented which indicate adequate performance given a 3:1 SWR.

3

TABLE OF CONTENTS

4

I. INTRODUCTION

A. NEED FOR THE STUDY

Shipboard HF and VHF antennas tend to protrude from the ship's silhouette and are quite fragile. This property increases the ship's profile and causes the antennas to be vulnerable to gun fire and bomb blast. Should a HF/VHF antenna be destroyed or damaged by gun fire or bomb blast the ship would suffer a loss in its HF/VHF communication capability. A loss of HF/VHF communications would degrade the ship's fighting ability. Therefore, a study of methods to make HF/VHF antennas more survivable is needed.

There are many survivable antenna designs which may be investigated. The antennas might be made an integral part of the ship's structure. This could be done by using patch or slot antennas imbedded in the hull or superstructure of the ship. An alternate approach would be to excite sections of the ship's superstructure allowing them to perform as antennas. For example, the ship's mast or stack might be excited and used as an antenna. Another possible design might take the form of a telescoping antenna. These and other possible survivable antenna designs should be investigated.

B. STATEMENT OF THE PROBLEM

Using a section of the ship's superstructure as an antenna is one possible survivable antenna design. This study

6

approximates a section of the ship's superstructure as a 12x12x12 meter metal box over a perfect ground. The problem is to excite this metal box and determine the impedance and radiation patterns of the antenna.

There are several ways to excite a metal box. One possible scheme is to insulate one or more sides of the box. A conductive patch may then be placed on the insulated face or faces and driven with a voltage or current source. The patch, in turn, excites the box. Another possible scheme is to utilize the same configuration but with slots instead of patches.

"Patch monopole" is the name chosen to describe the antenna used for exciting the box in this study. Figure 1.1 shows the three sizes of patch monopoles used in this study. The three patch sizes are: 4x4 meters, 6x6 meters, and 10x10 meters. The center of each patch section was chosen to coincide with the center of the box face. This was done to vary the spacing between the patch edges and the sides of the box. Figure 1.2 shows the middle sized patch monopole centered at the box face. To demonstrate the relative size differences of the three patch monopoles with respect to the box size, Figure 1.3 shows the three patch monopoles superimposed on each other at the box face.

A monopole structure is connected between the patch and ground to facilitate exciting the patch section, hence the name patch monopole. The monopole section is driven at its base by a voltage source. Since the monopole section serves
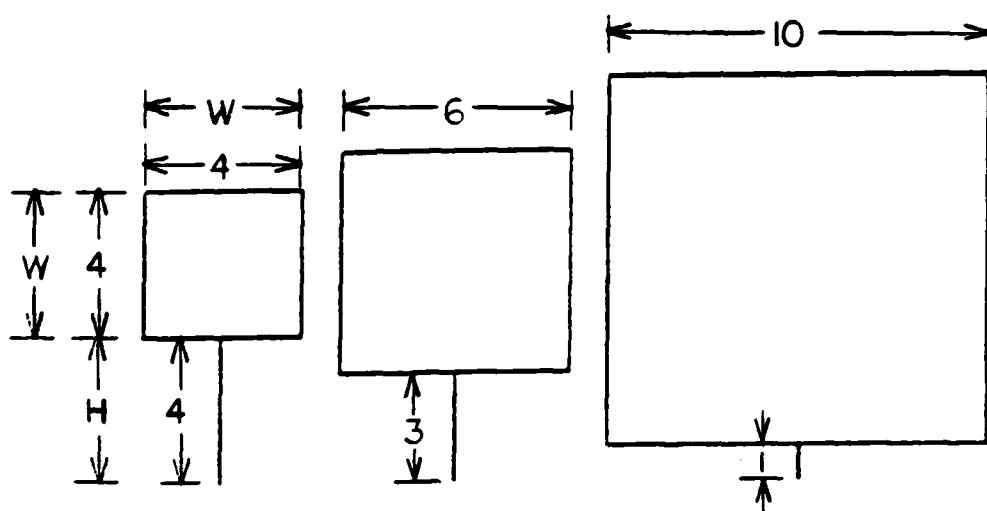
Figure 1.1.   The Three Patch Monopoles
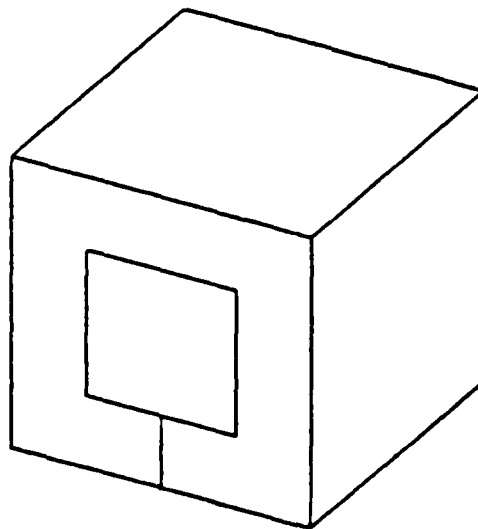
Figure 1.2.   The Middle Sized Patch Monopole at Box Face

8
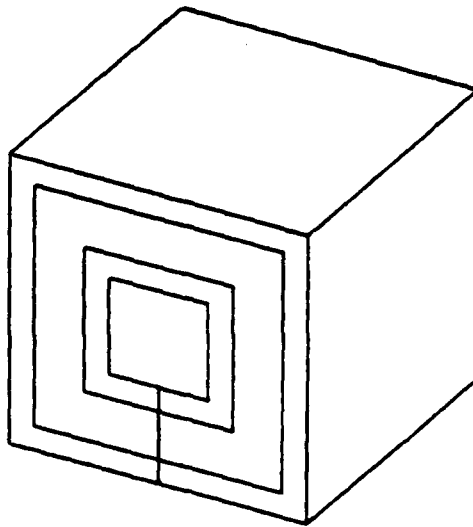
Figure 1.3.   All Three Patch Monopoles Superimposed
              at Box Face

as a voltage feed to the patch, it will be referred to as the
patch monopole's "feed line" at various times throughout this
study.

For ease in identifying the patch monopoles they will be
referred to by the ratio of their patch width (W) to feed line
height (H).   The three ratios are: W/H = 1, W/H = 2, and
W/H = 10.

C.   SCOPE AND LIMITATIONS

Although there are several ways to excite a rectangular
volume this study concentrates on the use of patch monopoles
for that purpose.

The frequency range investigated is limited to the HF
range of 2-24 MHZ.   This limitation is imposed due to computer

9

storage and time restraints. As frequency increases the wave-length decreases and the number of wire segments required to model the antenna increases. This will be discussed more in Section II.

The major emphasis of this study is the development of an adequate computer model for the patch monopole. The patch monopole and metal box are then modeled as a unit on the computer. The computer code used to model the antenna structures in this study is the Numerical Electromagnetics Code [Ref. 1].

Physical scale models of the patch monopoles were con-structed for impedance measurement purposes. There are accuracy limitations of the impedance measurements taken on the scale models.

The ground plane used with the scale models is an 11x11 meter ground plane. Since the ground plane is not infinite, some differences in theoretical and measured impedance values will occur due to edge effects. In addition there are several buildings located near the ground plane which may cause unwanted reflections.

The feed transition to the antenna on the ground plane does not physically fit the scale antenna models. The scale models are tapered at the base to correct this mismatch. However, the taper does cause some shift in the antenna impedance.

This thesis starts with a discussion of computer and physical antenna modeling in Chapter II. Chapter III describes

the computer models used in this study and Chapter IV describes the physical models built for comparison to the computer models. Chapters V and VI are presentations of the computer and physical model results. The results are compared in Chapter VII and conclusions and recommendations presented in Chapter VIII.

II. NUMERICAL AND PHYSICAL MODELING

A. WIRE ANTENNA COMPUTER MODELING

Wire antenna modeling programs typically solve integral equations for the antenna's current distribution. Once the current distribution is known other antenna parameters of interest may be calculated.

The electric field at an arbitrary observation point, $\bar{r}$, due to an arbitrary known current density located at a point $\bar{r}'$, (see Figure 2.1), can be found by integrating the product of the free space Green's function and the known current density over the surface on which the current density resides as shown in the following equation:

$$\bar{E}(\bar{r}) \;=\; \int_{s} \bar{\bar{G}}(\bar{r},\bar{r}') \cdot \bar{J}_{s}(\bar{r}')\,dA'$$
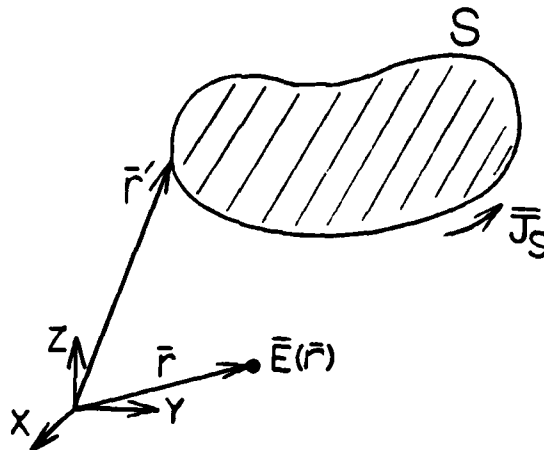

Figure 2.1. Electric Field Due to Current Distribution

12

The above equation becomes an integral equation when the electric field is known and the current unknown. When $\bar{r}$ is on a conducting surface, S, the electric field, $\bar{E}(\bar{r})$, must satisfy the following boundary condition:

$$\hat{n} \times [\bar{E}(\bar{r}) + \bar{E}^i(\bar{r})] = 0$$

and the electric field integral equation becomes [Ref. 2]:

$$\hat{n}(\bar{r}) \times \oint_S \bar{\bar{G}}(\bar{r},\bar{r}') \cdot \bar{J}_s(\bar{r}')dA' = -\hat{n}(\bar{r}) \times \bar{E}^i(\bar{r})$$

where:

$\oint_S$ indicates the principal value integral;

$\bar{J}_s$ is the surface current density;

$\hat{n}(\bar{r})$ is the surface unit normal vector at $\bar{r}$;

$\bar{E}^i(\bar{r})$ is the incident electric field at $\bar{r}$;

and

$$\bar{\bar{G}}(\bar{r},\bar{r}') = \frac{-j}{4\pi\omega\epsilon}(k^2\bar{\bar{I}} + \nabla\nabla)g(\bar{r},\bar{r}')$$

where:

$$g(\bar{r},\bar{r}') = \frac{e^{-jkR}}{R}$$

$$R = |\bar{r} - \bar{r}'|$$

13

$$\overline{\overline{I}} = \hat{x}\hat{x} + \hat{y}\hat{y} + \hat{z}\hat{z}, \quad \text{the identity dyad;}$$

$$k = \omega\sqrt{\mu\epsilon};$$

$$\mu = \text{permeability;}$$

$$\epsilon = \text{permittivity;}$$

$$\omega = \text{radian frequency.}$$

In the above equation $\overline{\overline{G}}(\overline{r},\overline{r}')$ is the kernel or Green's function, $-\hat{n}(\overline{r}) \times \overline{E}^i(\overline{r})$ is the forcing function, and $\overline{J}_s(\overline{r}')$ is the unknown current distribution. Figure 2.2 depicts the coordinate system utilized by the electric field integral equation.
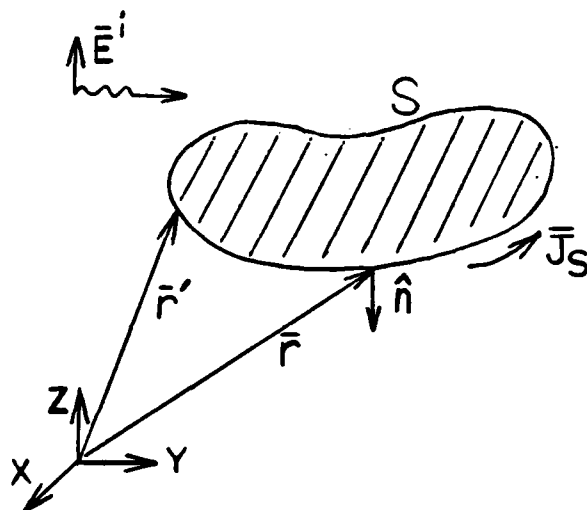

Figure 2.2. Electric Field Integral Equation Coordinate System

14

For the analysis of thin wire structures the electric field integral equation is reduced to a scalar integral equation by use of the thin wire approximation. Thin wire structures are wire structures for which the wire radius is small compared to a wavelength.

The thin wire approximation replaces the surface current density with a filament current at the center of the wire · being modeled. Circumferential variations of longitudinal currents are ignored as are effects of circumferential currents. Only the axial current is considered. A minimum distance of the wire radius is maintained between the filament current and the field observation points. Figure 2.3 illustrates the coordinate system used with the thin wire approximation. The resulting scalar integral equation is:

$$-\hat{s}\cdot\overline{E}^i(\overline{r}) = \frac{-j}{4\pi\omega\varepsilon} \int_{C(\overline{r})} I(s')(\hat{s}\cdot\hat{s}'k^2 - \frac{\partial^2}{\partial s\partial s'})g(\overline{r},\overline{r}')ds'$$

where $I(s')$ is the axial current.

A widely used technique for solving the integral equation is the application of the method of moments [Ref. 3]. The integral equation is of the form $L[\overline{J}_s(\overline{r}')] = \overline{F}(\overline{r})$ where L is a linear operator (here integration) having a domain D_L containing the vectors represented by $\overline{J}_s(\overline{r}')$.

$\overline{J}_s(\overline{r})'$ represents the unknown current distribution and $\overline{F}(\overline{r})$ is the known forcing function whose range is in the range R_L of L.

15
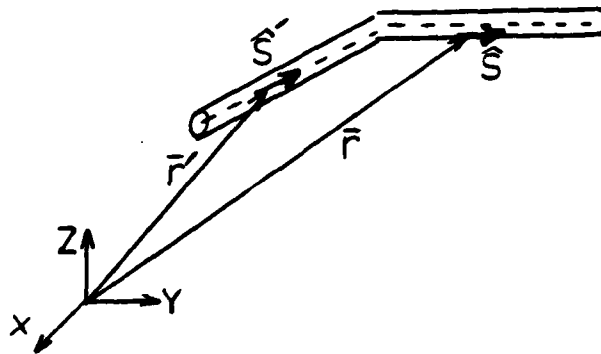
Figure 2.3. Thin Wire Approximation Coordinate System

The current is expanded in a set of N linearly independent basis functions as follows:

$$\bar{J}_s(\bar{r}') \;=\; \sum_{n=1}^{N} a_n \bar{J}_n(\bar{r}')$$

Here the a_n's are not known but are determined in the solution process and the $\bar{J}_n$'s are the basis functions chosen by the individual. The integral equation now has the form

$$\bar{F}(\bar{r}) \;=\; \sum_{n=1}^{N} a_n L[\bar{J}_n(\bar{r}')] \tag{1}$$

Next, a set of N linearly independent weighting or testing functions are postulated which span a N-dimensional vector

space S. These weighting functions are denoted by W_m with $m = 1, \ldots, N$.

The N projections of $\overline{J}_s(\overline{r}')$ and of $\sum\limits_{n=1}^{N} a_n \overline{J}_n(\overline{r}')$ upon the subspace S_w are then forced to be equal by taking the inner products with the weighting functions. This forces the right and left sides of Equation (1) to be equal. Taking the inner products with the set of N weighting functions the following system of N linearly independent equations is arrived at:

$$\sum_{n=1}^{N} a_n < \overline{W}_m(\overline{r}), L[\overline{J}_n(\overline{r}')] > \; = \; <\overline{W}_m(\overline{r}), \overline{F}(\overline{r}) >$$

This linear algebraic system is then solved for the N unknown coefficients a_n, and an approximation to $\overline{J}_s(\overline{r}')$ is obtained.

The selection of basis functions and weighting functions affects the accuracy of the solution and the efficiency of the computation. Different computer codes use different combinations of these functions. Each has its advantages and disadvantages for different antenna geometries. E.K. Miller and F.J. Deadrick present an excellent comparison of the different combinations of basis and weighting functions [Ref. 4].

Having solved the system of linear equations an approximation of the current distribution is obtained. Knowing the current distribution the antenna's radiation patterns, input impedance, gain, efficiency, and other parameters may be calculated.

17

The Numerical Electromagnetics Code (NEC) is a method of moments computer code for the analysis of the electromagnetic response of antennas and other metallic structures. NEC is the computer code used for modeling in this thesis.

NEC's application to wire antennas requires the structure to be modeled with strings of short straight wire segments. These segments should follow as closely as possible the geometry of the conductors of the structure being modeled. NEC uses the method of moments to numerically solve the thin wire integral equation for the currents on the wire segments and consequently the entire structure.

The weighting functions used by NEC are Dirac delta functions located at the center of the wire segments. The weighting functions have the form:

$$W_m(\overline{r}) = \delta(S - S_m)$$

where S_m are the set of match points found at the center of each segment S. This is known as the collocation method of solution.

NEC uses a three term basis function for the current expansion. The basis function is the sum of a constant, sine, and cosine term. Each basis function extends over the segment for which it is defined and onto the segments on either side of the segment for which it is defined, see Figure 2.4. The result is a continuous current distribution and charge density over the segmented wire.
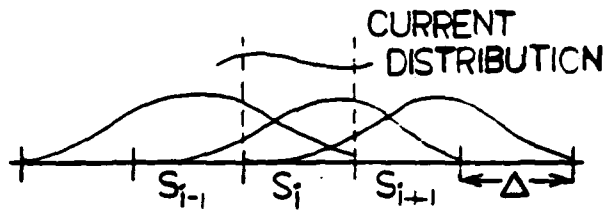
Figure 2.4.   Basis Function Configuration

NEC has the capability of modeling active or passive structures.   The structure may be located over a perfect or imperfect ground.   A model may be composed of perfect or imperfect conductors and include lumped element loading. if desired.   NEC is capable of using symmetry where it exists in the structure .to significantly reduce the computer storage and time requirements.   NEC allows the 'self-interaction matrix' of a .structure to be computed, factored for solution, and stored on tape or file.   This matrix may then be used when a new antenna or structure is added to the environment of the original structure, reducing the computation time required. Once NEC has computed the current distribution it will output, as requested, the following quantities: input impedance, input power, antenna efficiency; radiation patterns, gain, coupling, near field values, polarization, currents, and charge distribution.

NEC allows several types of excitation.   The structure may be excited by an applied source or an incident plane wave with various polarization schemes.   Of primary interest in this thesis are the applied voltage source models.   There

19

are two such models used by NEC, the E-gap voltage source
and the current-slope-discontinuity voltage source.

The E-gap or applied field voltage source places the
E-field at the match point of the source segment. The
result is a nearly rectangular field spread over the width
of the source segment, mathematically:

$$V_o = - \int_{\ell_1}^{\ell_2} \overline{E} \cdot \hat{s} \, ds \approx - E\Delta$$

The current-slope-discontinuity model forces a discontinuity
in the charge density between segments such that
$V_o \approx I(S_o^+) - I(S_o^-)$. The resulting source obeys the following
mathematical expression:

$$\Delta \frac{\partial I}{\partial I_s} = \frac{-j \, V_o}{60[\ell n(\Delta/a) - 1]}$$

Note that since the current-slope source is a more localized
source it is less dependent on segment length than the E-gap
voltage source. Also, the E-gap source is applied at the
center of the wire segment while the current-slope-discon-
tinuity source is applied to the base of the segment.

There are several wire structure modeling guidelines
which should be adhered to: When using a voltage source,
the segment lengths on either side of the segment to which
the source is applied should be equal to the length of the

20

segment on which the source is applied. When the current-slope-discontinuity source is used, adjacent segments should have radii equal to the radius of the segment to which the source is applied. Wire segment lengths, d, should be less than a tenth of a wavelength, in critical regions making $d < .05\lambda$ may be necessary. Extremely short segments, less than $10^{-4}\lambda$ should be avoided. The radius 'a' of a wire segment should be small relative to both wavelength and segment length, the guidelines are:

$$a < .5d$$
$$a < .1\lambda$$

Equal radii and length segments should be used at junctions. Large changes in radius should be avoided, however, if such changes are necessary the radius change should be done in successive steps. Sharp bends in thick wires should be avoided. Wires must not be overlaid. Wires which are to be connected must contact at segment ends. Contact is considered made when following inequality is satisfied:

$$\frac{\text{separation of segment ends}}{d} < 10^{-3}$$

In general, while remaining within the above guidelines, the more segments used to model the structure the more accurate the solution.

Metallic surfaces may be modeled with varying degrees of success by a wire grid. This is possible since as the grid

21

size becomes small relative to a wavelength, the grid supports a current distribution which approximates that of the continuous surface. The current is only an approximation, however, and as such can be expected to predict far fields and impedances reasonably well but possible not near fields.

The wire grid will approximate a surface if the mesh is dense enough, a tenth of a wavelength is considered adequate for most models. The ratio of segment length to radius should obey the following inequality: $10 < d/a < 30$, where d is the segment length and a the wire radius. As a mesh is sparser than a continuous surface its currents will tend to be concentrated and exhibit a higher inductance than would normally be present on the continuous surface. Possible solutions are to use distributed loads of negative inductance or fat, rod-like wires.

B. SCALE MODELING

Antenna engineers often use scale models of antennas as tools in antenna analaysis and design. Such models predict the response of the full size antenna well and are less expensive to build than the full-sized antenna. Scale models also require less test area to conduct measurements in.

As a consequence of the linearity of Maxwell's equations an antenna with certain properties at a given frequency, f, will have identically the same properties at another frequency, nf, provided all linear dimensions are scaled by the ratio 1/n [Ref. 5]. Thus a 10 meter monopole at a frequency of 10 MHZ

may be modeled by a 1 meter monopole at 100 MHZ. Problems do arise in scaling the conductivity however. To properly scale the antenna the models conductivity should be 10 times that of the original monopole. If the original antenna is made of copper or some other highly conductive material it may not be possible to build the model from a material of 10 times the conductivity. This is not too serious a problem, however, since conductivity losses affect the operation of most antennas only to a small degree.

Selection of a ground plane for the scale model antenna measurements is important. The ideal ground plane is infinite in extent and made of a perfect conductor. The radiation fields of a monopole of height h over such a ground plane are identical to those of a center driven dipole of length 2h. This follows from the image theory [Ref. 6]. The monopole's input impedance is one-half that of the dipole. The above properties hold for all antennas over a perfect ground.

When a finite imperfect ground plane is used the radiation patterns are distorted due to the edge effects of the ground plane [Ref. 7]. In addition the ground plane size affects the input impedance of the antenna. It is reported that for a quarterwave monopole above a circular ground plane of diameter greater than 10 wavelengths the variation of the resistance or reactance from that of an ideal monopole over a perfect ground is less than an ohm. This variation in impedance gets progressively worse as the ground size is reduced.

Meir and Summers [Ref. 8] have made measurements of mono-
poles over finite ground planes. Their results indicate a
square ground plane produces less variations in impedance than
does a circular ground plane. Also, broad monopoles produce
less variations in impedance than do thin monopoles. Typical
variations for a $L/\lambda = .488$ monopole of $.0258\lambda$ diameter over
a square ground plane were $\pm 10\%$ in resistance and $\pm 17\%$ in
reactance for a ground plane 2 wavelengths wide. When the
ground plane width was increased to 4 wavelengths the variations
were 4% in resistance and 8% in reactance. Thus the ground
plane used should be as large as possible and preferably square.

The feed transition to the scale antenna is also an impor-
tant consideration. The feed transition should present a
smooth 50 ohm (or any other characteristic impedance desired)
to the antenna. The antenna should fit the transition so as
not to present any discontinuities in the network. Such dis-
continuities could cause reflections which change the standing
wave ratio and other properties of the antenna.

If the antenna's radius is not the same size as the feed
transition radius, it may be altered by tapering the base of
the antenna to fit the feed transition radius. Such tapering
will minimize the discontinuities seen by the electromagnetic
transmission to the antenna. Tapering the antenna will also
change the properties of the antenna but to a lesser degree
than an inadequate fit to the feed transition.

III. COMPUTER MODELS

This section presents the various computer models used in this study. The models range from monopoles to patch monopoles at the face of box structures. All models were run over a perfect ground.

A. MONOPOLE MODELS

Two monopoles were modeled on the computer. Both monopoles were of height 13.986 meters and run over the frequency range: 2-24 MHZ. The first monopole had a constant radius of .054 meters and was constructed of fourteen equal length wire segments, each .999 meters long. This monopole is a computer model of one whose impedance characteristics over the frequency range in question have been tabulated by R.W.P. King [Ref. 9]. This monopole computer model will serve as a check between NEC's calculated impedance and that of theory.

The second monopole modeled with NEC was of identical height as the first but had a tapered base similar to the physical scale models of this study. The base of the monopole was "step tapered" over 2 segments. The first segment had a radius of .13387 meters and a length of .2925 meters. The second segment had a radius of .09337 meters and a length of .2925 meters. The remaining thirteen segments were of radii .054 meters and length 1.0308 meters each. Figure 3.1 shows the shapes of the scale model taper and the computer model taper.
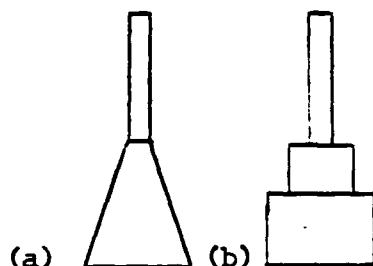
25

Figure 3.1.   Taper Shapes of Models.   a) Scale Model;
b) Computer Model

Both monopoles were driven at their base with a 1 volt
E-gap voltage source.

B.   PATCH MONOPOLE MODELS

The patch monopole is a generic antenna used in this.
study for the excitation of a metallic box as discussed in
Chapter I.

Wire grid computer models of the W/H = 1 and W/H = 10
patch monopoles with various grid densities were built to
determine the effect of grid density on the computer models'
impedances.   To conserve computer resources the W/H = 2 patch
monopole was not run.   The assumption was that the behavior
of the W/H = 2 patch monopole would lie somewhere between
that of the W/H = 1 and W/H = 10 patch monopole models.

The grid models were run at three frequencies: 2 MHZ,
6 MHZ, and 10 MHZ.   These frequencies corresponded to below,
near, and above resonance, respectively.   The radius of the
wire segments used was .05 meters.   Figure 3.2 shows the
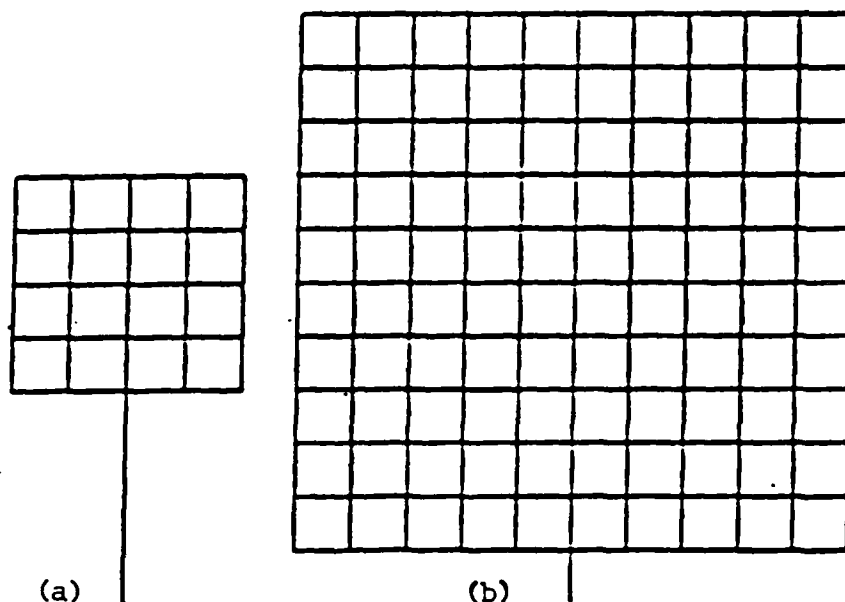typical grid structure used for modeling the patch monopoles.

Figure 3.2. Wire Grid Models. a) W/H = 1; b) W/H = 10

Tables 1 and 2 provide a summary of the different grid densities used with the wire grid models.

TABLE 3.1

GRID DENSITIES OF W/H = 1 ANTENNA MODEL

Grid Spacing in Meters	Grid Spacing in Wavelengths		
	f = 2 MHZ	f = 6 MHZ	f = 10 MHZ
2	.0133	.0400	.0667
1	.0067	.0200	.0336
.5	.0033	.0100	.0167
.4	.0027	.0080	.0133

27

TABLE 3.2

GRID DENSITIES OF W/H = 10 ANTENNA MODEL

Grid Spacing in Meters	Grid Spacing in Wavelengths		
	f = 2 MHZ	f = 6 MHZ	f = 10 MHZ
5	.0334	.1001	.1668
2.5	.0167	.0500	.0834
1.25	.0083	.0250	.0417
1	.0067	.0200	.0334
.625	.0042	.0125	.0209

To determine the effect of the different voltage sources on the computer models, each of the wire grid models of Tables 3.1 and 3.2 were run with an E-gap voltage source and a current-slope-discontinuity voltage source, separately. The voltage sources were applied to the wire segments which contacted the ground plane, i.e., the lowest wire segment of the feed line on each model.

The number of wire segments used to construct the patch monopole feed lines was also varied. This investigated the effect of equal and unequal length segments at junctions as well as the effect of varying the number of equal length segments on either side of a voltage source. Note that when a ground plane is present it appears to the code as if, in addition to the modeled antenna, a mirror image of the antenna above the ground plane is also below the ground plane.

28

Thus placing the voltage source at the segment touching the ground plane is like placing it at the center of the two antennas, and does not violate the modeling guideline of having equal length segments on either side of the voltage source.

The W/H = 10 patch monopole was modeled with a one segment feed line and a 3 segment feed line. The W/H = 1 patch monopole was modeled with a 3 segment feed line and a feed line whose segment lengths were of the same length as those used for the grid structure of that particular wire grid model. Tables 3.3 and 3.4 summarize these segment lengths in terms of wavelengths.

TABLE 3.3

NUMBER OF FEED SEGMENTS AND THEIR LENGTHS IN
WAVELENGTHS FOR W/H = 1 ANTENNA MODEL

Number of Feed Segments	Feed Segment Length in Wavelengths		
	$f = 2$ MHZ	$f = 6$ MHZ	$f = 10$ MHZ
2	.0133	.0400	.0667
3	.0089	.0267	.0444
4	.0067	.0200	.0333
8	.0033	.0100	.0167
10	.0027	.0080	.0133

TABLE 3.4

NUMBER OF FEED SEGMENTS USED AND THEIR LENGTHS IN WAVELENGTHS FOR W/H = 10 ANTENNA MODEL

Number of Feed Segments	Feed Segement Length in Wavelengths		
	f = 2 MHZ	f = 6 MHZ	f = 10 MHZ
1	.0067	.0200	.0333
3	.0022	.0067	.0111

The number of feed lines and voltage sources driving the wire grid models was changed from 1 to 3. This was done to determine the effect of multiple feed points on the patch monopole models. Each. of the three feed lines was composed of three equal length wire segments. The feed line segment sizes in wavelengths was the same as the three segment feed line cases of Tables 3.3 and 3.4. The three feed lines were each driven at the base by a 1 volt E-gap voltage source. Figure 3.3 shows typical three feed line models.

Three "sparse" computer models were modeled with NEC. These models were run to investigate the modeling of the patch monopole with a non-grid structure. The configurations of these models were selected because their geometry approximated the major distribution of current on the 2 MHZ wire grid model.

For ease in identifying the sparse model configurations the following abbreviations will be used:

sparse patch monopole with no vee--SPMNV
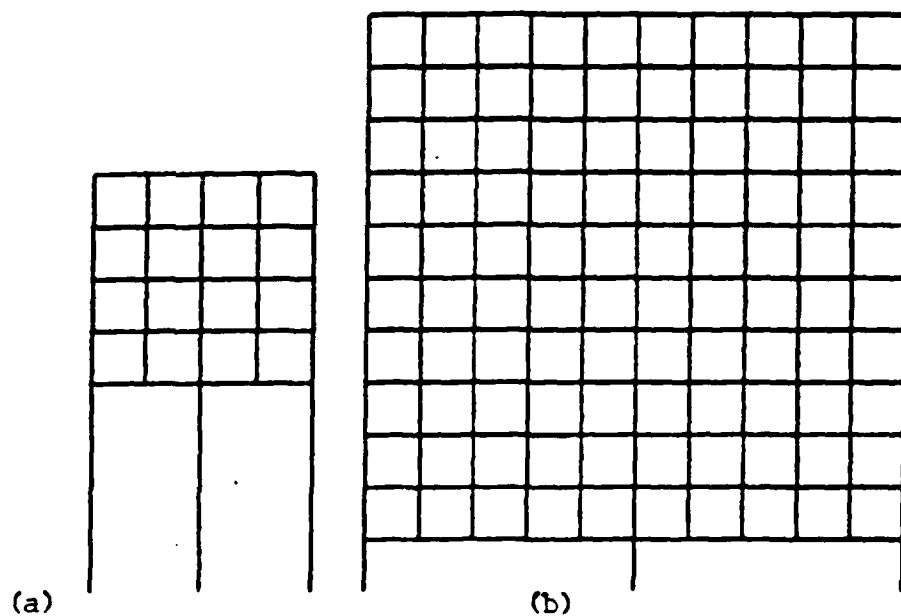
sparse patch monopole with vee--SPMV

30

(a)   (b)

Figure 3.3.   Three Feed Line Wire Grid Models.
              a)   W/H = 1, b) W/H = 10

sparse patch monopole with vee and vertical center--SPMVC
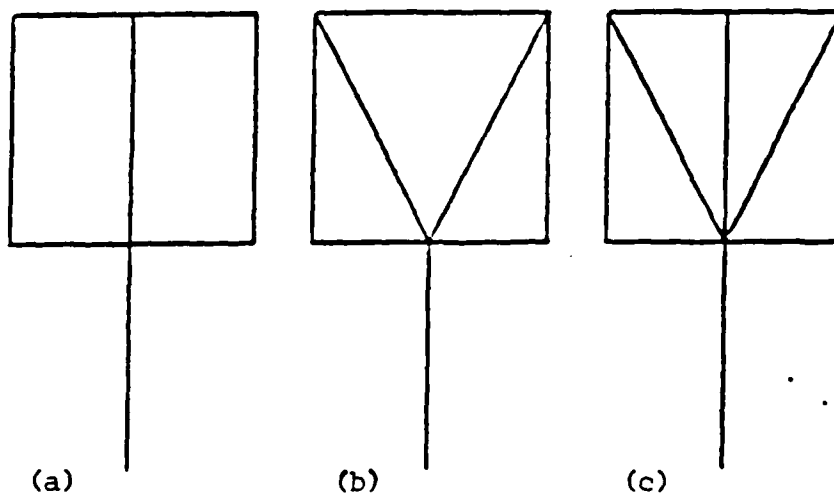
Figure 3.4 shows the models and their abbreviated names.

(a)   (b)   (c)

Figure 3.4.   Sparse Models.   a) SPMNV, b) SPMV, c) SPMVC

31

The sparse models were modeled with one feed line. The W/H = 1 models each had three segments on their feed lines. The W/H = 10 models were modeled twice, one with one segment feed line and once with three segment feed lines.

Each of the wires composing the W/H = 1 patch monopole patch section was made of two wire segments. Each of the wires used in the W/H = 10 patch section was divided into four segments. Tables 3.5 and 3.6 provide segment lengths in terms of wavelength for the sparse models.

TABLE 3.5

W/H = 1 SPARSE MODEL SEGMENT LENGTHS

Segment Size in Wavelengths

Segment Type	2 MHZ	6 MHZ	10 MHZ
Vertical	.0133	.0400	.0667
Horizontal	.0133	.0400	.0667
Diagonal	.0149	.0448	.0746
Feed	.0089	.0267	.0445

The sparse models were run with their wire radii equal to .005 meters as well as .05 meters. This was to determine the effect of wire radius variations on calculated impedance.

Three patch monopole configurations were run over the frequency range of 2-24 MHZ. The three patch monopoles were of the wire grid type with the following W/H ratios: W/H = 1, W/H = 2, and W/H = 10. These patch monopoles were each driven

32

TABLE 3.6

W/H = 10 SPARSE MODEL SEGMENT LENGTHS

Segment Size in Wavelengths

Segment Type	2 MHZ	6 MHZ	10 MHZ
Vertical	.0167	.0500	.0834
Horizontal	.0167	.0500	.0834
Diagonal	.0187	.0559	.0932
Feed (1 seg/feed)	.0067	.0200	.0334
Feed (2 seg/feed)	.0022	.0067	.0111

with a 1 volt E-gap voltage source at the segment connecting the patch monopole to the ground. Each of the patch monopoles was constructed of .05 meters radii wires and a grid separation of one meter. The W/H = 1 and the W/H = 2 models' feed lines were three equal length wire segments. The W/H = 10 model's feed line had one segment. Table 3.7 lists the range of the models grid sizes, feed segment lengths, and antenna heights in terms of wavelengths. Figure 3.5 shows the three models.

TABLE 3.7

ANTENNA DIMENSIONS AT 2 MHZ AND 24 MHZ

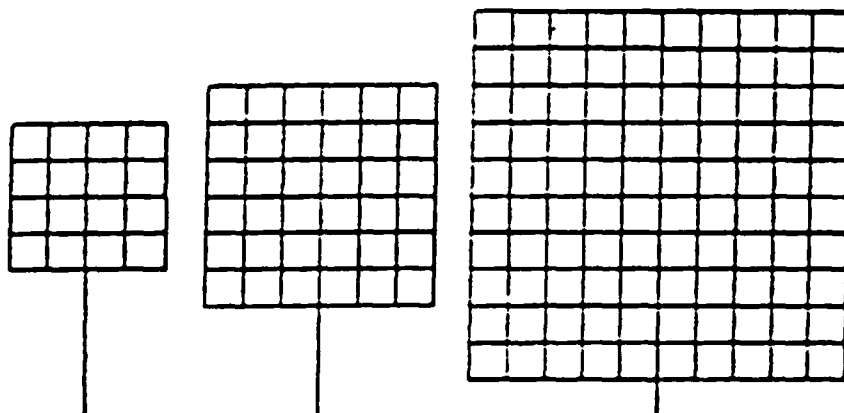| Measurements in Wavelengths	W/H = 1		W/H = 2		W/H = 10	
	2 MHZ	24 MHZ	2 MHZ	24 MHZ	2 MHZ	24 MHZ
Height	.0534	.6405	.0600	.7206	.0734	.8807
Grid Size	.0067	.0801	.0067	.0801	.0067	.0801
Feed Segment Length	.0089	.1068	.0067	.0801	.0067	.0801

Figure 3.5.   Wire Grid Path Monopole Models

C.   METAL BOX COMPUTER MODELS

A 12x12x12 meter box above a perfect ground was modeled with .05 meter radii wires over the frequency range 2-24 MHZ. One side (or face) of the box was left open for later insertion of a patch monopole at the box face.

Three different grid densities were chosen for three frequency ranges. This was done to minimize computer time and storage while still maintaining the less than one-tenth a wavelength per wire segment length criteria. Table 3.8 lists the frequency ranges and corresponding grid spacings. Figures 3.6-3.8 show the wire grid box models used.

Finally, the metal box with a patch monopole at its open face was modeled over a perfect ground. The box was run for a W/H = 1, W/H = 2, and a W/H = 10 patch monopole at the face of the box, separately. The patch monopoles were those

TABLE 3.8

BOX MODEL FREQUENCY RANGES AND GRID SPACINGS IN WAVELENGTHS

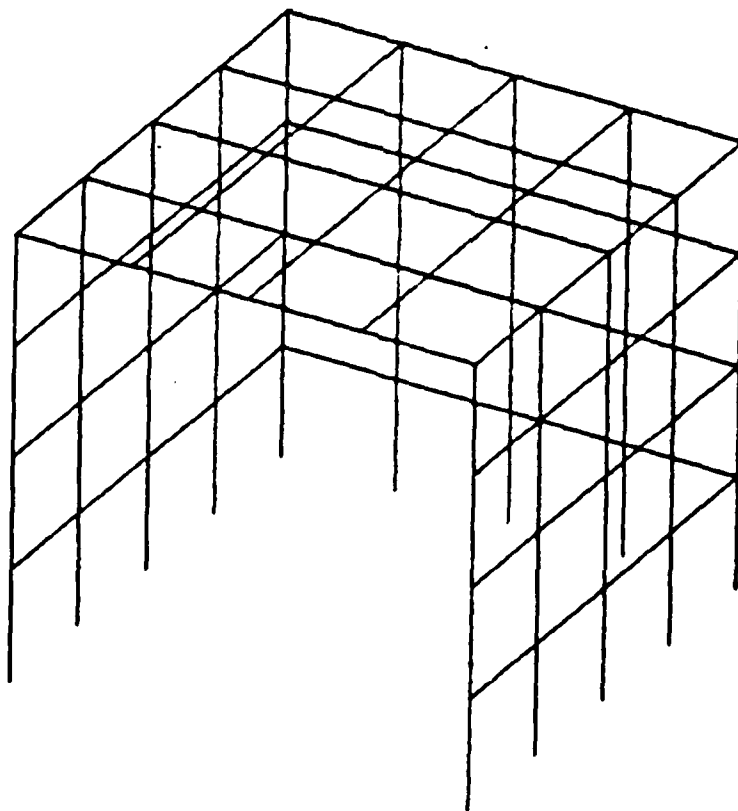| Frequency Range in MHZ	Grid Spacing in Meters	Low Freq. End Grid Spacing in Wavelengths	High Freq. End Grid Spacing in Wavelengths
2-10	3	.0200	.1001
11-15	2	.0733	.1001
16-24	1.2	.0640	.0961

Figure 3.6.   Box Model for Frequency Range 2-10 MHZ
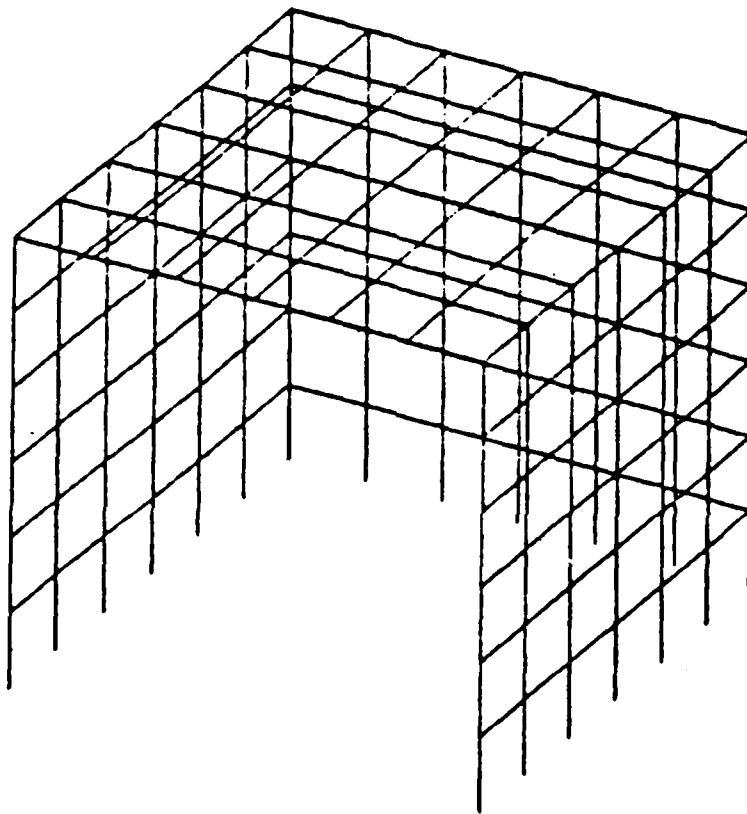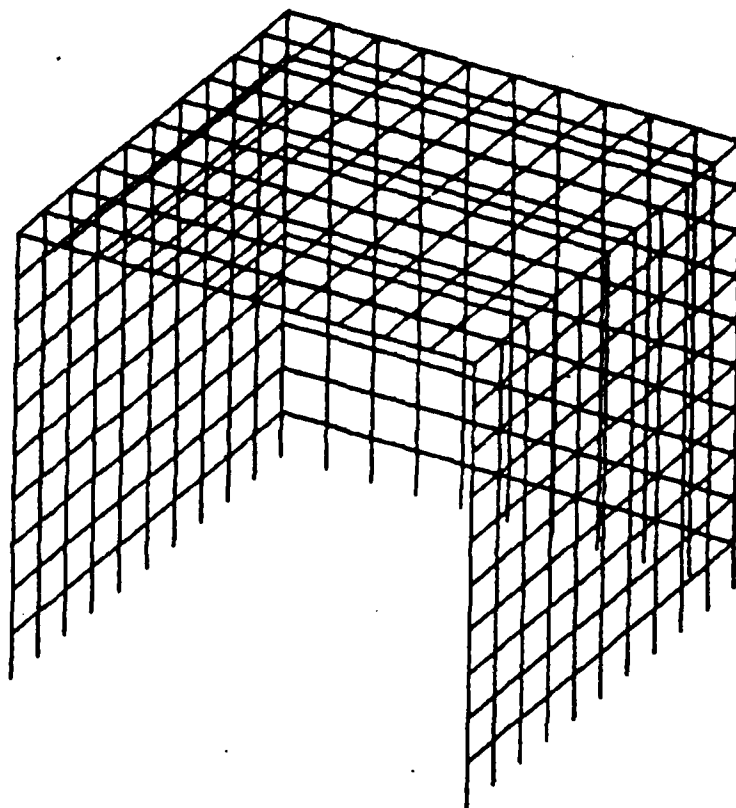
Figure 3.7.   Box Model for Frequency Range 11-15 MHZ

36

Figure 3.8.   Box Model Frequency Range 16-24 MHZ

which had been run over the frequency range 2-24 MHZ with the one meter grid spacing, discussed earlier.   Figure 3.9 shows a typical gridded box model with a wire grid patch monopole at its open face.

37
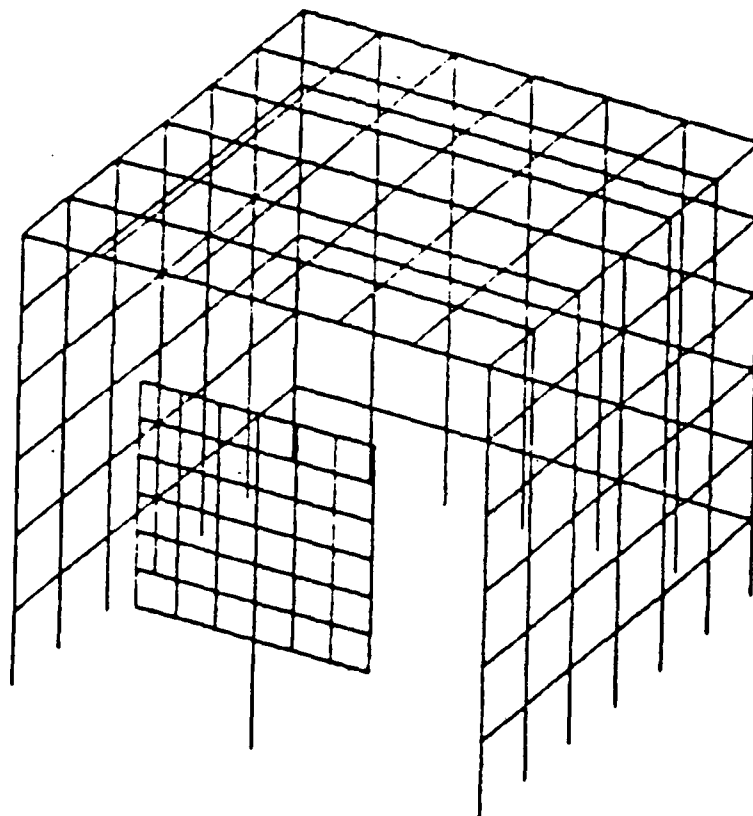
Figure 3.9. Typical Box with Patch Monopole Wire
Grid Model

IV. SCALE MODELS

Physical scale models of the patch monopoles and of a monopole whose theoretical impedance values are known, were constructed to provide a correlation between physical impedance measurements and the impedances predicted by NEC. The impedance measurements were performed with the physical models over an 11 x 11 meter ground plane. A scale factor of 1/45 was used on the physical models to ensure the ground plane was at least three wavelengths across at the lowest frequency. The frequency range used for the impedance measurements was 90-1080 MHZ. This corresponded to the computer model frequency range of 2-24 MHZ. Appendix A provides a block diagram of the experimental set up.

A. SCALE MONOPOLE

To determine the accuracy of the experimental set up a monopole whose theoretical characteristics have been tabulated by R.W.P. King [Ref. 9] was built. The physical monopole was a flat-top cylindrical brass rod of height .3108 meters. The bottom of the monopole was tapered from a diameter of .685 cm at the base to the monopole diameter of .24 cm at a height 1.3 cm from the monopole base. Although this taper presents a deviation from the theoretical monopole it was necessary to match the diameter to that of the feed transition's center conductor. (This taper is also used

with each of the patch monopole models to be discussed in this chapter.)

B. SOLID PATCH MONOPOLES

Scale patch monopole models of the W/H = 1 and W/H = 10 patch monopoles were constructed. The patch sections of the two models were made of .215 cm thick brass plate while the monopole sections were made from .24 cm diameter brass rods. The taper described in Section A was used on both models. Figures 4.1 and 4.2 are photographs of the W/H = 1 and W/H = 10 scale models respectively.
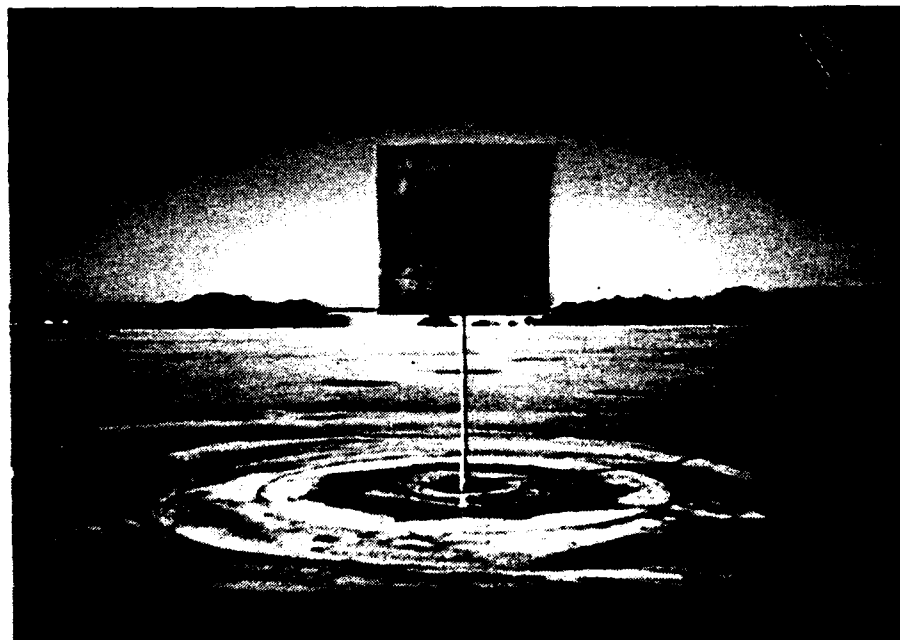

Figure 4.1. W/H = 1 Patch Monopole 1/45 Scale Model
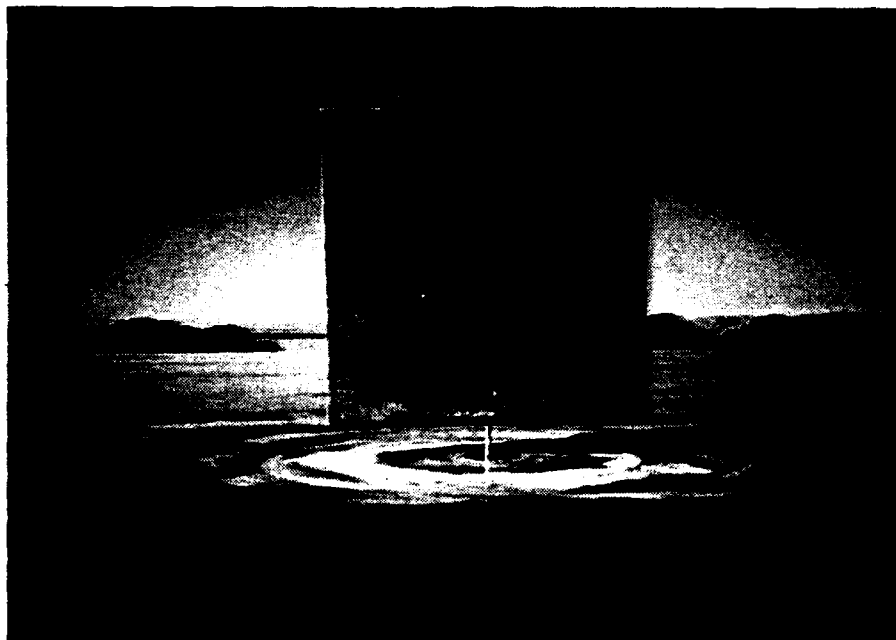
Figure 4.2. W/H = 10 Patch Monopole 1/45 Scale Model

C. GRID PATCH MONOPOLE MODELS

Wire grid scale patch monopole models were built to pro-
vide a comparison between the computer patch monopole models
and the physical models, as well as to determine the degree
to which a wire grid approximates a solid plate.

Scale models of the W/H = 1, W/H = 2, and W/H = 10 wire
grid computer models were built. The grid spacing of the
scale models was 2.22 cm corresponding to the computer wire
grid models with grid spacings of one meter. The diameter of
the brass rods used to construct the grids and the monopole
sections was .24 cm. Again the taper described in Section A

41

was used with each model. Figures 4.3, 4.4, and 4.5 are
photographs of the W/H = 1, W/H = 2, and W/H = 10 wire grid
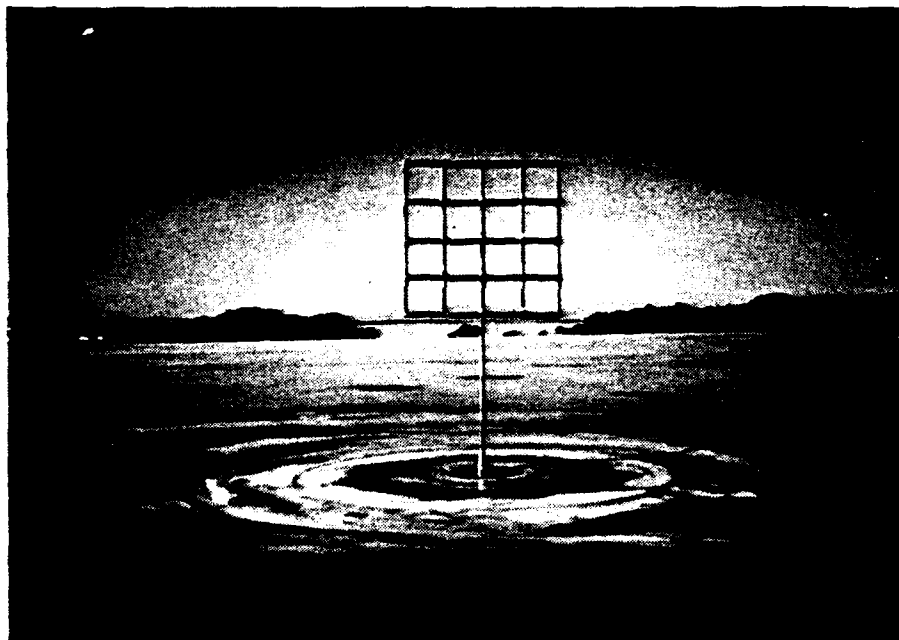scale models, respectively.

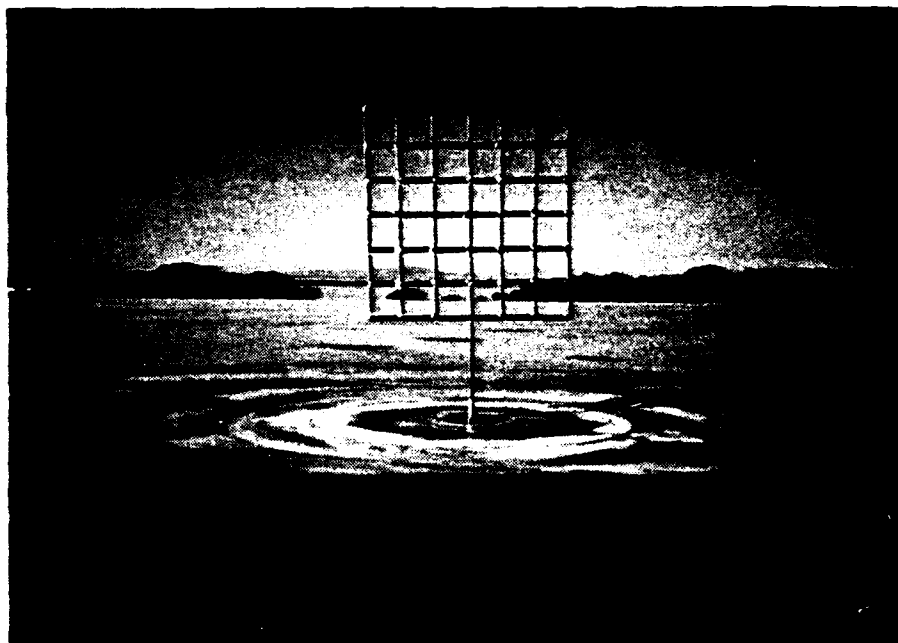Figure 4.3. W/H = 1 Scale Wire Grid Patch Monopole Model

Figure 4.4. W/H = 2 Scale Wire Grid Patch Monopole Model
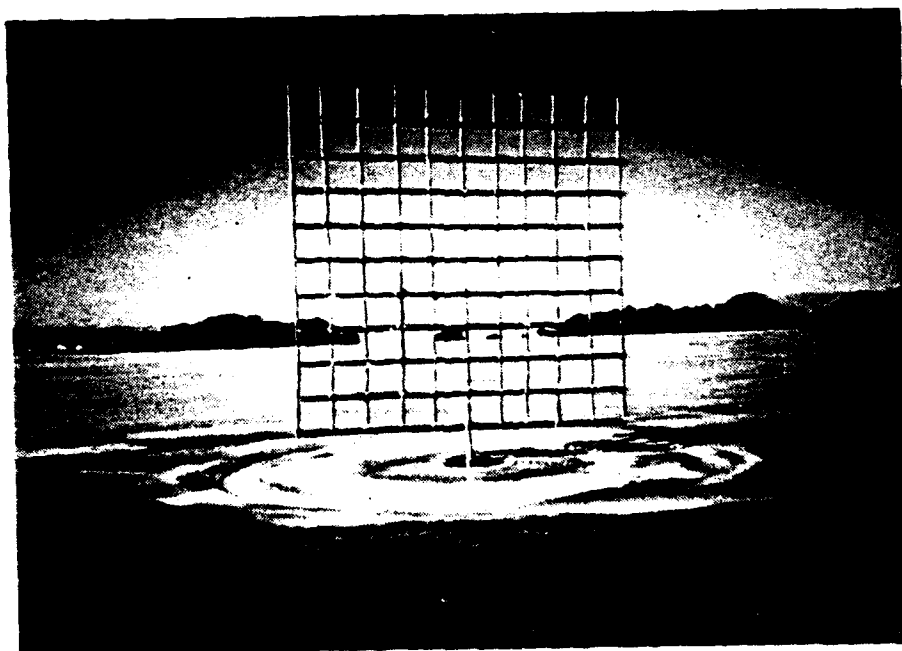

Figure 4.5. W/H = 10 Scale Wire Grid Patch Monopole Model

V. COMPUTER MODEL RESULTS

This section is devoted to presenting the results of the computer models described in Chapter III.

A. COMPUTER MONOPOLE MODELS

As discussed in Chapter III a computer monopole model of a monopole whose characteristics were calculated and tabulated by R.W.P. King was modeled with NEC. A second monopole but with a tapered base was also modeled on the computer. Figure 5.1 is a plot of the resistance versus monopole height of King's monopole, the non-tapered computer monopole model and the tapered computer monopole model. Figure 5.2 is a plot of the reactance versus monopole height of the three monopoles. From the graphs it is seen that NEC models the monopole well, particularly at heights less than .4 wavelengths. The effect of the taper at the base of the monopole is to make the resistance and reactance lower than that for the uniform radius. Also notice the tapered model correlates to King's monopole better at the high frequency end while the non-tapered model correlates better at the low frequency end.

B. PATCH MONOPOLE COMPUTER MODELS

The W/H = 1 and W/H = 10 patch monopole grid models were run at 2, 6, and 10 MHZ varying their grid size. The results indicate that changing the grid size does affect the impedance
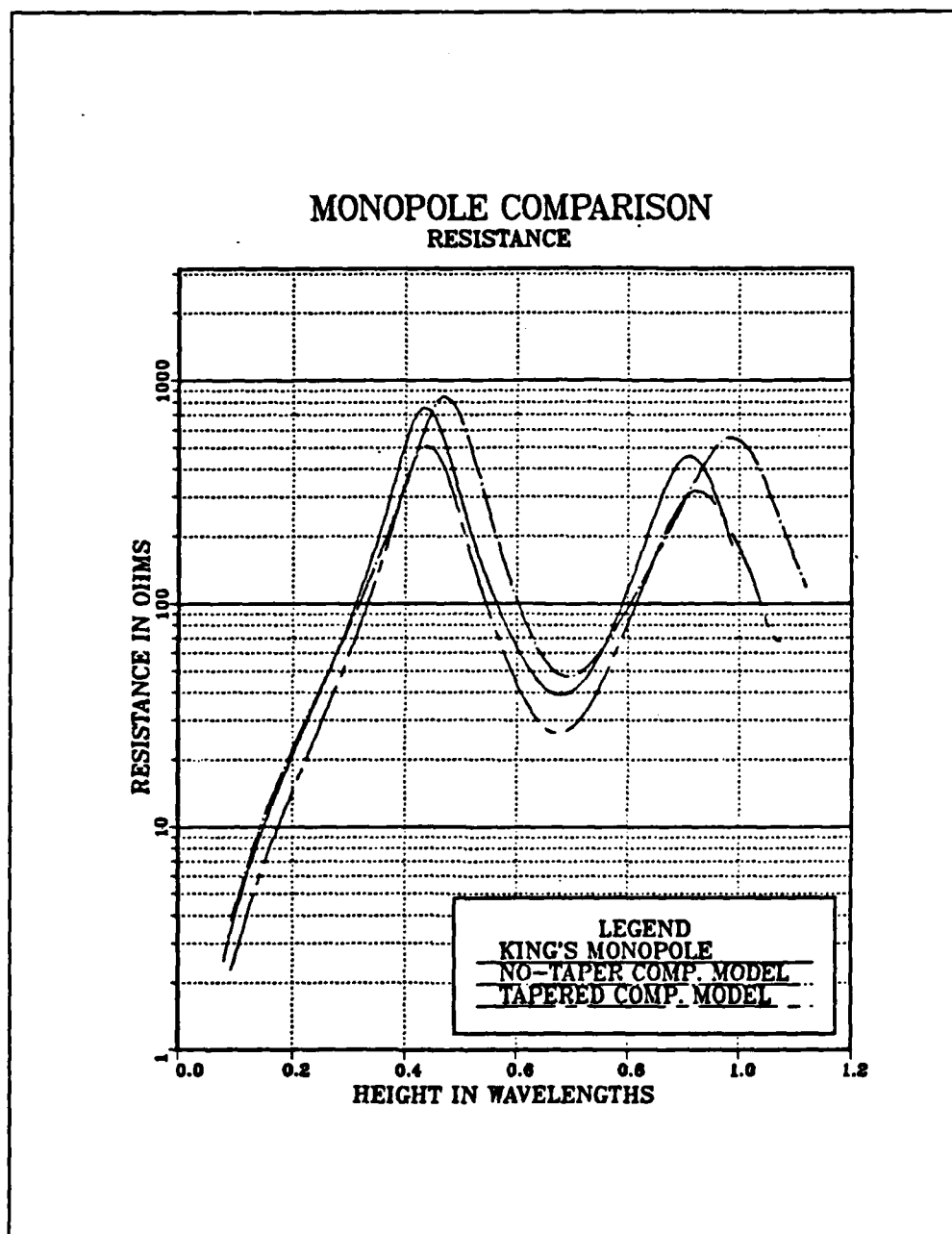
MONOPOLE COMPARISON
RESISTANCE

Figure 5.1.   Monopole Resistance Versus Electrical Height
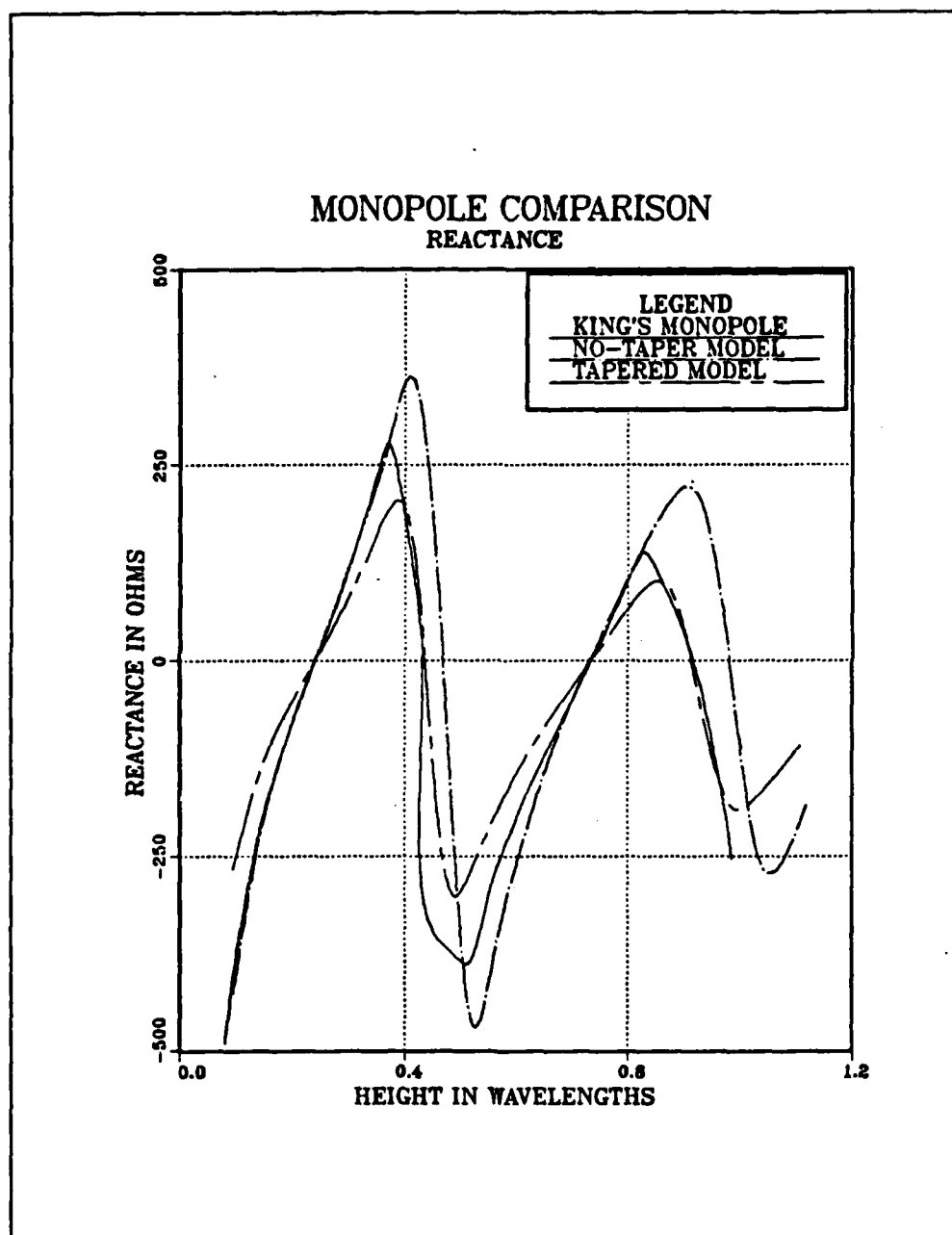
45

MONOPOLE COMPARISON
REACTANCE

Figure 5.2. Monopole Reactance Versus Monopole Height

46

of the antenna model. Figures 5.3 through 5.6 are typical plots of resistance and reactance versus grid size for the two antenna models. From these plots it is seen that, with the exception of the W/H = 1 antenna resistance values, it is not apparent to what value of resistance or reactance the computer models will converge or if they will ever converge as grid size is decreased. Also it is seen that the grid density has a much greater effect on the large antenna's impedance than on that of the small antenna's.

The wire grid patch monopoles with various grid densities were run on the computer with the E-gap voltage source and the current-slope-discontinuity voltage source for comparison, at frequencies of 2, 6, and 10 MHZ. The two voltage sources produce different results. However, for the W/H = 10 antenna the two values tend to converge as grid size is decreased. For the W/H = 1 antenna the two voltage soruces result in impedances that tend to track each other at a fairly constant separation as the grid size is varied. In both cases the current-slope-discontinuity voltage source produces greater resistive and reactive impedance values than the E-gap source. Figures 5.7-5.10 illustrate these trends.

The W/H = 1 and W/H = 10 grid models were also modeled as the number of segments in the feed line varied. This investigated the effect of changing the segment length on either side of the applied voltage source and the effect of unequal segments at wire junctions, in particular at the
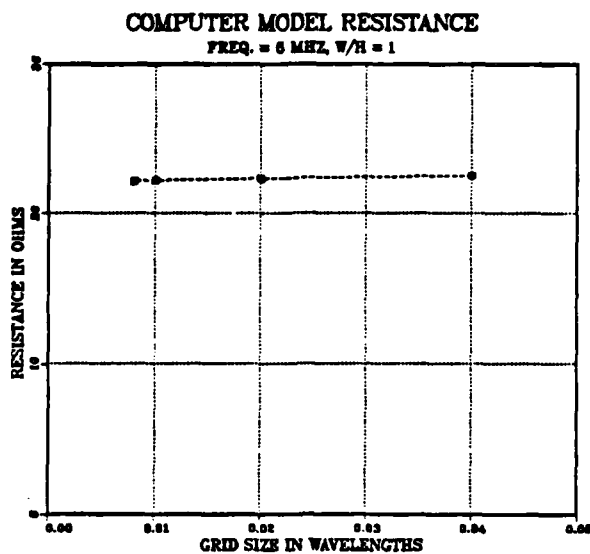
47

COMPUTER MODEL RESISTANCE
FREQ. = 6 MHZ, W/H = 1

Figure 5.3.   Resistance Versus Grid Size for W/H = 1
               Antenna Model at 6 MHZ

COMPUTER MODEL REACTANCE
FREQ. = 6 MHZ, W/H = 1
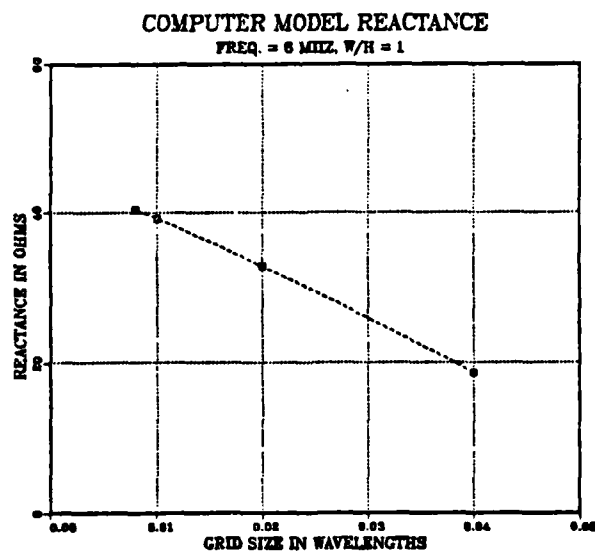
Figure 5.4.   Reactance Versus Grid Size for W/H = 1
               Antenna Model at 6 MHZ

COMPUTER MODEL RESISTANCE

FREQ. = 6 MHZ, W/H = 10
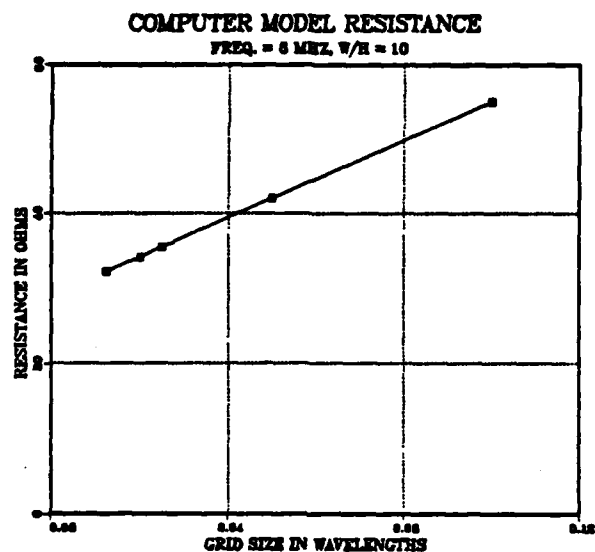
Figure 5.5.   Resistance Versus Grid Size for W/H = 10
Antenna Model at 6 MHZ

COMPUTER MODEL REACTANCE

FREQ. = 6 MHZ, W/H = 10
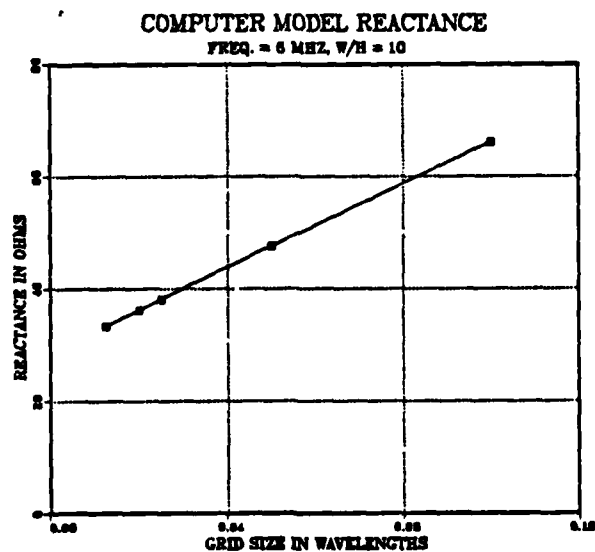
Figure 5.6.   Reactance Versus Grid Size for W/H = 10
Antenna Model at 6 MHZ

COMPUTER MODEL RESISTANCE

FREQ. = 10 MHZ, W/H = 1
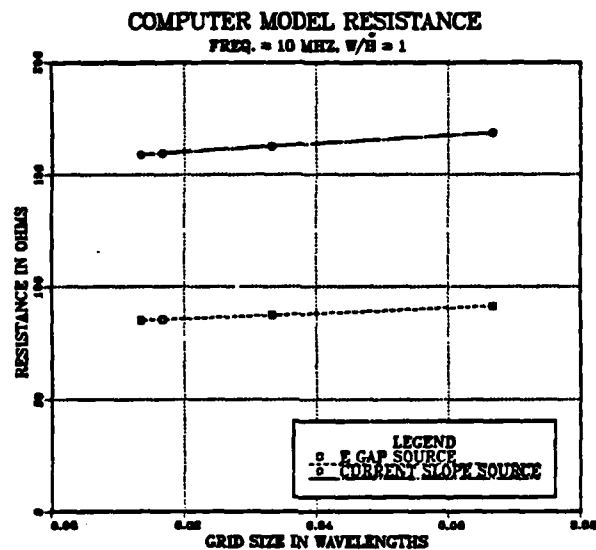
Figure 5.7.   Comparison of Voltage Sources on Resistance
Versus Grid Size for W/H = 1 Antenna Model

COMPUTER MODEL REACTANCE

FREQ. = 10 MHZ, W/H = 1
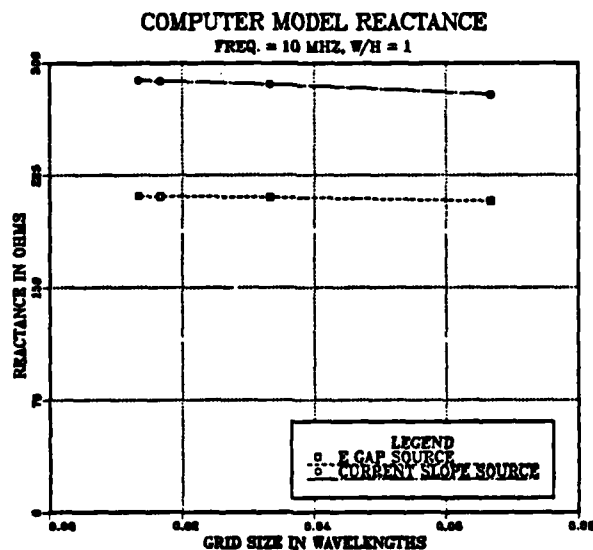
Figure 5.8.   Comparison of Voltage Sources on Reactance
Versus Grid Size for W/H = 1 Antenna Model

COMPUTER MODEL RESISTANCE
FREQ. = 10 MHZ, W/H = 10
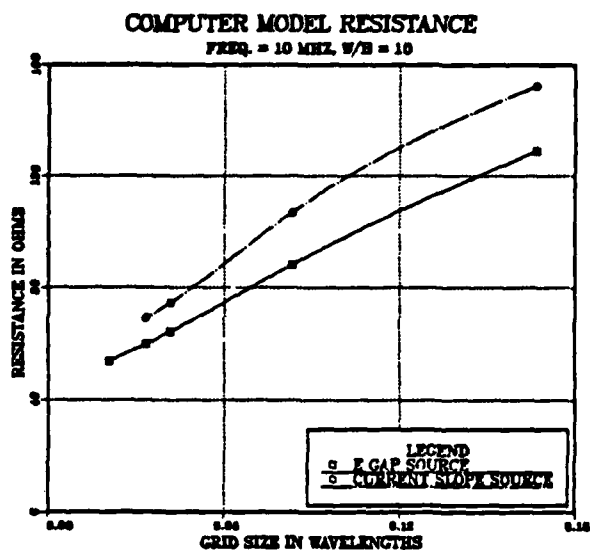
Figure 5.9.   Comparison of Voltage Sources on Resistance
Versus Grid Size for W/H = 10 Antenna Model

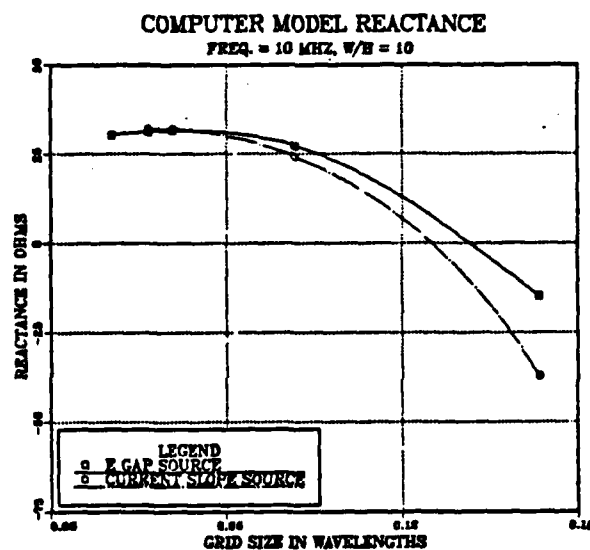**COMPUTER MODEL REACTANCE**
FREQ. = 10 MHZ, W/H = 10

Figure 5.10.   Comparison of Voltage Sources on Reactance
Versus Grid Size of W/H = 10 Antenna Model

51

junction of the wire grid patch and its feed line. Figures 5.11 through 5.14 are typical graphs of how the resistance and reactance values change with grid size for different number of feed segments.

The impedances of the small antenna model (W/H = 1) with feed segment size equal to the grid segment size, tends to diverge from the impedance values obtained with the feed line broken into three segments, as the grid size is decreased. The three segment feed line W/H = 1 model has more stable resistance versus grid size than does the model with its feed segment lengths equal to its grid segment lengths; the opposite is true for reactance. It was expected that the model with equal length segments in the feed line and grid would produce the most stable impedance with respect to grid size since it satisfied the guideline of equal length segments at junctions as well as on either side of the voltage source, but this was not the case.

As the graphs of Figures 5.13 and 5.14 show the impedances of the W/H = 10 antenna models with different length feed segments tend to converge as the grid size is decreased. Also the one segment feed line model has a more stable impedance versus grid size model than the three segment feed line model has. This is reasonable since the length of the one segment feed line is closer in size to the grid segment lengths than are the three feed line segment lengths, and as such, more closely satisfies the guideline for equal length segments at junctions.
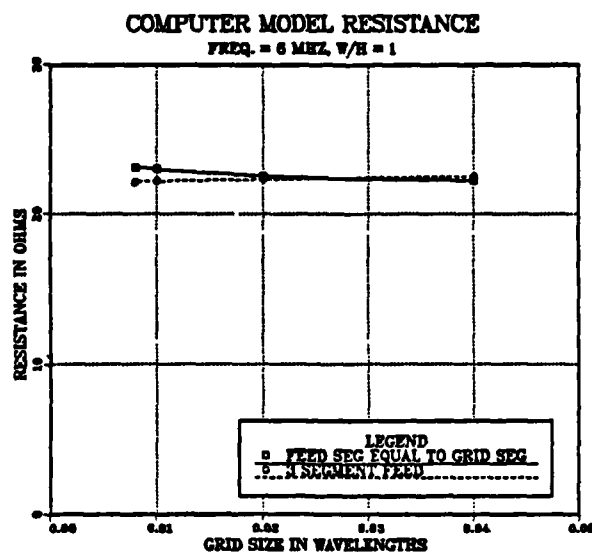
52

COMPUTER MODEL RESISTANCE

FREQ. = 6 MHZ, W/H = 1

Figure 5.11.   Comparison of Different Length Feed Line
Segments on Resistance Versus Grid Size
for W/H = 1 Antenna

COMPUTER MODEL REACTANCE

FREQ. = 6 MHZ, W/H = 1

Figure 5.12.   Comparison of Different Length Feed Line
Segments on Reactance Versus Grid Size
for W/H = 1 Antenna

COMPUTER MODEL RESISTANCE

FREQ. = 6 MHZ, W/H = 10

Figure 5.13. Comparison of Different Length Feed Line Segments on Resistance Versus Grid Size for W/H = 10 Antenna

COMPUTER MODEL REACTANCE

FREQ. = 6 MHZ, W/H = 10

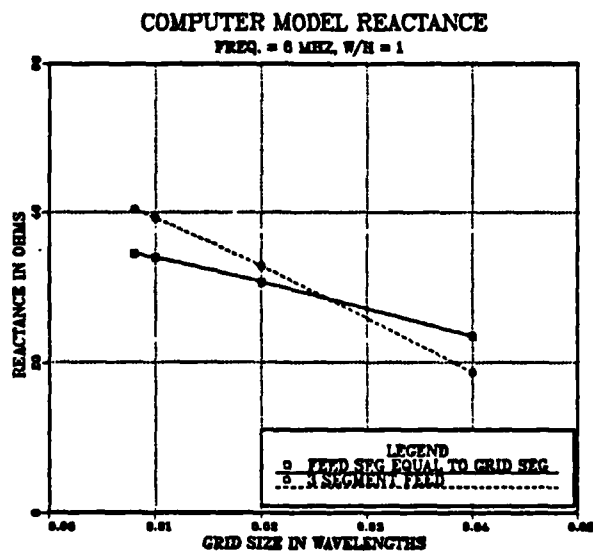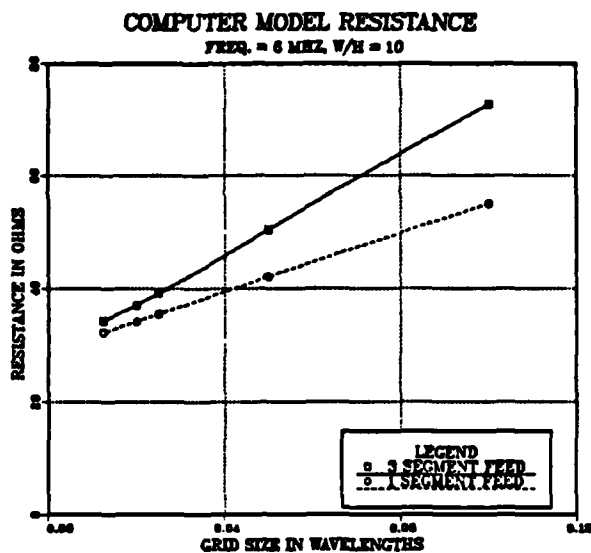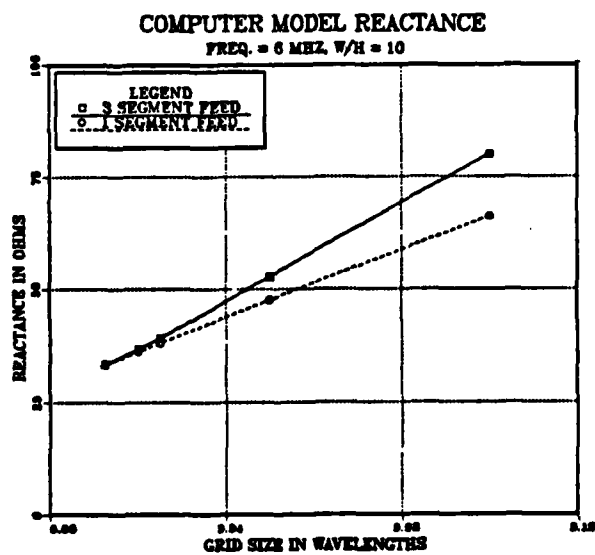Figure 5.14. Comparison of Different Length Feed Line Segments on Reactance Versus Grid Size for W/H = 10 Antenna

54

The W/H = 1 and W/H = 10 patch monopole modles were also modeled with the three sparse models described in Chapter III. Tables 5.1 and 5.2 present their impedances along with the impedances of the one meter grid size models driven with the E-gap voltage source. The W/H = 1 models each used a three segment feed line while the W/H = 10 models used a one segment feed line. Tables 5.3 and 5.4 present the percent change in resistance and reactance for each of the sparse models with respect to the corresponding one meter grid separation model.

TABLE 5.1

IMPEDANCE COMPARISON OF W/H = 1 SPARSE AND GRID MODELS

Freq in MHZ	GRID	SPMVC	SPMV	SPMNV
2	2.08-320j	2.07-333j	2.04-359j	2.06-378j
6	22.3+32.8j	22.1+27.5j	21.8+17.9j	22.3+13.3j
10	87.3+210j	86.1+206j	85.8+200j	89.9+202j

TABLE 5.2

IMPEDANCE COMPARISON OF W/H = 10 SPARSE AND GRID MODELS

Freq in MHZ	GRID	SPMVC	SPMV	SPMNV
2	2.07-98.9j	2.23-125j	2.28-142j	2.48-157j
6	34.2+36.2j	37.1+39.6j	42.3+44.3j	51.3+58.6j
10	59.9+31.31j	78.2+24.3j	89.1+1.59j	116-1.14j

55

TABLE 5.3

PERCENT CHANGE IN RESISTANCE AND REACTANCE OF SPARSE MODELS
FROM WIRE GRID MODEL, W/H = 1

| Freq in MHZ	SPMVC		SPMV		SPMNV	
	Δ%R	Δ%Xj	Δ%R	Δ%Xj	Δ%R	Δ%Xj
2	.53	3.89	2.16	12.3	1.15	18.3
6	.89	19.2	2.26	45.6	.29	59.5
10	1.15	2.21	1.75	4.93	2.97	3.70

TABLE 5.4

PERCENT CHANGE IN RESISTANCE AND REACTANCE OF SPARSE MODELS
FROM WIRE GRID MODEL, W/H = 10

Freq in MHZ	SPMVC		SPMV		SPMNV	
	Δ%R	Δ%Xj	Δ%R	Δ%Xj	Δ%R	Δ%Xj
2	6.96	21.1	10.0	43.7	18.6	58.9
6	8.38	8.55	19.2	18.3	33.3	38.2
10	23.4	28.9	48.9	94.9	94.1	103.

The W/H = 1 sparse models are relatively good over the frequency range 2-10 MHZ with the worst case percent change in resistance being 2.97%. The reactances are less comparable, reaching a percent change of about 60% at 6 MHZ. However, 6 MHZ is the near resonance frequency of the grid model and computer models typically result in resonances which are shifted from the physical resonance. This results in greater deviations in impedances between the physical and modeled antennas near resonance. The above and below resonance

frequencies give a better correlation with a maximum percent change of 18.32%.

The W/H = 10 sparse models correlate less and less in impedance with the grid model as frequency increases and as the model becomes sparser, i.e., the SPMVC model's impedance correlates with the grid model's impedance better than the SPMV model's impedance. The tables also show that the reactances correlate worse than the resistances. This is expected since the sparse models have fewer wires available for current distribution. This results in larger currents on the sparse model's individual wires than what would be found on the grid models individual wires. Larger current concentrations result in greater reactances. Also the sparse models were designed to mimic the current distribution on the grid models at 2 MHZ and as the antenna's height and breadth increase in wavelength the current distribution becomes more complex and the sparse models are less capable of supporting these currents and thus produce different impedances.

The sparse models were also run with the wire radii reduced from .05 meters to .005 meters. As expected the results indicate that thinner wire tends to increase the antenna's impedance.

To determine the effect of multiple feed points on the antenna model the W/H = 1 and W/H = 10 wire grid models were run with three feed points for various grid sizes. Figures 5.15 and 5.16 show the manner in which resistance and reactance changed with respect to grid size for the three feed models.
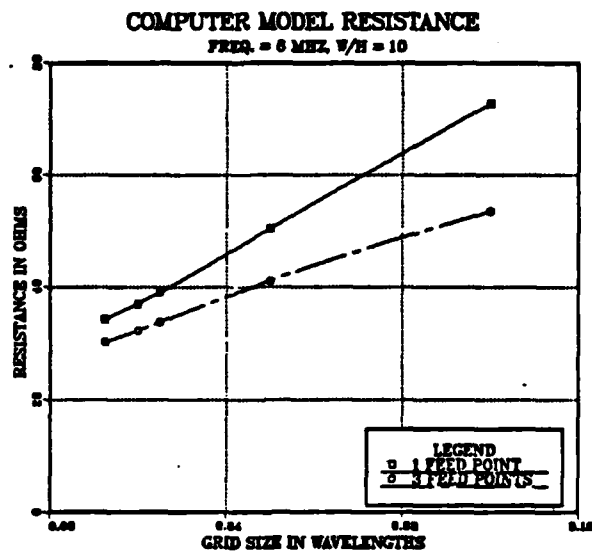
Figure 5.15.   Resistance Comparison of 3 Feed Model
                and 1 Feed Model Versus Grid Size
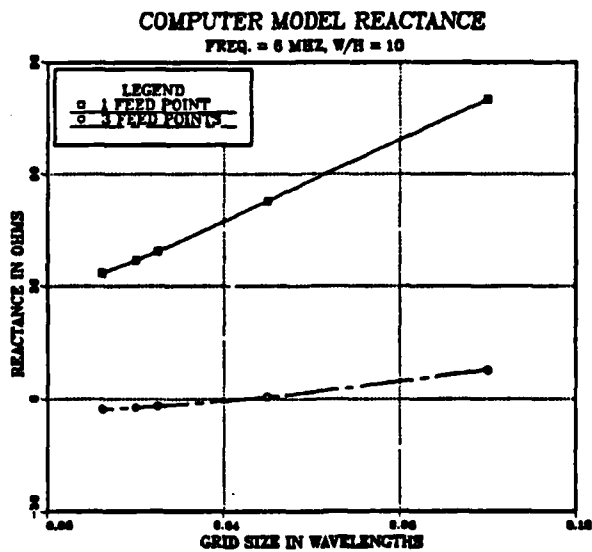
Figure 5.16.   Reactance Comparison of 3 Feed Model
                and 1 Feed Model Versus Grid Size

The resistance and reactance curves of a single feed model are included in the plots for comparison.

The impedance for the three feed models tend to be more stable than for the single feed point models, with respect to grid size. The resistances of the three feed model are typically less than those of the single feed model. In addition the reactances are typically more capacitive than the reactances of the single feed model.

Radiation patterns for the one meter grid separation patch monopole models driven with the E-gap voltage source were obtained over the frequency range 2-24 MHZ. The W/H = 1 and W/H = 2 antenna models each used a three segment feed line and the W/H = 10 antenna model used a single segment feed line.

For heights less than .3 wavelength, the radiation patterns of the W/H = 1 and W/H = 2 patch monopoles looked like patterns of equal height monopoles. The horizontal patterns became slightly elliptical at electrical heights greater than .5 wavelengths. At heights greater than .5 wavelengths the vertical patterns looked similar to those of an equal size monopole but with less lobing. Figure 5.17 is typical of the horizontal patterns of the W/H = 1 and W/H = 2 antennas showing the elliptical shape. Figure 5.18 is a typical vertical pattern. Notice the less severe lobing compared to an equal sized monopole radiation pattern. Figure 5.19 is the vertical pattern of a monopole of equal height provided for comparison.

MEDIUM ANTENNA OVER GROUND

FREQ = 18 MHZ, THETA = 90 DEG, PHI = 1 — 360 DEGS.
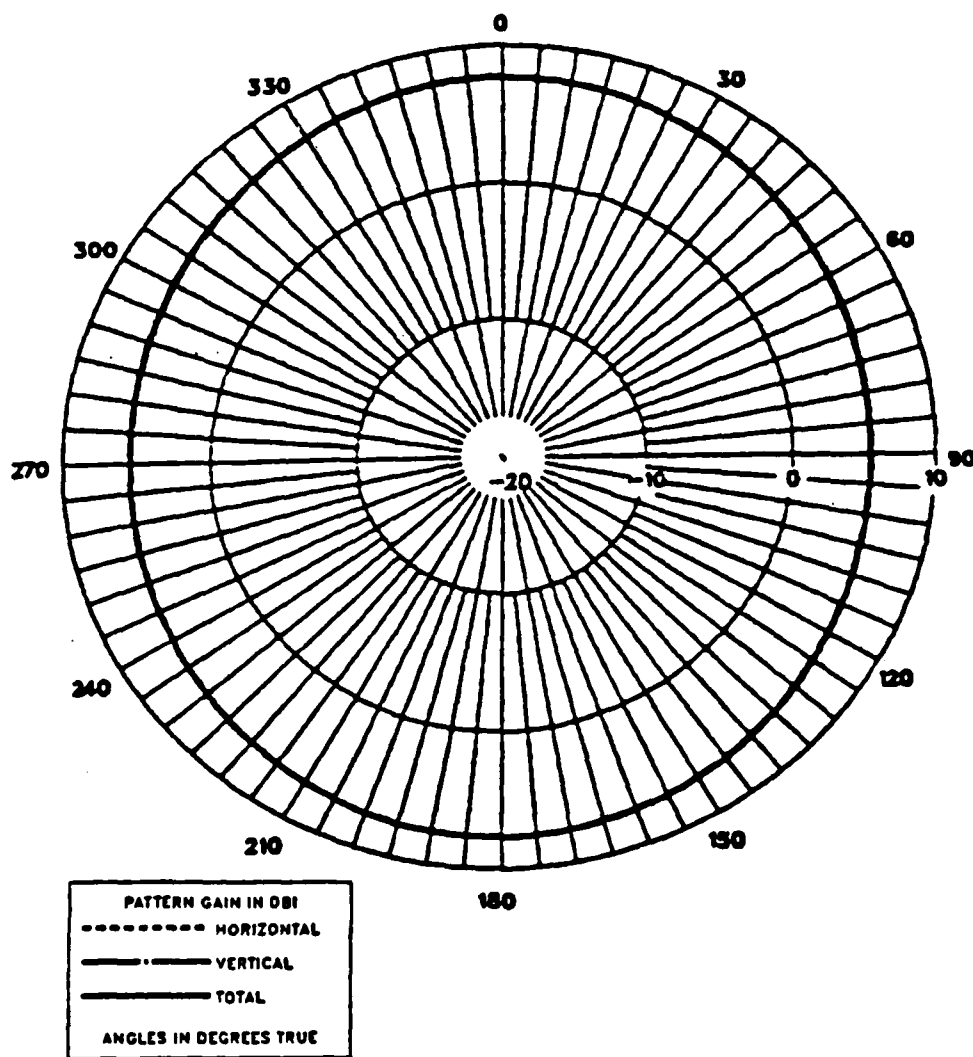
Figure 5.17. Typical Horizontal Pattern of W/H = 1 and W/H = 2 Antenna for Height Greater Than .5 Wavelengths

60

SMALL ANTENNA OVER GROUND

FREQ = 24 MHZ, PHI = 0 DEG.

PATTERN GAIN IN DBI
---------- HORIZONTAL
————·———— VERTICAL
———————— TOTAL
ANGLES IN DEGREES TRUE
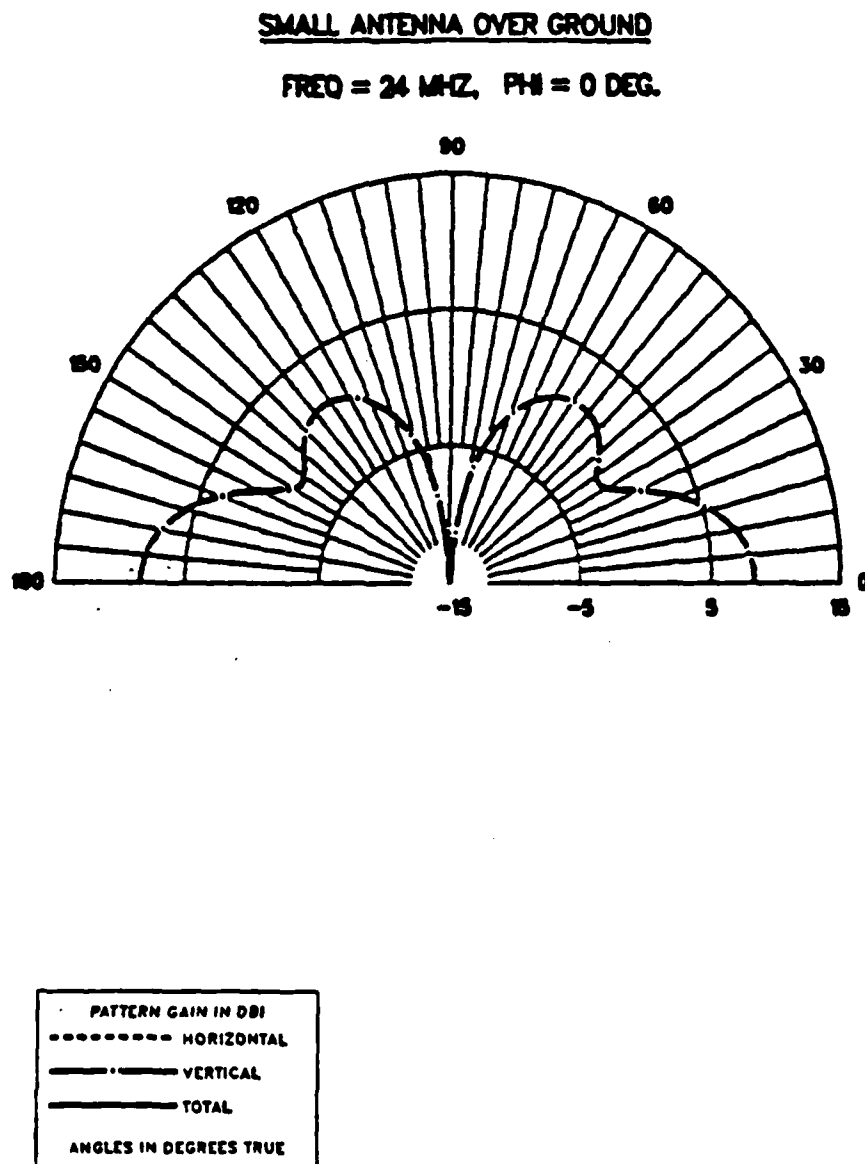
Figure 5.18.   Typical Vertical Pattern of W/H = 1 and
                W/H = 2 Antennas for Height Greater
                Than .5 Wavelengths

61

8 METER MONOPOLE

FREQ = 24 MHZ

PATTERN GAIN IN DBI
- - - - - - - - HORIZONTAL
———·——— VERTICAL
——————— TOTAL
ANGLES IN DEGREES TRUE
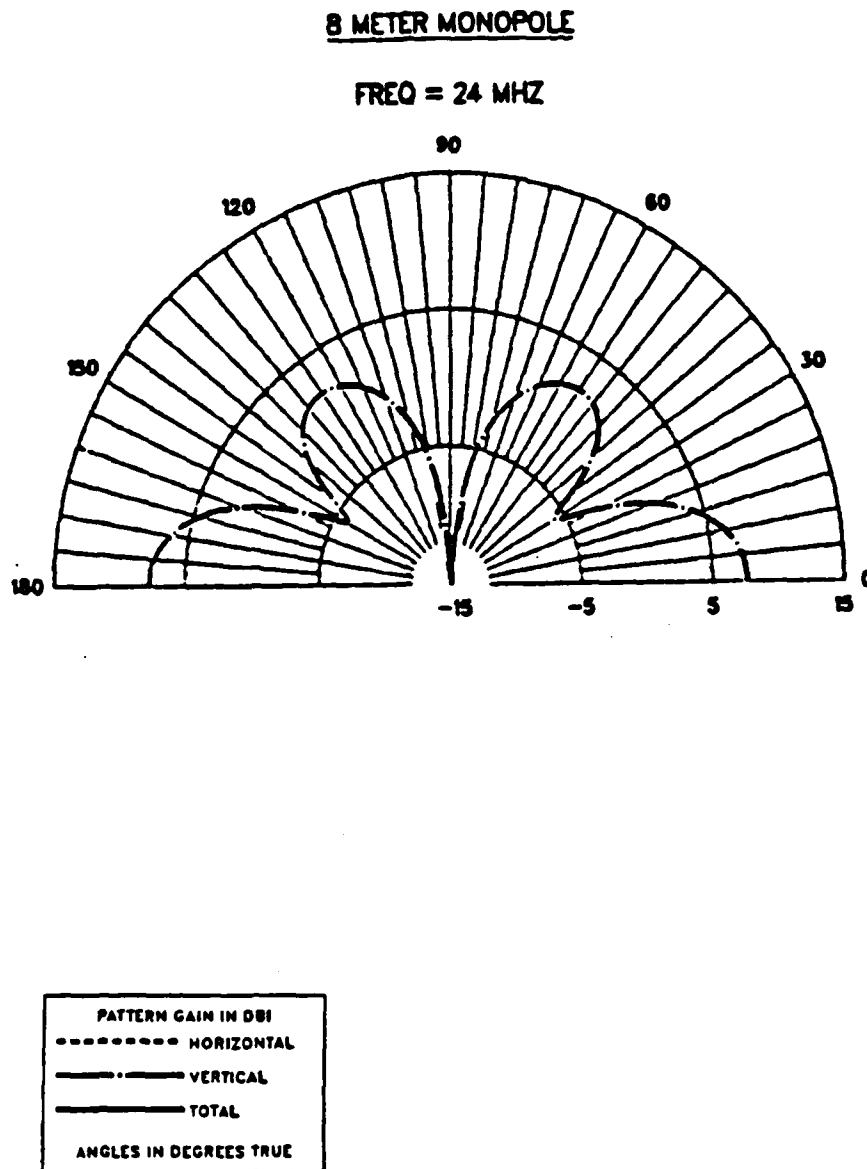
Figure 5.19. Vertical Pattern of Monopole with Electrical Height Equal to That of the Antenna of Figure 5.18

62

The W/H = 10 patch monopole has horizontal patterns
similar to those of the other two antennas but the ellipticity
is more prominent. Figure 5.20 is a typical horizontal pat-
tern. For electrical heights greater than .5 wavelengths,
the vertical patterns of the W/H = 10 antenna lose the
circular symmetry that the vertical patterns of an equal height
monopole possess, as seen in Figures 5.21 and 5.22. Note the
vertical pattern's shape is dependent on the azimuth angle
of the antenna. This is expected as the breadth of the patch
monopole face causes the antenna to appear like a very broad
monopole from the face aspect while it looks like a thin
monopole from the side aspect. Figure 5.23 is the vertical
pattern of a monopole whose electrical height is equal to the
antenna whose patterns are shown in Figures 5.21 and 5.22.

The following is a summarization of the patch monopole .
computer model results: There are many modeling parameters
which affect the impedance of the computer model. Among these
parameters are grid size, type of voltage source, feed line
segmentation and the radius of the wire segments. The small
antenna model's impedance is less dependent on these parameters
than is the large antenna model's impedance. The impedances
of the various large antenna models tend to converge in value
as the grid size is reduced. Sparse models are adequate in
terms of impedance for electrically short antennas and repre-
sent a savings in computer storage and time requirements.
The horizontal patterns of the patch monopoles become elliptical

LARGE ANTENNA OVER GROUND

FREQ = 18 MHZ, THETA = 60 DEG, PHI = 1 – 360 DEGS.

PATTERN GAIN IN DBI
----------- HORIZONTAL
———·——— VERTICAL
——————— TOTAL
ANGLES IN DEGREES TRUE
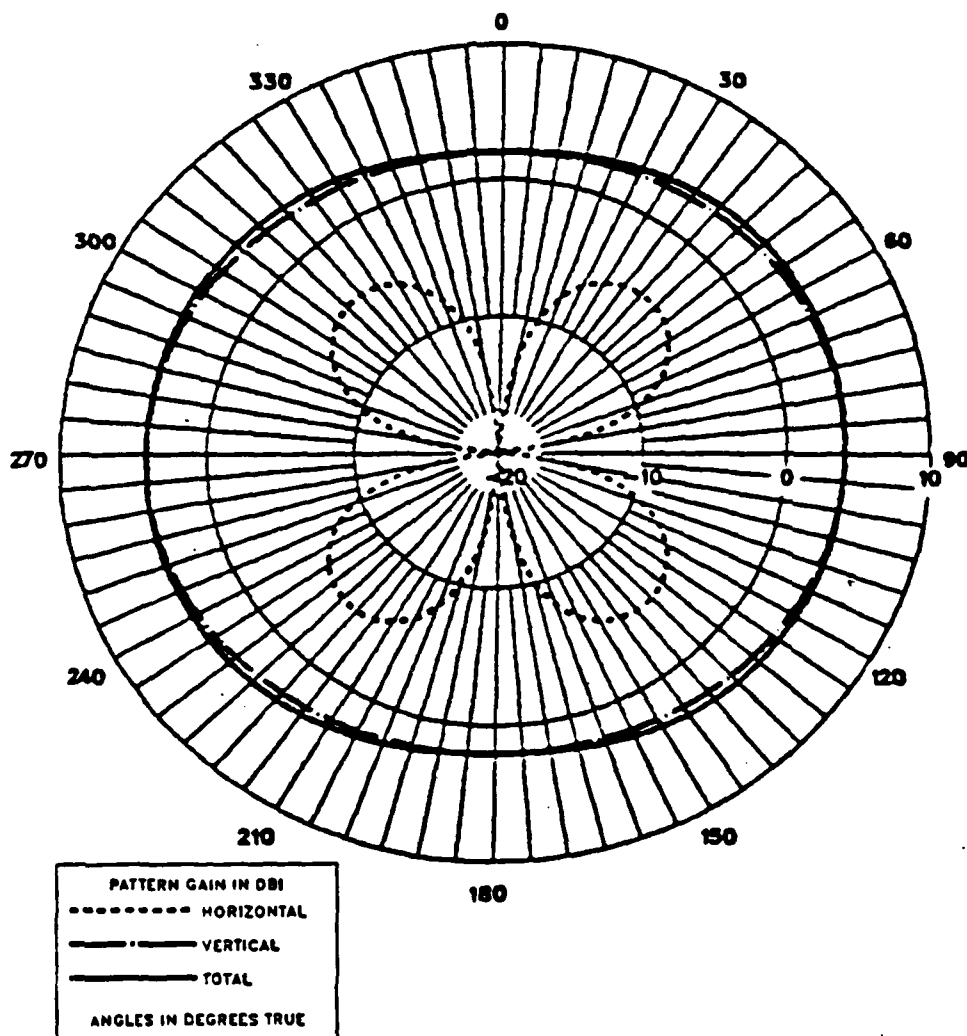
Figure 5.20. Typical Horizontal Pattern of the
W/H = 10 Antenna

64

LARGE ANTENNA OVER GROUND

FREQ = 18 MHZ, PHI = 0 DEG.
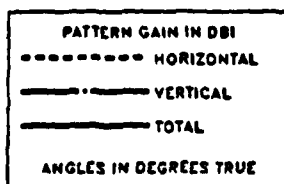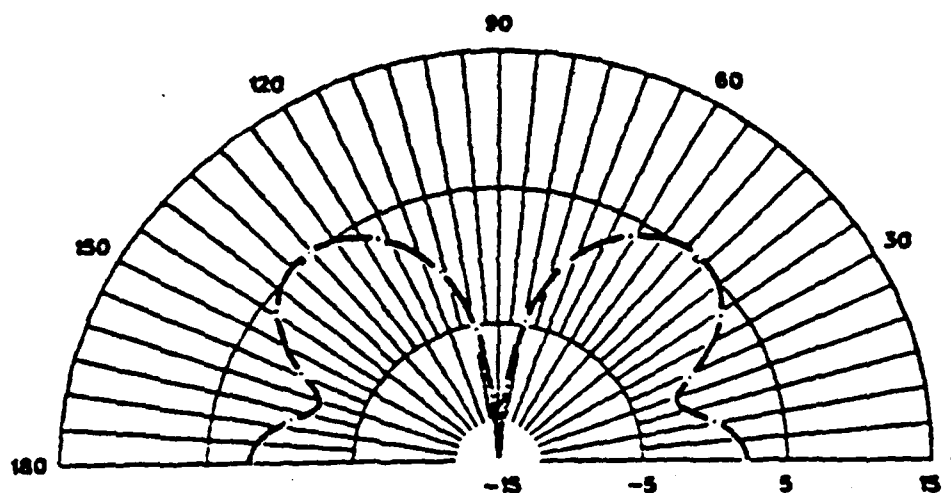
Figure 5.21. Typical Vertical Pattern of the W/H = 10
Antenna for Heights Greater than .5
Wavelengths (Face on View)

65

LARGE ANTENNA OVER GROUND

FREQ = 18 MHZ, PHI = 90 DEG.
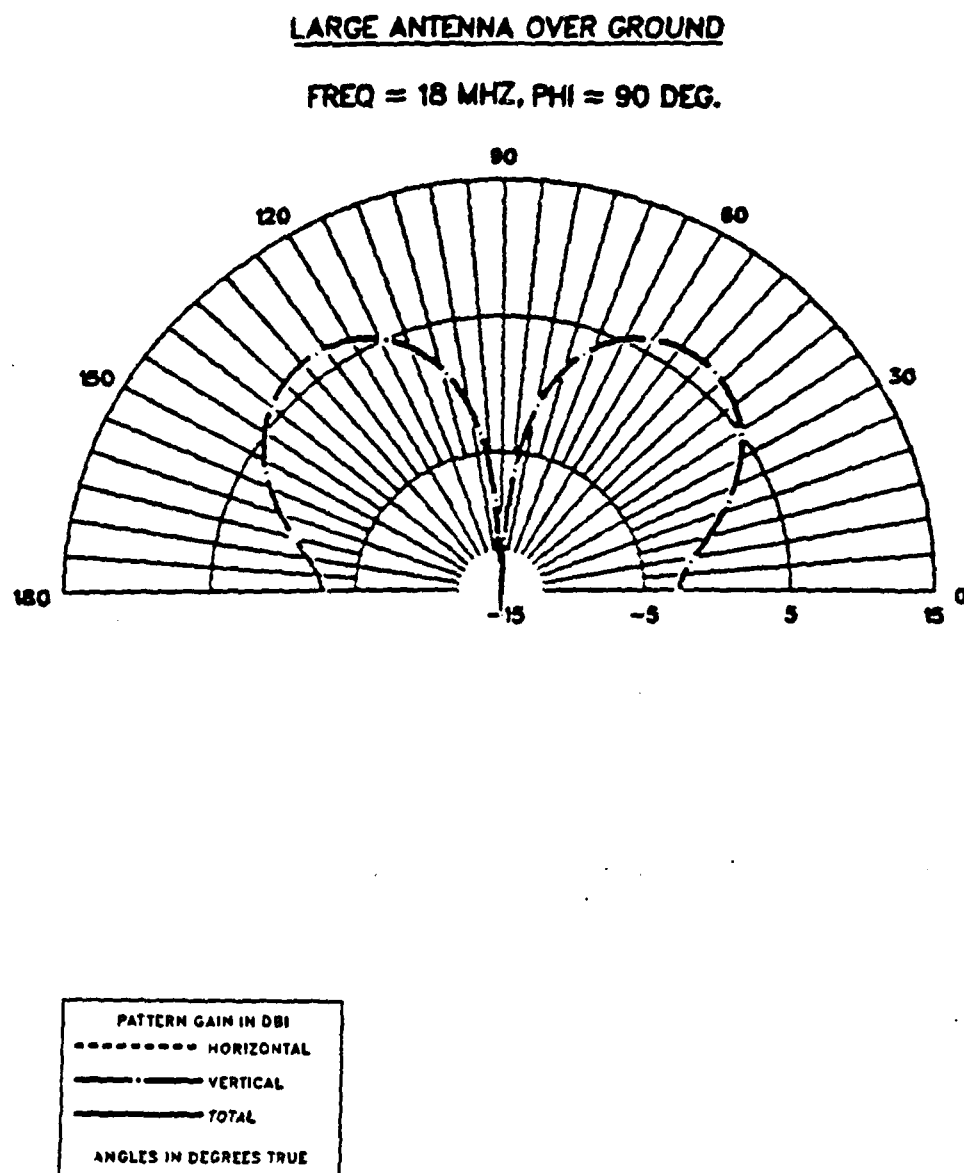
Figure 5.22.   Typical Vertical Pattern of the W/H = 10
              Antenna for Heights Greater Than .5
              Wavelengths (Side Aspect)

66

11 METER MONOPOLE

FREQ = 18 MHZ
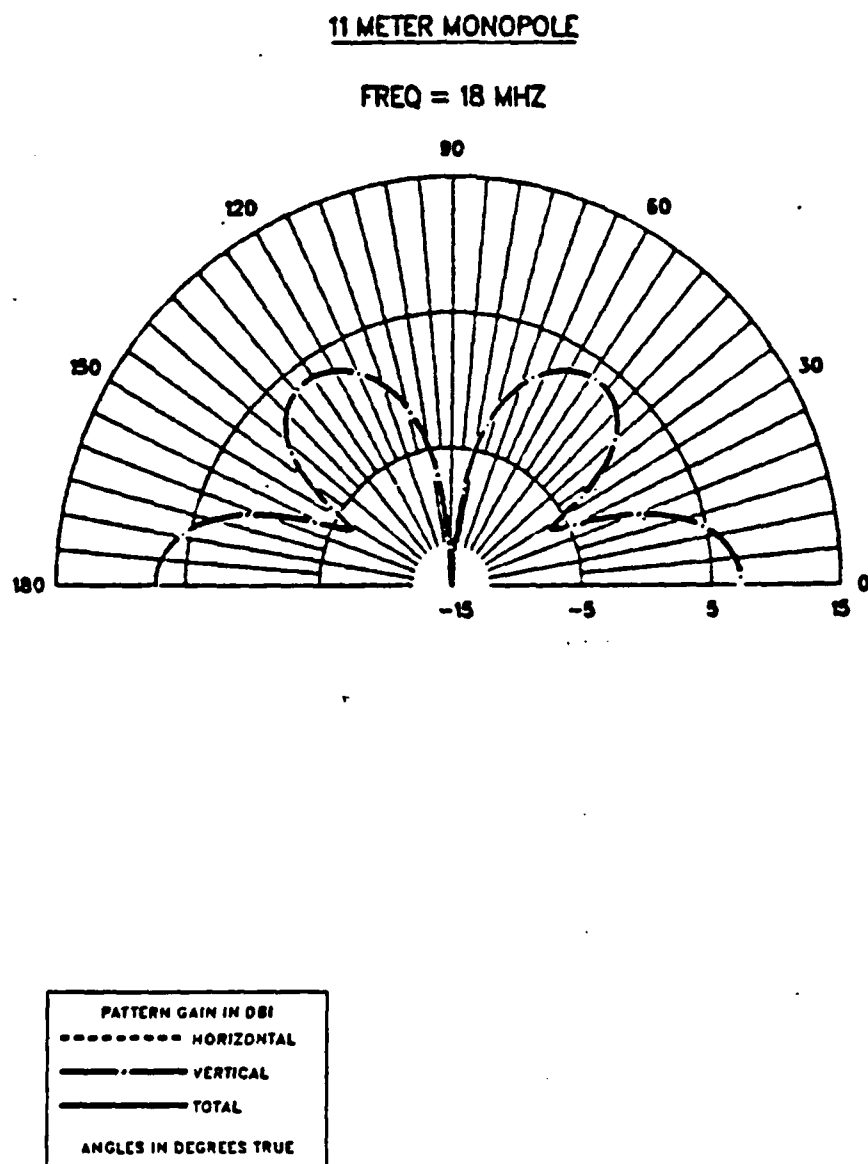
Figure 5.23. Vertical Pattern of Monopole Whose Electrical Height Is Equal to That of the Antenna of Figures 5.21 and 5.22

67

for antenna heights greater than .5 wavelengths. The vertical patterns display less severe lobing than the patterns of an equal height monopole. However the circular symmetry characteristic of a monopole's vertical pattern is also lost as the patch monopole's vertical pattern becomes more directional.

C. PATCH MONOPOLE AT BOX FACE COMPUTER MODELS

Computer models of each of the patch monopoles at the open face of a metal box were run on the computer using NEC. The frequency range was 2-24 MHZ. This frequency range corresponded to the box electrical height range of .08 wavelengths to .96 wavelengths. The patch monopole models were the W/H = 1, W/H = 2, and W/H = 10 wire grid models with one meter grid spacing driven by the E-gap voltage source. These models and the box models were described in Chapter III.

Figures 5.24 and 5.25 are plots of the resistance and reactances versus box height of each of the three patch monopoles at the open face of the wire grid box model (henceforth referred to as the survivable antenna). From these plots it is apparent that the W/H = 10 survivable antenna (the largest patch monopole at the box face) produces lower resistances and reactances than the other two antennas. The first resonances of all three antennas are close together, around .18 wavelengths. Also, the reactance of the W/H = 10 survivable antenna drops away from that of the other two at a box height of about .25 wavelengths.

A 3:1 SWR is considered a reasonable criterion for broadband antenna operation [Ref. 10]. Not too many antennas

68

PATCH MONOPOLE AT BOX FACE
RESISTANCE
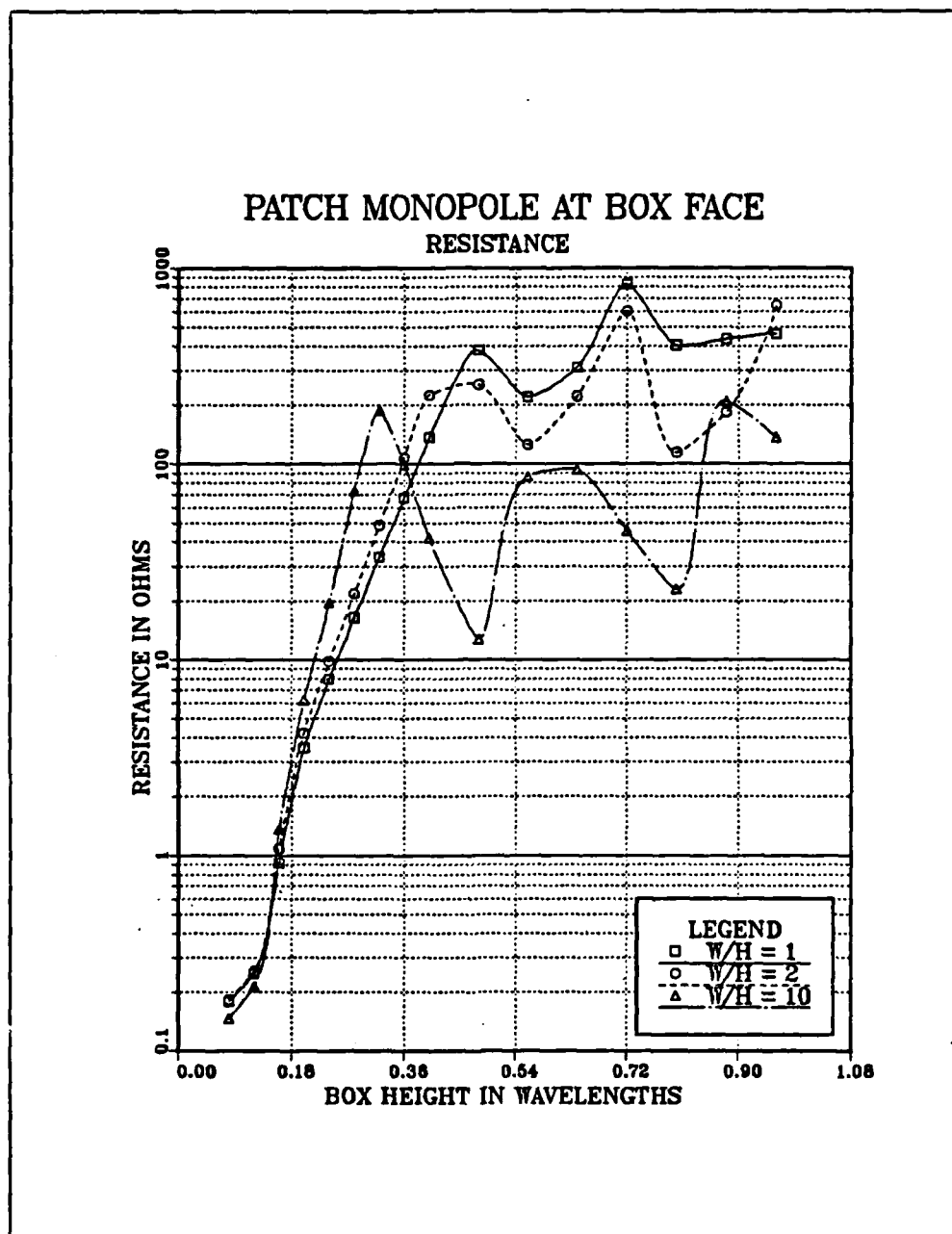
Figure 5.24.   Resistance Versus Box Height of Survivable
Antenna Models

69

PATCH MONOPOLE AT BOX FACE
REACTANCE
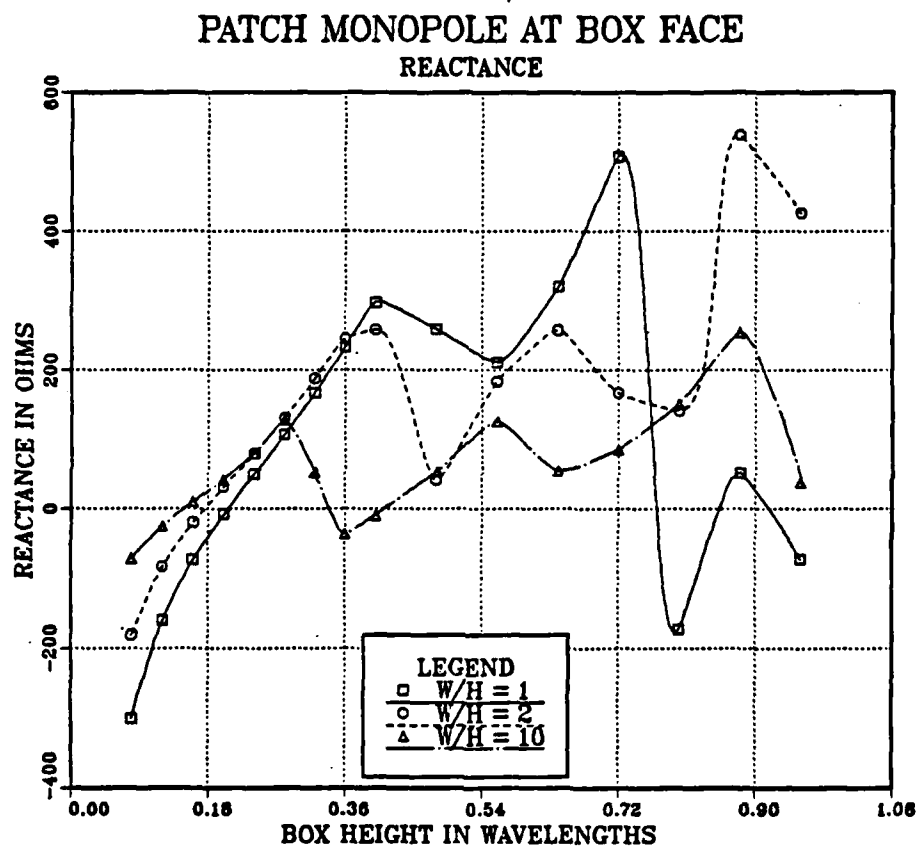
Figure 5.25.   Reactance Versus Box Height of Survivable
Antenna Models

70

satisfy this criterion over an operating band of interest but many may be brought into this region by use of series inductance or capacitance. Figure 5.26 shows the 3:1 SWR circle. The shaded region represents the impedance region of the Smith chart which may be moved into the 3:1 SWR circle by use of series reactances. This thesis will consider impedances that fall in this region and the 3:1 SWR circle as acceptable impedances for operational requirements.

Figures 5.27 through 5.29 are Smith Chart plots of the impedance characteristics for the W/H = 1, W/H = 2, and W/H = 10 survivable antennas. Table 5.5 presents the frequency ranges which fall in the 3:1 SWR circle or are matchable by series reactance to the 3:1 SWR circle for the three antennas.

TABLE 5.5

FREQUENCIES SATISFYING 3:1 SWR CRITERIA

	W/H = 1	W/H = 2	W/H = 10
Frequency Range in MHZ	7-10	7-9, 14, 20	6-7.5, 8.5-22, 24

This table reveals that the W/H = 10 survivable antenna design has the superior bandwidth of the three. Based on the frequency ranges over which the antenna's impedance is series matchable to a 3:1 SWR, this antenna has an acceptable frequency range from 6-7.5 MHZ and 8.5-22 MHZ. Also the antenna has an SWR which lies within the 3:1 circle without need of

71
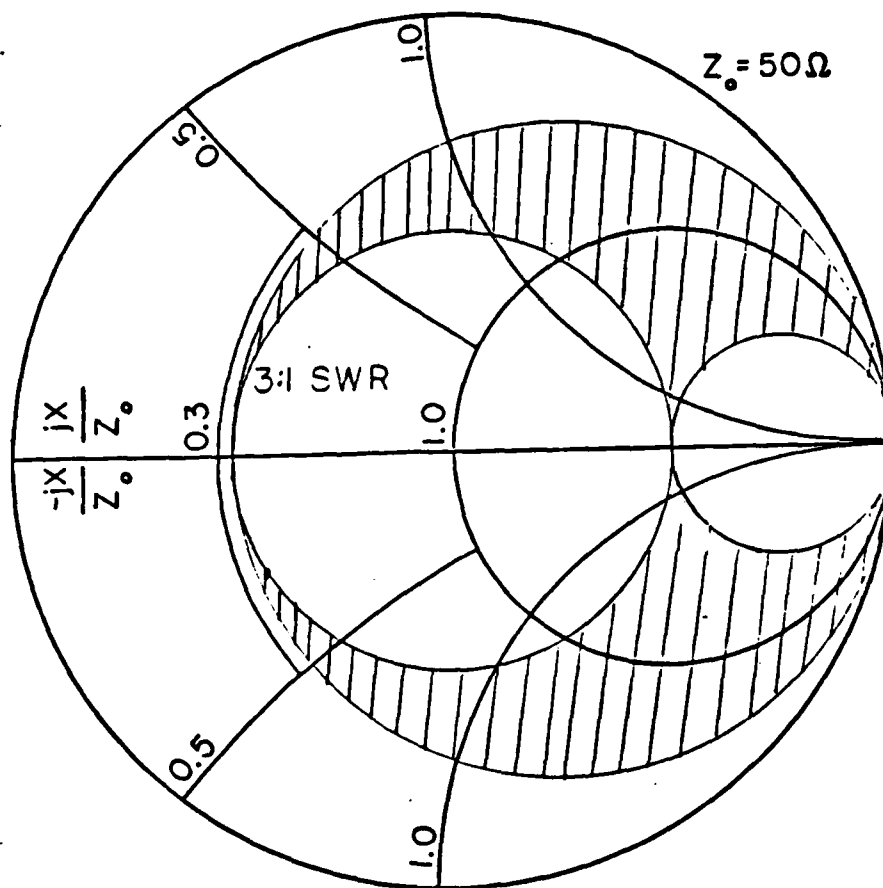
Figure 5.26.   Smith Chart Showing 3:1 SWR Matchable Region

72
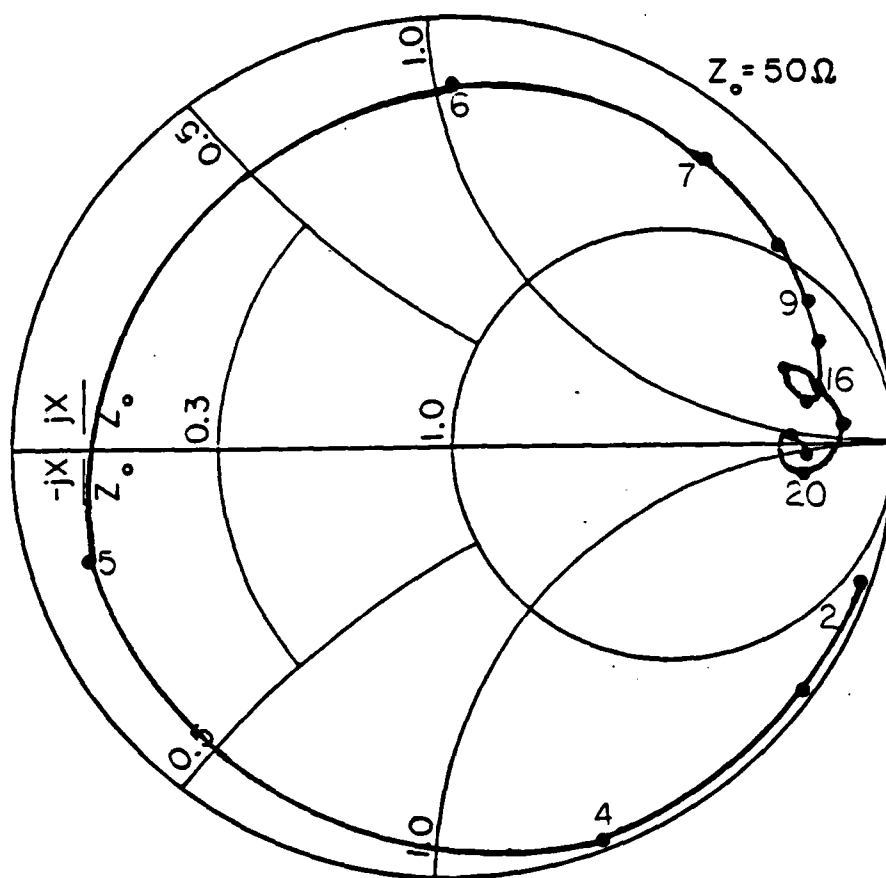
Figure 5.27. Impedance Plot of W/H = 1 Survivable Anténna

Figure 5.28.   Impedance Plot of W/H = 2 Survivable Antenna

74

Figure 5.29.   Impedance Plot of W/H = 10 Survivable Antenna

75

a matching network over the frequency range of 8.5-11 MHZ.

Radiation patterns were obtained for the three survivable antenna designs. For box heights of up to .4 wavelengths the patterns of the three antennas tended to be similar (though not identical) indicating the box was the dominant factor in the patterns at these frequencies. At very low frequencies, where the box height was less than a tenth of a wavelength, the patterns closely resemble those of an electrically short monopole. As frequency increases the box height becomes near .25 wavelength and the patterns become cardioidal in the direction of the box face. Figures 5.30-5.32 are typical of these patterns. Notice the heart-shaped patterns with the greatest gain in the direction of the box face.

As the box height nears half a wavelength, the horizontal patterns become less directional and the vertical patterns differ greatly from those of an equal-sized monopole. Figures 5.33-5.35 illustrate these properties. From these figures it is observed that the horizontal pattern no longer presents a cardioidal shape. The vertical patterns have lost the null at the 90 degree elevation angle which is characteristic of a vertical monopole pattern. The patterns are also less lobey than the vertical patterns of an equal-sized monopole. Also the patch monopole has better gain at higher elevation angles than does a monopole of equal height. Figure 5.36 is the vertical pattern of a monopole whose electrical height is

76

LARGE ANTENNA AT BOX FACE

FREQ = 6 MHZ, THETA = 60 DEG, PHI = 1 – 360 DEGS.
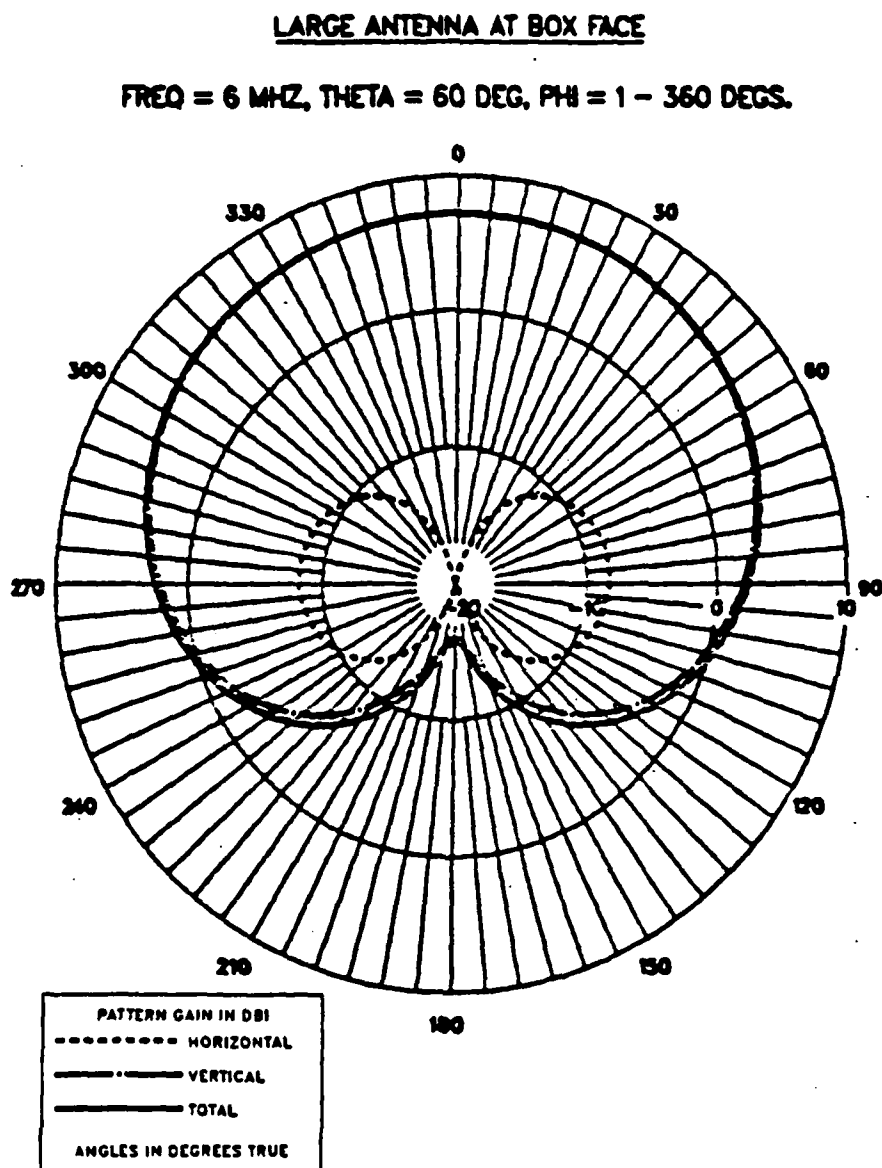
Figure 5.30.   Typical Horizontal Pattern for Box Height
              Near .25 Wavelength

LARGE ANTENNA AT BOX FACE

FREQ = 6 MHZ. PHI = O DEG.
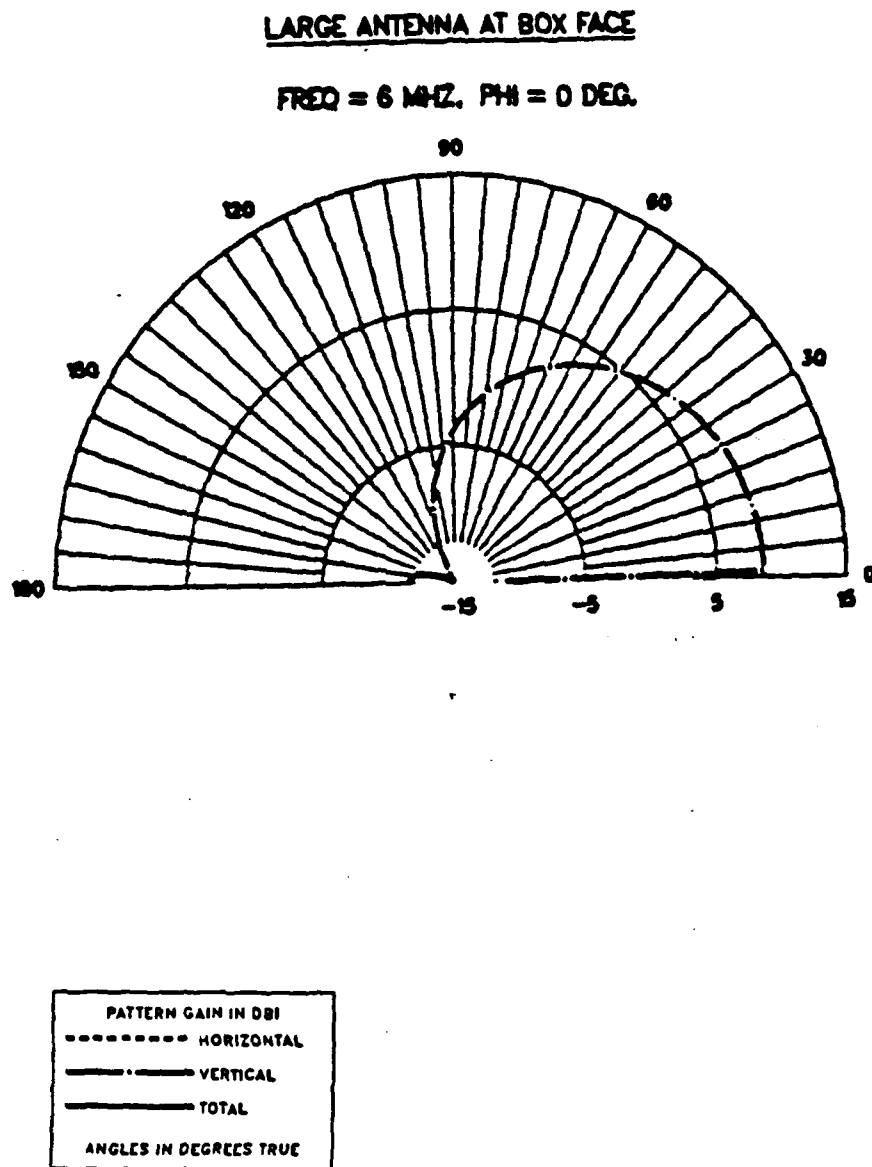
Figure 5.31. Typical Vertical Pattern for Box Height
Near .25 Wavelength (Face Aspect)

LARGE ANTENNA AT BOX FACE

FREQ = 6 MHZ, PHI = 90 DEG.

PATTERN GAIN IN DBI
•••••••••• HORIZONTAL
————— VERTICAL
————— TOTAL
ANGLES IN DEGREES TRUE
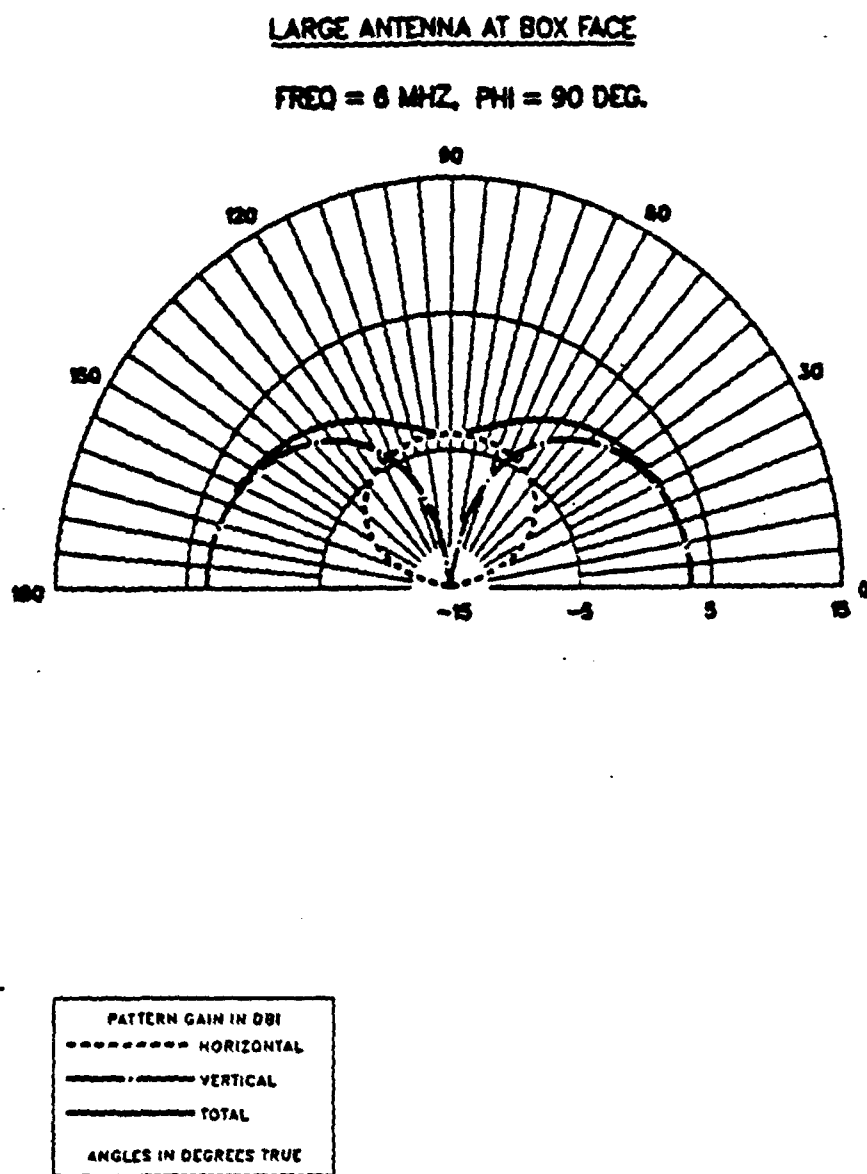
Figure 5.32.   Typical Vertical Pattern for Box Height
              Near .25 Wavelength (Side Aspect)

79

LARGE ANTENNA AT BOX FACE

FREQ = 14 MHZ, THETA = 60 DEG, PHI = 1 - 360 DEGS.
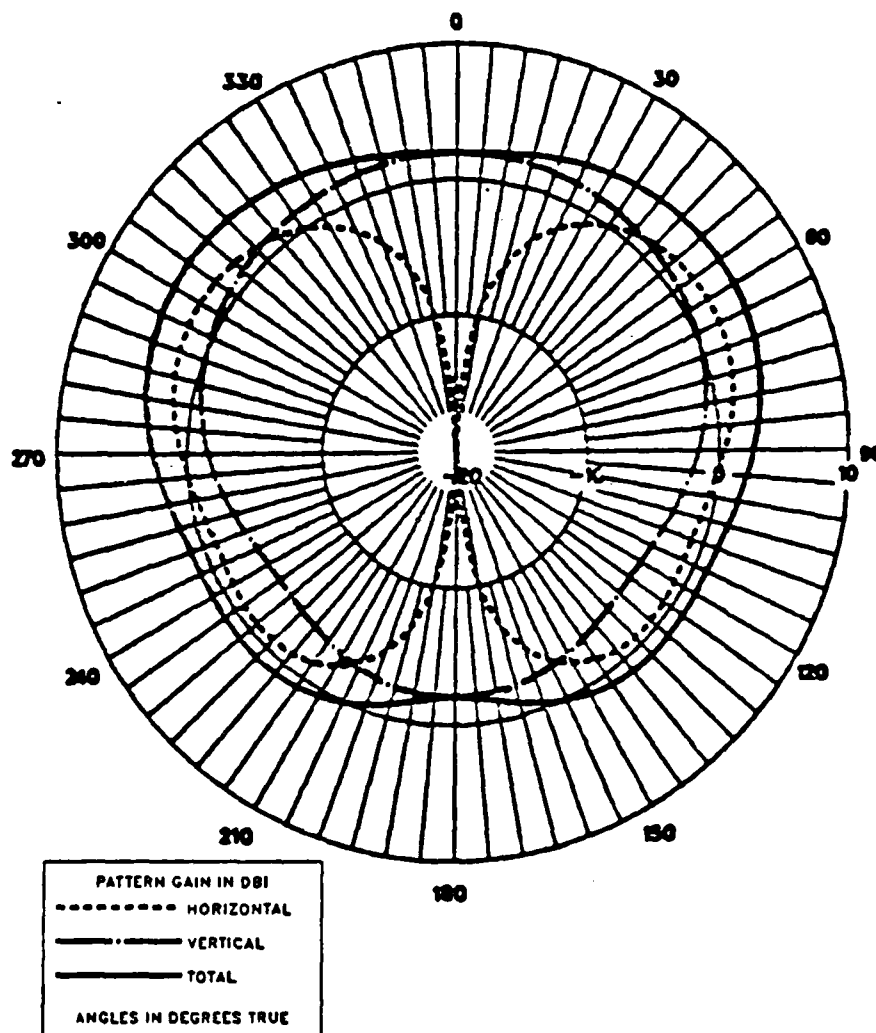
Figure 5.33.   Typical Horizontal Pattern for Box Height
Near .5 Wavelength

80

LARGE ANTENNA AT BOX FACE

FREQ = 14 MHZ, PHI = 0 DEG.

PATTERN GAIN IN DBI
- - - - - - - - HORIZONTAL
——— · ——— VERTICAL
————— TOTAL
ANGLES IN DEGREES TRUE
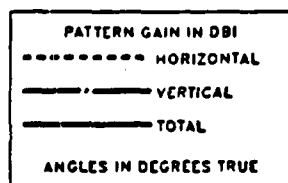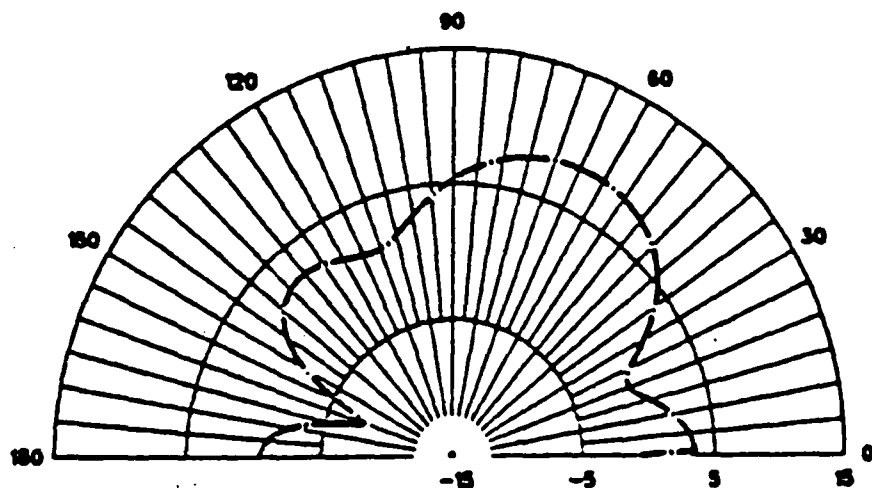
Figure 5.34.   Typical Vertical Pattern for Box Height
Near .5 Wavelength (Face Aspect)

LARGE ANTENNA AT BOX FACE

FREQ = 14 MHZ, PHI = 90 DEG.

PATTERN GAIN IN DBI
● ● ● ● ● ● ● HORIZONTAL
━ · ━ · ━ VERTICAL
━━━━━ TOTAL
ANGLES IN DEGREES TRUE
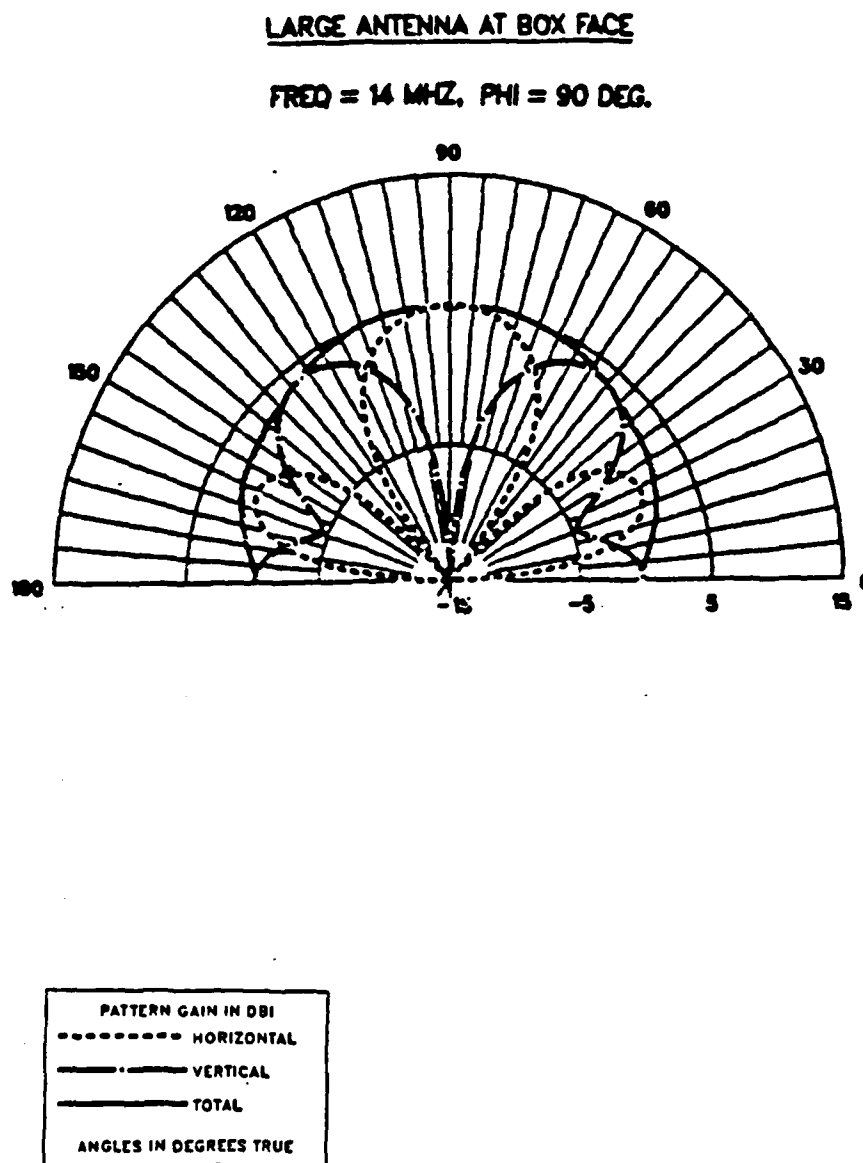
Figure 5.35.   Typical Vertical Pattern for Box Height
Near .5 Wavelength (Side Aspect)

12 METER MONOPOLE

FREQ = 14 MHZ
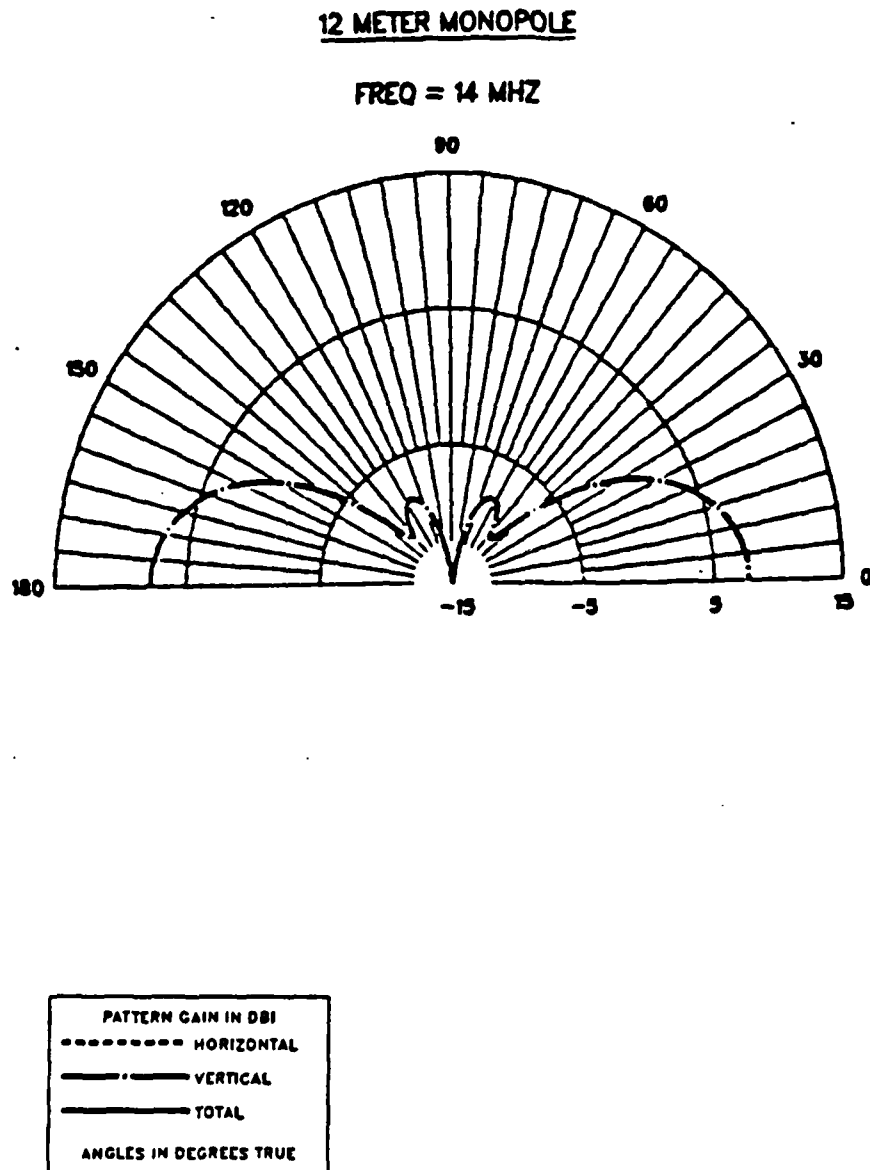
Figure 5.36.   Vertical Pattern of a .56 Wavelength
Tall Monopole

83

equal to the antenna whose patterns are shown in Figures 5.33-5.35.

As the frequency is increased and the box nears .8 wavelengths in height the vertical patterns become more lobey and the horizontal patterns become more directional. Figures 5.37 and 5.38 are vertical patterns of the $W/H \doteq 10$ antenna which show the lobey radiation pattern of the antenna for a box height of .8 wavelengths. Figures 5.39 and 5.40 are horizontal radiation patterns for the same antenna and frequency which display the directional properties of the pattern.

LARGE ANTENNA AT BOX FACE

FREQ = 20 MHZ, PHI = 0 DEG.

PATTERN GAIN IN DBI
- - - - - - - - HORIZONTAL
————·———— VERTICAL
———————— TOTAL
ANGLES IN DEGREES TRUE
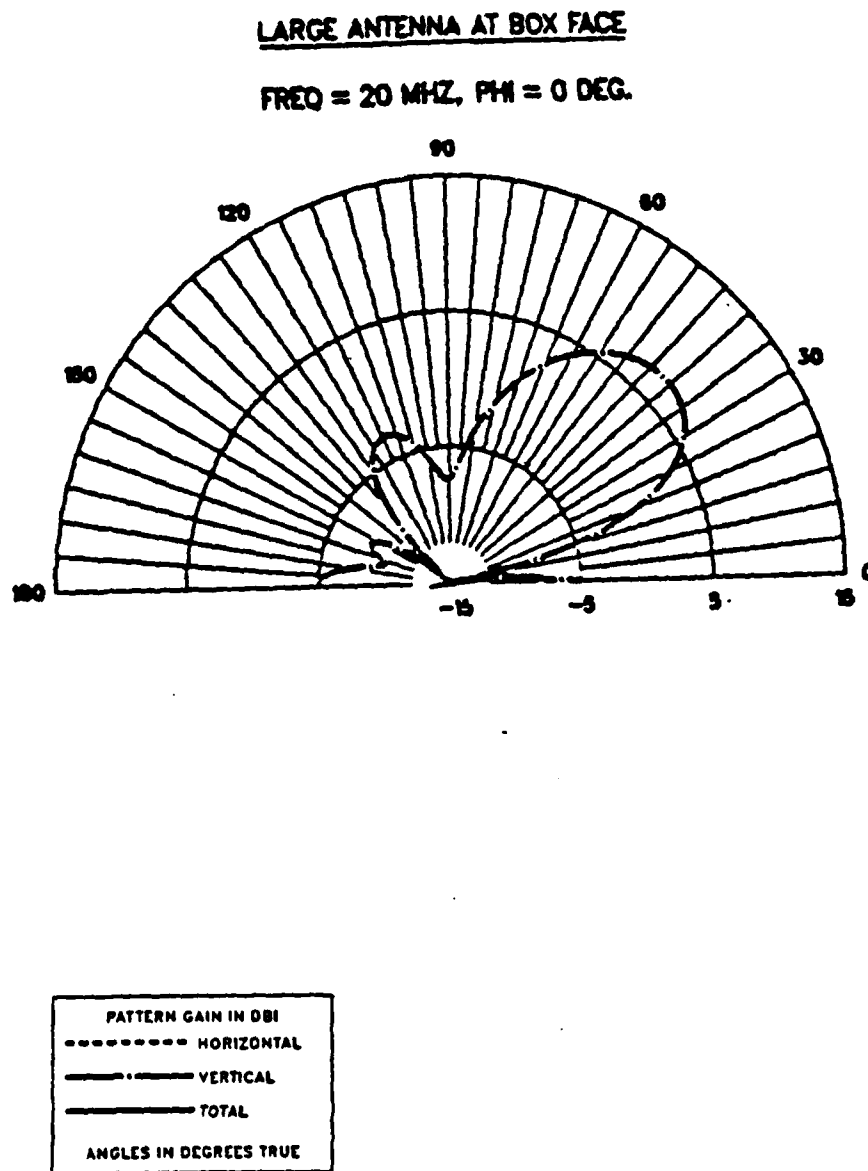
Figure 5.37.   Vertical Pattern of W/H = 10 Survivable
Antenna at a Box Height of .8 Wavelength
(Face Aspect)

85

LARGE ANTENNA AT BOX FACE

FREQ = 20 MHZ, PHI = 90 DEG.

PATTERN GAIN IN DBI
••••••••• HORIZONTAL
———·——— VERTICAL
———————— TOTAL
ANGLES IN DEGREES TRUE
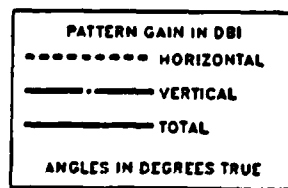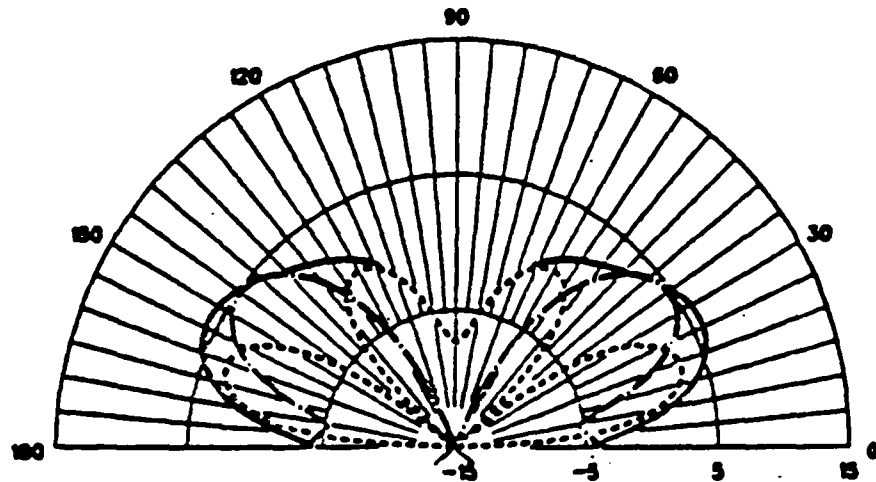
Figure 5.38.   Vertical Pattern of W/H = 10 Survivable
Antenna at a Box Height of .8 Wavelength
(Side Aspect)

LARGE ANTENNA AT BOX FACE

FREQ = 20 MHZ, THETA = 60 DEG, PHI = 1 – 360 DEGS.

PATTERN GAIN IN DBI

- - - - - - - HORIZONTAL

———·——— VERTICAL

———————— TOTAL

ANGLES IN DEGREES TRUE
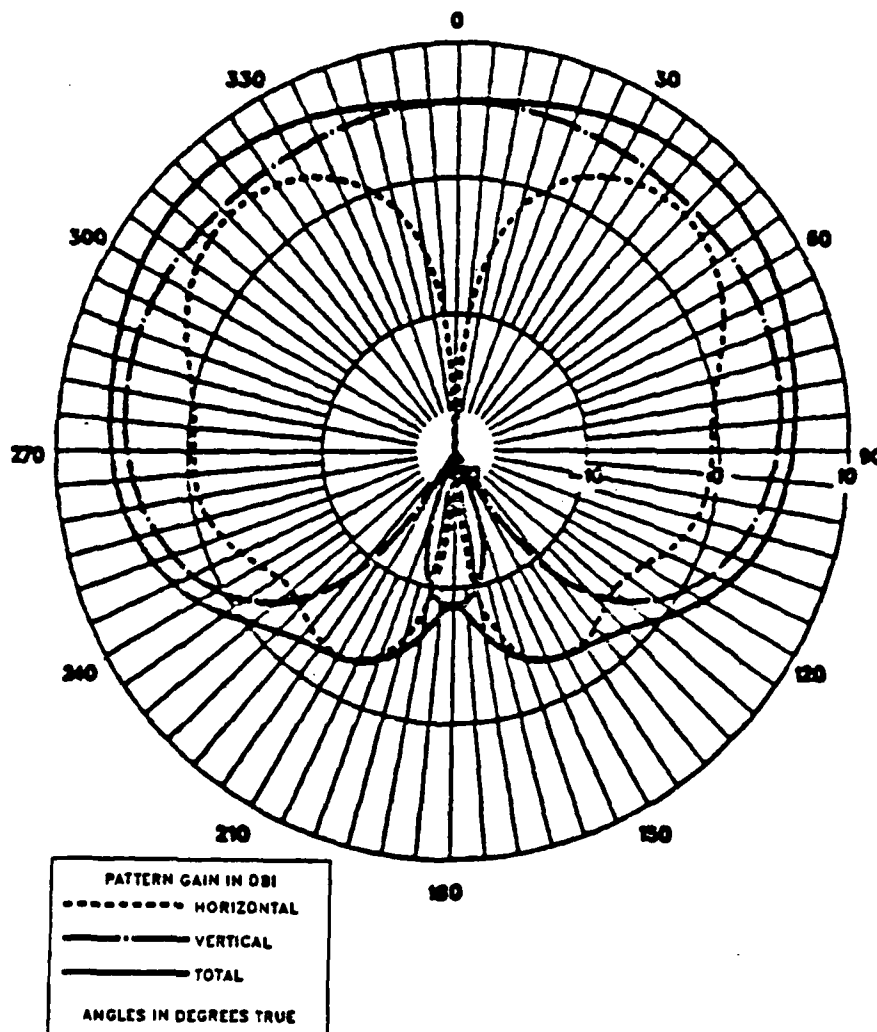
Figure 5.39. Horizontal Pattern of W/H = 10 Survivable Antenna at a Box Height of .8 Wavelength (Elevation Angle of 30 Degrees)

LARGE ANTENNA AT BOX FACE

FREQ = 20 MHZ, THETA = 90 DEG, PHI = 1 – 360 DEGS.
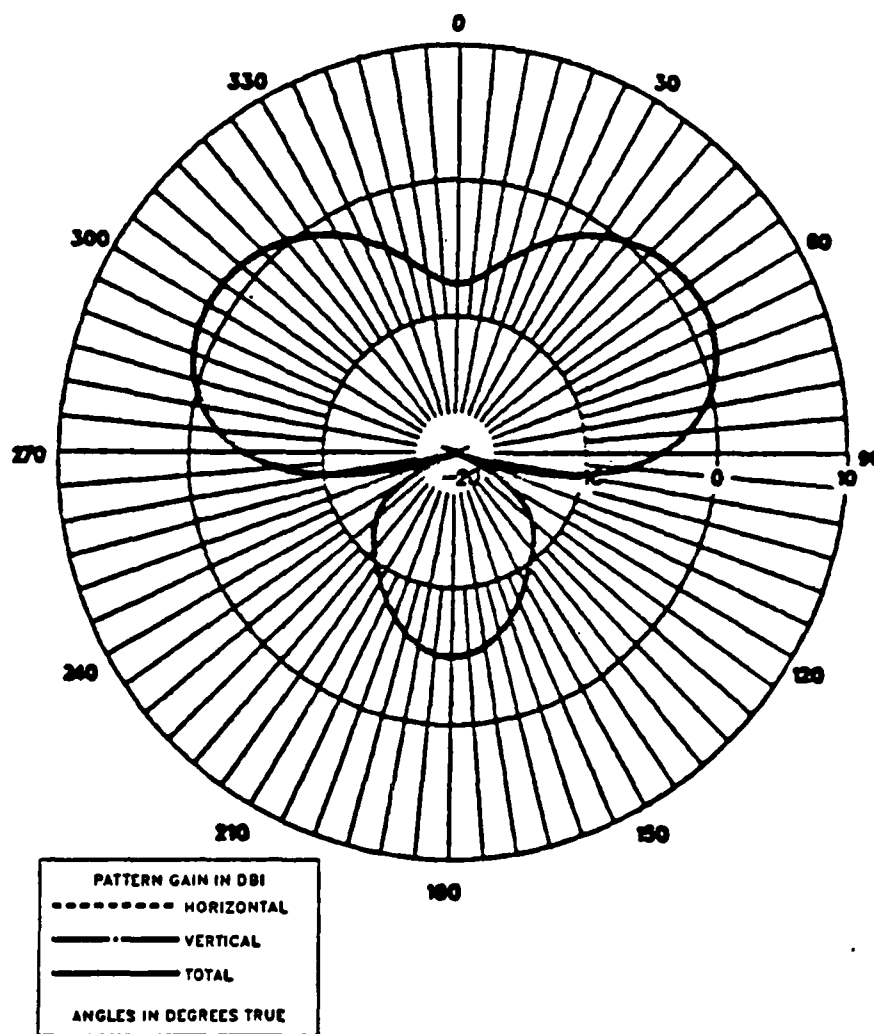
Figure 5.40. Horizontal Pattern of W/H = 10 Survivable
Antenna at a Box Height of .8 Wavelength
(Elevation Angle of 0 Degrees)

88

VI.   PHYSICAL MEASUREMENTS

Impedance measurements were made on the patch monopole scale models and the replica of a monopole whose impedance characteristics were tabulated by R.W.P. King.   These antennas were described in Chapter IV.   The measurements were taken with the antenna on an 11x11 meter ground plane.   The procedure described in Hewlett Packard Application Note 77-3 [Ref. 11] was followed.   This required a directional coupler, vector voltmeter, and a frequency sweep oscillator.   Appendix A contains a block diagram of the experimental set up.

To ensure the test equipment was operating properly the impedance of a known 200 ohm load was measured.   The measured values produced a 4:1 SWR circle on a Smith Chart indicating proper test equipment operation over the frequency range in question, 90-1080 MHZ.

It was necessary to determine the effect of the feed transition and finite ground plane on the impedance measurements.   Impedance measurements were done on a monopole whose theoretical impedance characteristics were known.   Figure 6.1 is the plot of the measured impedances.   There is a definite digression from the expected clockwise spiral on the Smith Chart which characterizes monopole impedance plots.   The data points in the frequency range 337.5-562.5 MHZ appear to be erroneous.

89
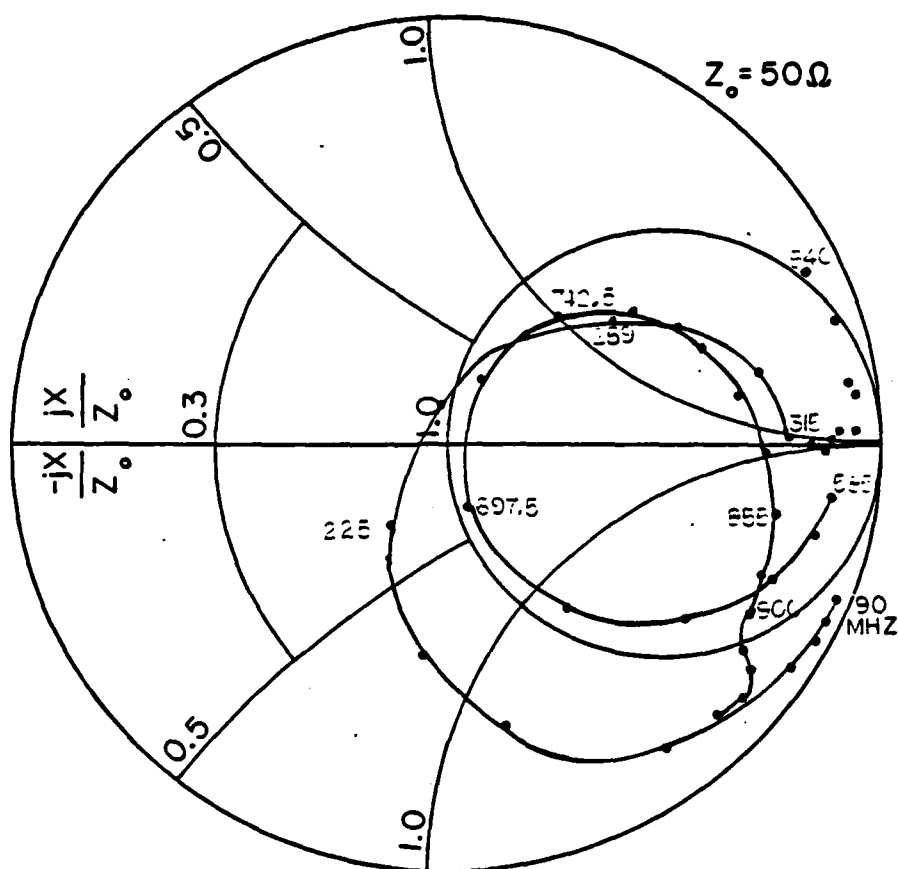
Figure 6.1. Plot of Measured Monopole Impedances

90

Figures 6.2 and 6.3 are plots of the resistance and
reactance of the physical monopole and the theoretical mono-
pole, referred to as King's monopole. These plots show dis-
agreement between the theoretical and measured impedance values.
The frequency ranges of disagreement are 427.5-675 MHZ for
resistance and 315-630 MHZ for reactance. The impedance values
are also questionable at frequencies greater than 900 MHZ and
less than 112.5 MHZ. Note that the physical measurements
correlate well with the theoretical data in the frequency
ranges 112.5-315 MHZ and 630-900 MHZ.

Having determined the frequency ranges where measured
data are likely to be accurate and inaccurate, the physical
scale patch monopole models impedance characteristics were
measured.

The impedance plots of the W/H = 1 solid and grid scale
models are presented in Figures 6.4 and 6.5 respectively.
Figure 6.6 is the W/H = 2 grid scale model measured impedance
characteristics. Figures 6.7 and 6.8 are the W/H = 10 solid
and grid scale impedance measurements respectively.

The impedance plots of the W/H = 1 and W/H = 2 patch
monopole models show erratic impedance values in the frequency
range 337.5-675 MHZ. This was the same frequency range for
which the monopole measurement resulted in questionable data
and as such was not unexpected.

The W/H = 10 scale solid and grid model measurements do
not have the regions of erratic data points the previous models

91
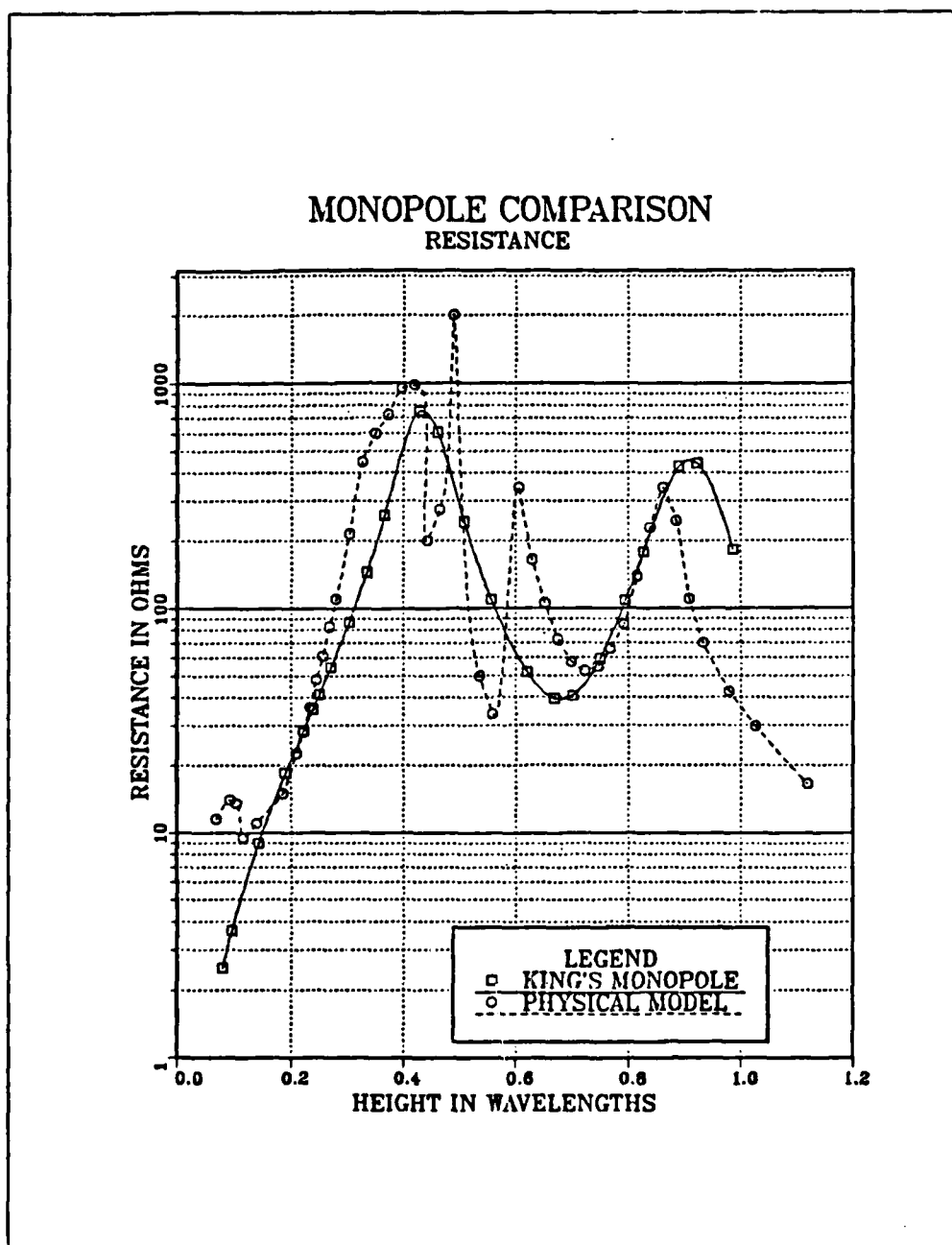
Figure 6.2.   Monopole Comparison of Theoretical
             and Measured Resistances

MONOPOLE COMPARISON
REACTANCE
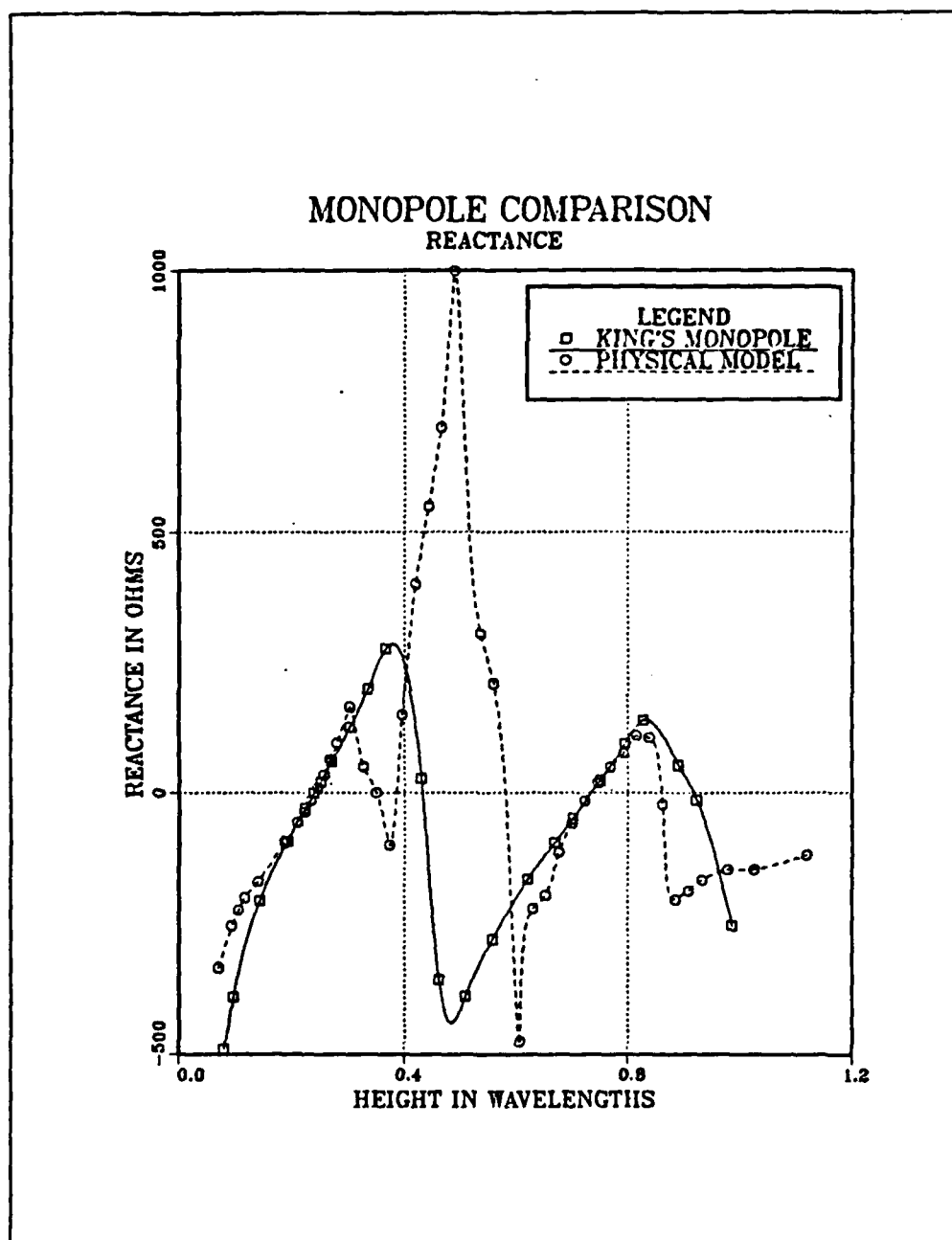
Figure 6.3.   Monopole Comparison of Theoretical and
              Measured Reactances

93

Figure 6.4. W/H = 1 Solid Scale Model Impedance
Characteristics

MICROCOPY RESOLUTION TEST CHART
NATIONAL BUREAU OF STANDARDS 1963 A
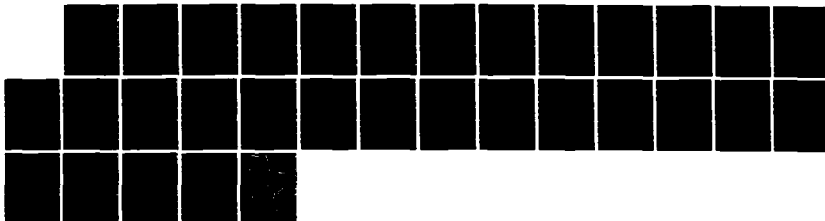
Figure 6.5.   W/H = 1 Grid Scale Model Impedance
              Characteristics

95
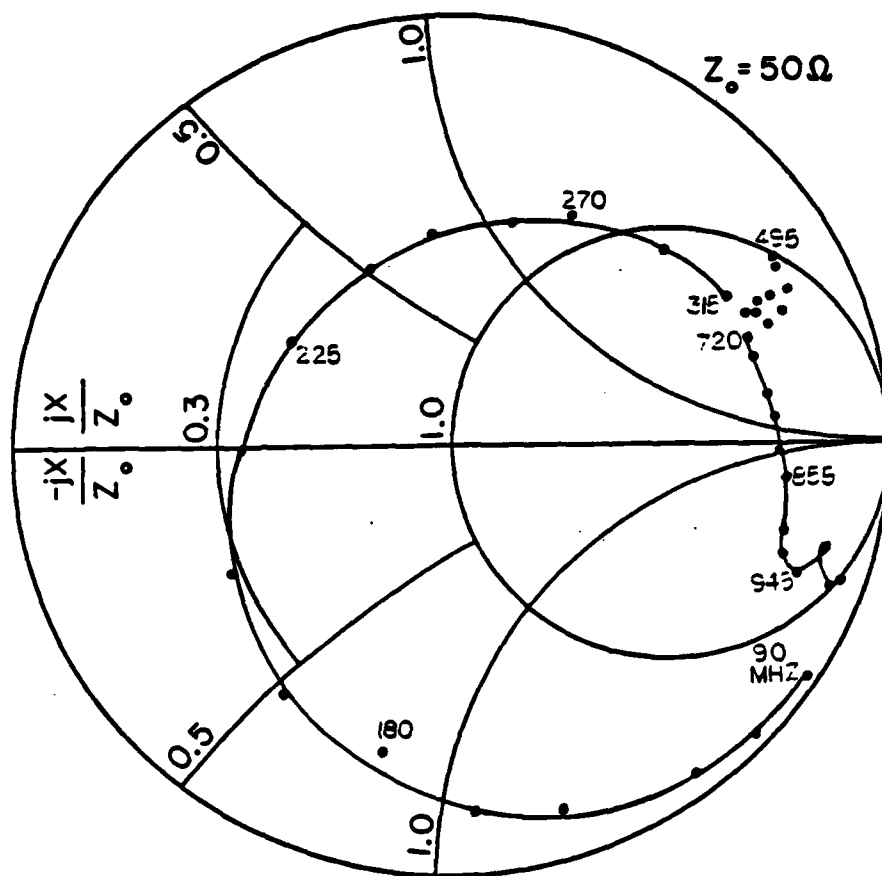
Figure 6.6. W/H = 2 Grid Scale Model Impedance
Characteristics

Figure 6.7.   W/H = 10 Solid Scale Model Impedance
              Characteristics

97

Figure 6.8.   W/H = 10 Grid Scale Model Impedance
             Characteristics

98

experienced. The reason is not certain, but one possible explanation is the model's larger size. Broad monopoles are affected less in impedance by finite ground planes than are slendor monopoles.

The Smith Chart impedance plots of the W/H = 1 and W/H = 10 models show that the wire grid models and solid plate models have similar impedance characteristics. Thus the use of a wire grid structure to model or approximate a solid structure is valid.

VII. <u>PHYSICAL MODEL AND COMPUTER MODEL COMPARISONS</u>

This chapter provides a comparison between the computer generated and measured impedances of the various patch monopole models. These comparisons may be used to determine how well the computer models of the survivable antenna, used in Chapter V, predict the physical performance of the antenna.

Tables 7.1 and 7.2 present the percent change in resistance and reactance values of a representative number of the computer models of Chapter V with respect to the solid scale patch monopole models of the W/H = 1 and W/H = 10 antennas. The W/H = 1 antenna is compared at 2 and 6 MHZ while the W/H = 10 antenna is compared at 2, 6, and 10 MHZ. The W/H = 1 antenna models were not compared at 10 MHZ due to the erratic nature of the measured impedance at this frequency. Note 10 MHZ corresponded to 450 MHZ when scaled by 45 for the scale model measurement.

Several observations may be made from Table 7.1. The various W/H = 1 computer models yield similar values of resistance. At 2 MHZ the correlation between physical and computed impedances is poor. This was expected as the frequency range below 112.5 MHZ, or 2.5 MHZ for the computer models, was determined to be questionable in Chapter VI. At 6 MHZ the models with the current-slope-discontinuity source seem to yield more accurate resistances. Of the computer

100

TABLE 7.1

PERCENT CHANGE BETWEEN MEASURED AND COMPUTED IMPEDANCES OF THE W/H = 1 ANTENNA

4x4

	2 MHZ		6 MHZ	
	Δ%R	Δ%Xj	Δ%R	Δ%Xj
Grid Sep = .5 m Equal Feed Seg E Gap Source	78.7	46.2	36.1	12.4
Grid Sep = 1 m Equal Feed Seg E Gap Source	78.0	55.0	37.3	20.8
Grid Sep ≈ .5 m 3 Seg Feed E Gap Source	77.5	43.4	38.3	1.2
Grid Sep = 1 m 3 Seg Feed E Gap Source	77.5	53.9	38.0	15.3
Grid Sep = .5 m 3 Seg Feed C/S Source	77.6	52.0	26.9	16.0
Grid Sep = 1 m 3 Seg Feed C/S Source	77.8	62.3	27.1	3.6
SPMVC	77.6	60.1	38.5	28.9
SPMV	78.0	72.8	39.4	53.9
SPMNV	77.7	82.0	38.2	65.7

TABLE 7.2

PERCENT CHANGE BETWEEN MEASURED AND COMPUTED
IMPEDANCES OF THE W/H = 10 ANTENNA

W/H = 10

	2 MHZ		6 MHZ		10 MHZ	
	$\Delta\%R$	$\Delta\%Xj$	$\Delta\%R$	$\Delta\%Xj$	$\Delta\%R$	$\Delta\%Xj$
Sep = 1 m 3 Seg Feed E Gap Source	33.5	29.4	21.1	15.0	6.8	6.4
Sep = 2.5 m 3 Seg Feed E Gap Source	17.5	76.8	7.2	64.8	50.2	27.5
Sep = 1 m 1 Seg Feed E Gap Source	36.4	21.4	27.3	13.2	14.5	1.0
Sep = 2.5 m 1 Seg Feed E Gap Source	27.0	52.1	10.6	48.7	26.0	11.9
Sep = 1 m 3 Seg Feed C/S Source	19.1	59.6	1.7	43.8	21.1	6.9
Sep = 2.5 m 3 Seg Feed C/S Source	.8	117	39.8	106	92.5	39.8
Sep = 1 m 1 Seg Feed C/S Source	31.7	32.3	16.9	25.3	1.4	3.6
Sep = 2.5 m 1 Seg Feed C/S Source	18.2	74.1	9.5	74.3	52.7	21.7
SPMVC	31.7	53.8	21.2	23.8	11.7	21.6
SPMV	30.1	74.4	10.0	38.6	27.4	94.9
SPMNV	24.0	77.4	9.0	83.2	66.0	103

models, the sparse models have the poorest correlation in reactance and this becomes progressively worse as the sparseness of the models increases, i.e., the SPMNV model is worse than the SPMV model which is worse than the SPMVC model. Among the E-gap wire grid models the three segment feed line models produce better reactances, while the models with equal feed segment and grid segment lengths yield slightly better resistances.

From Table 7.2 several trends concerning the W/H = 10 model types are evident. The sparse models again get progressively worse as their sparseness is increased. The 1 meter grid separation models are generally better than the 2.5 meter grid separation models, particularly in reactance. This indicates that tighter grids produce more accurate results. The current-slope-discontinuity voltage source models are generally better in resistance than are the E-gap voltage source models, but the opposite is true in reactance. There are exceptions to this generality noted, particularly at 10 MHZ. Among the wire grid models with one meter grid separation, the three segment feed line models generally produce resistances which correlate better to measured values than do the one segment feed models. Here again, the opposite is true for reactance.

If all models with a percent change greater than 50% in either resistance or reactance for any of the three frequencies are discarded, only three models remain. These are the one

meter separation wire grid models. Two of these use the E-gap voltage source and the other uses the current-slope-discontinuity voltage source. The current-slope-discontinuity voltage source model has a one segment feed line as does one of the E-gap voltage source models. The remaining E-gap voltage source model uses a three segment feed line. These three models are fairly close to each other in impedance value and it is difficult to determine which is the better model over the frequency range in question.

It was noted that for some models an average gain which was much less than 2.0 produced better results in resistance than models with an average gain near 2.0. Appendix B contains a discussion of these results.

It is apparent that for different frequency ranges, the various models result in different impedances. Some are better than others at one frequency and worse than others at another frequency. To properly choose the most accurate model over a broad frequency range, the models in question should each be exercised over the frequency range and compared to physical measurements.

Impedances for the wire grid patch monopole computer models of the W/H = 1, W/H = 2, and W/H = 10 antennas were obtained over the frequency range 2-24 MHZ. The models used had a grid separation of one meter and were driven by the E-gap voltage source. The W/H = 1 and W/H = 2 models used a three segment feed line while the W/H = 10 model had a one segment feed line.

104

Figures 7.1 and 7.2 are plots of the W/H = 1 solid and grid scale patch monopole measured resistance and reactance values. Included in the plots are the computer generated resistance and reactance values. Figures 7.3 and 7.4 are the resistance and reactance values for the W/H = 2 computer model and the wire grid scale model. Figures 7.5 and 7.6 are the W/H = 10 resistance and reactance plots of the computer model, solid scale model, and wire grid scale model. The following paragraphs are observations from these figures.

These plots show the close correlation in impedance between the wire grid scale models and the solid scale models, affirming the fact that wire grids can be used to approximate solid plate structures.

The computer model reactances and the measured reactances correlate well for the three antenna sizes. The resistance values do not possess such a close correlation. For the W/H = 1 and W/H = 2 antennas the correlation between computer model and scale model resistances is relatively poor for frequencies greater than around 7 MHZ, which corresponds to the scale model frequency of 315 MHZ. In Chapter VI it was noted that for the W/H = 1 and W/H = 2 scale models there was questionable data in this frequency range so these results are not too surprising. It is noted that the computer generated resistance curves do pass through the measured resistance curves and with the same general increasing trend, indicating that a loose correlation does exist.

PATCH MONOPOLE
RESISTANCE, W/H = 1
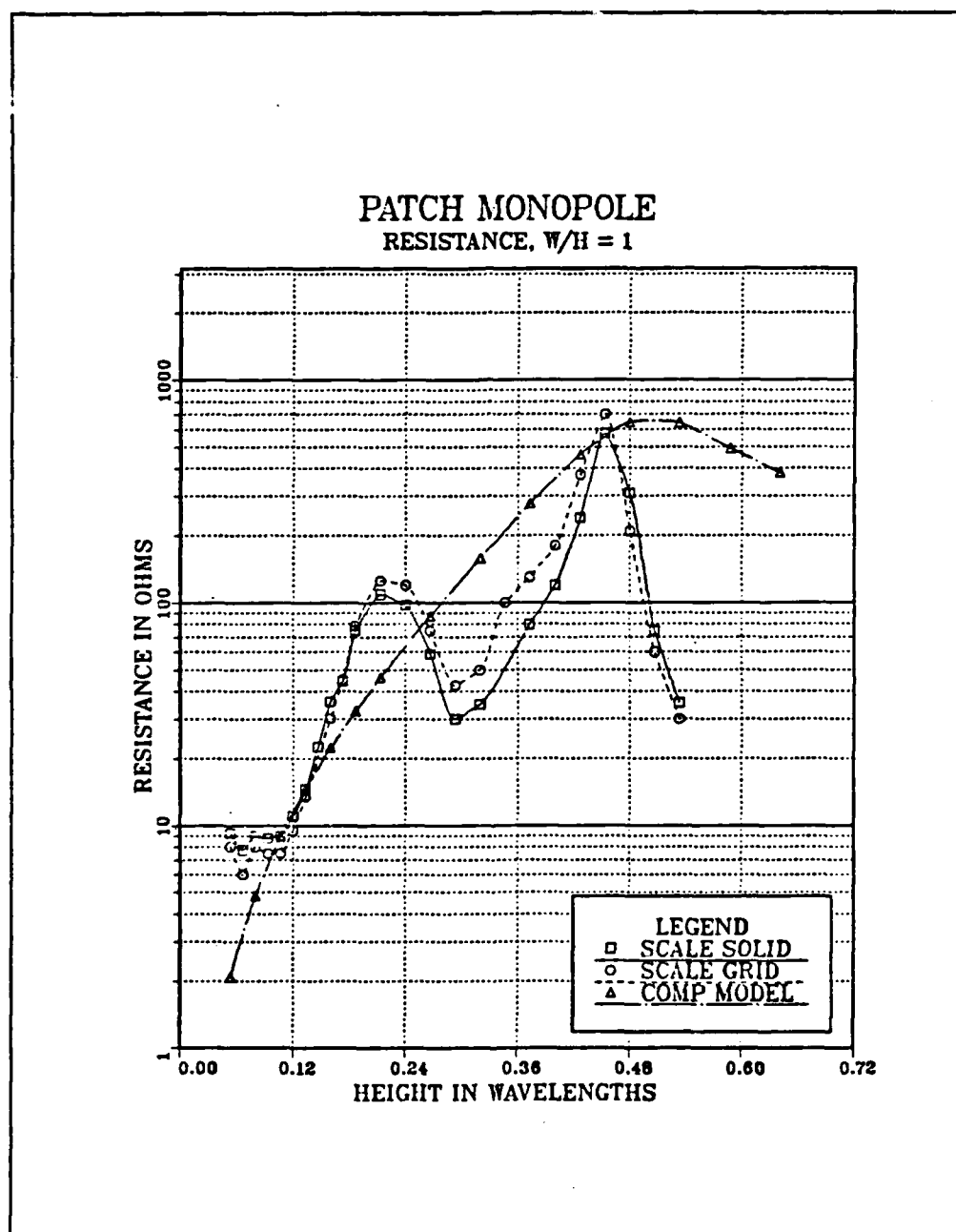
Figure 7.1.   W/H = 1 Computer and Scale Model Resistance
Comparisons

106
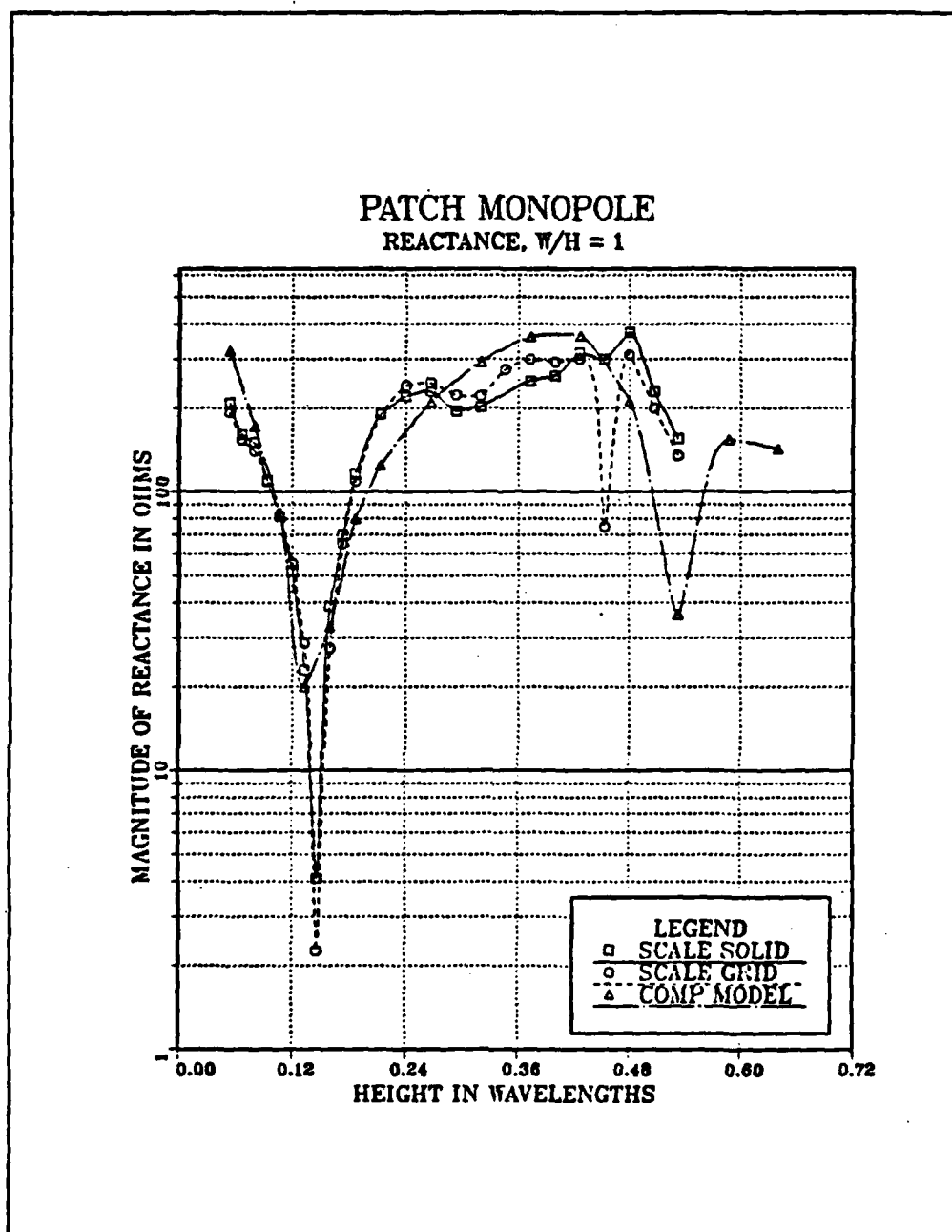
Figure 7.2.   W/H = 1 Computer and Scale Model Reactance
Comparisons

107
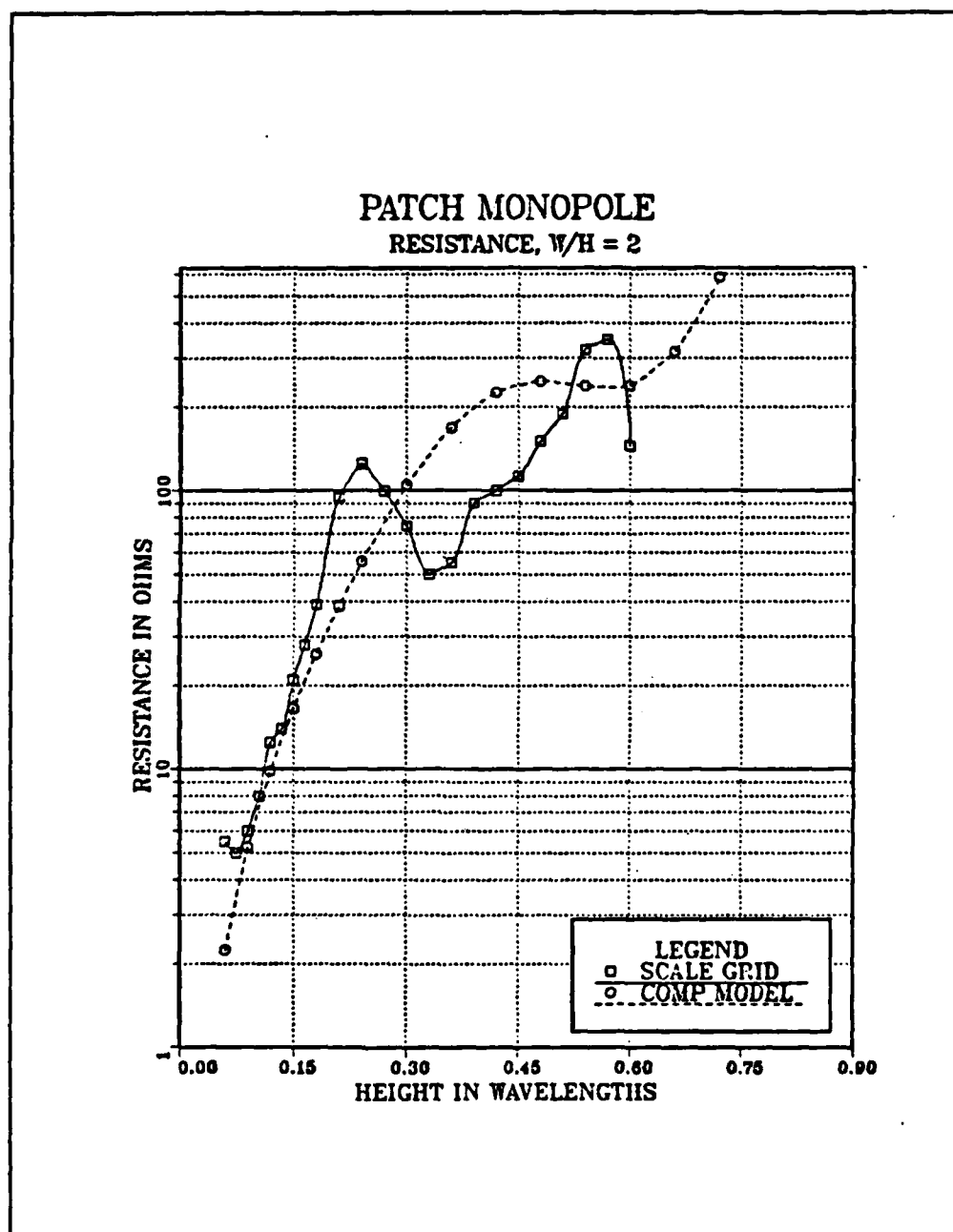
Figure 7.3. W/H = 2 Computer and Scale Model Resistance
Comparisons

108
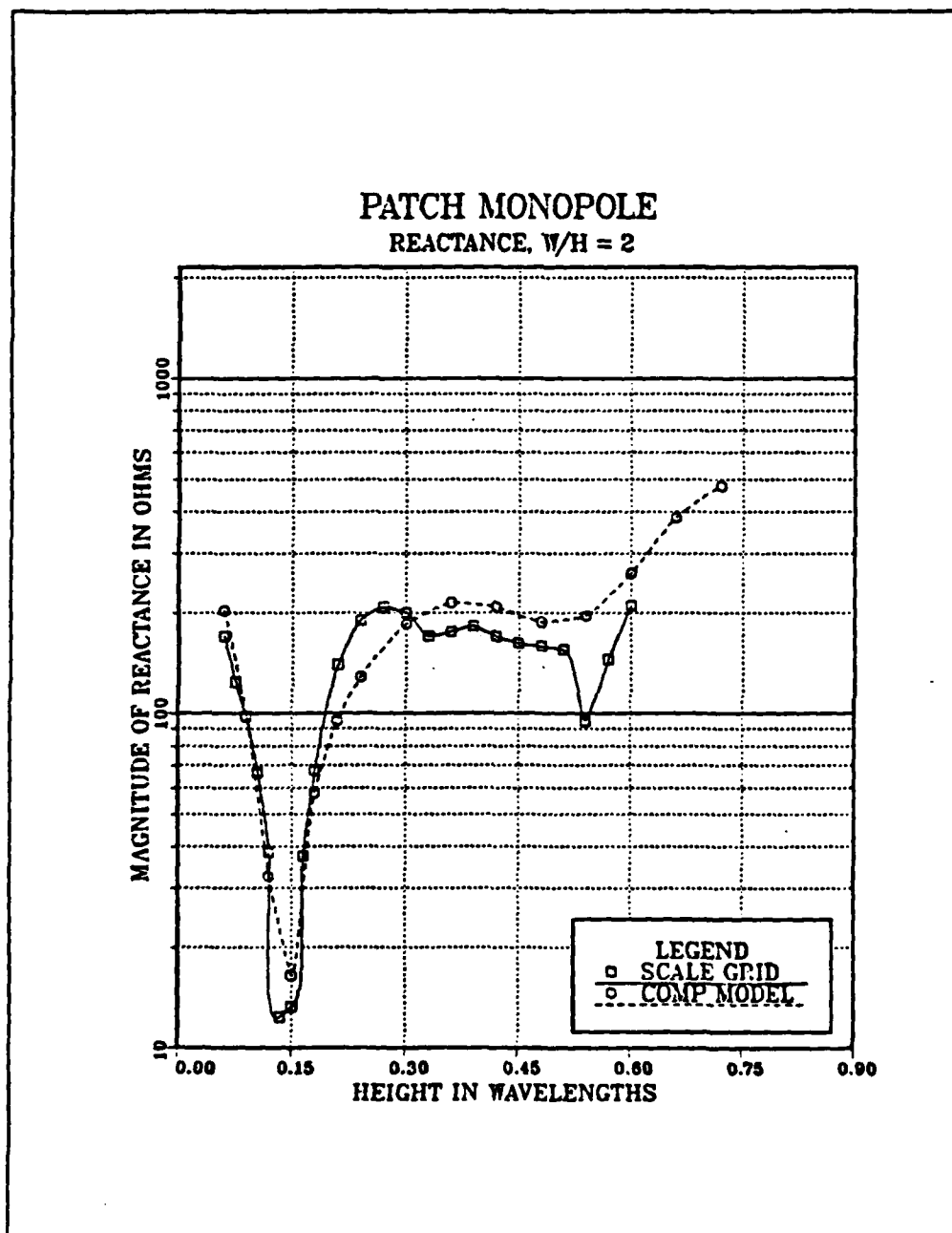
Figure 7.4.   W/H = 2 Computer and Scale Model Reactance
              Comparisons

109
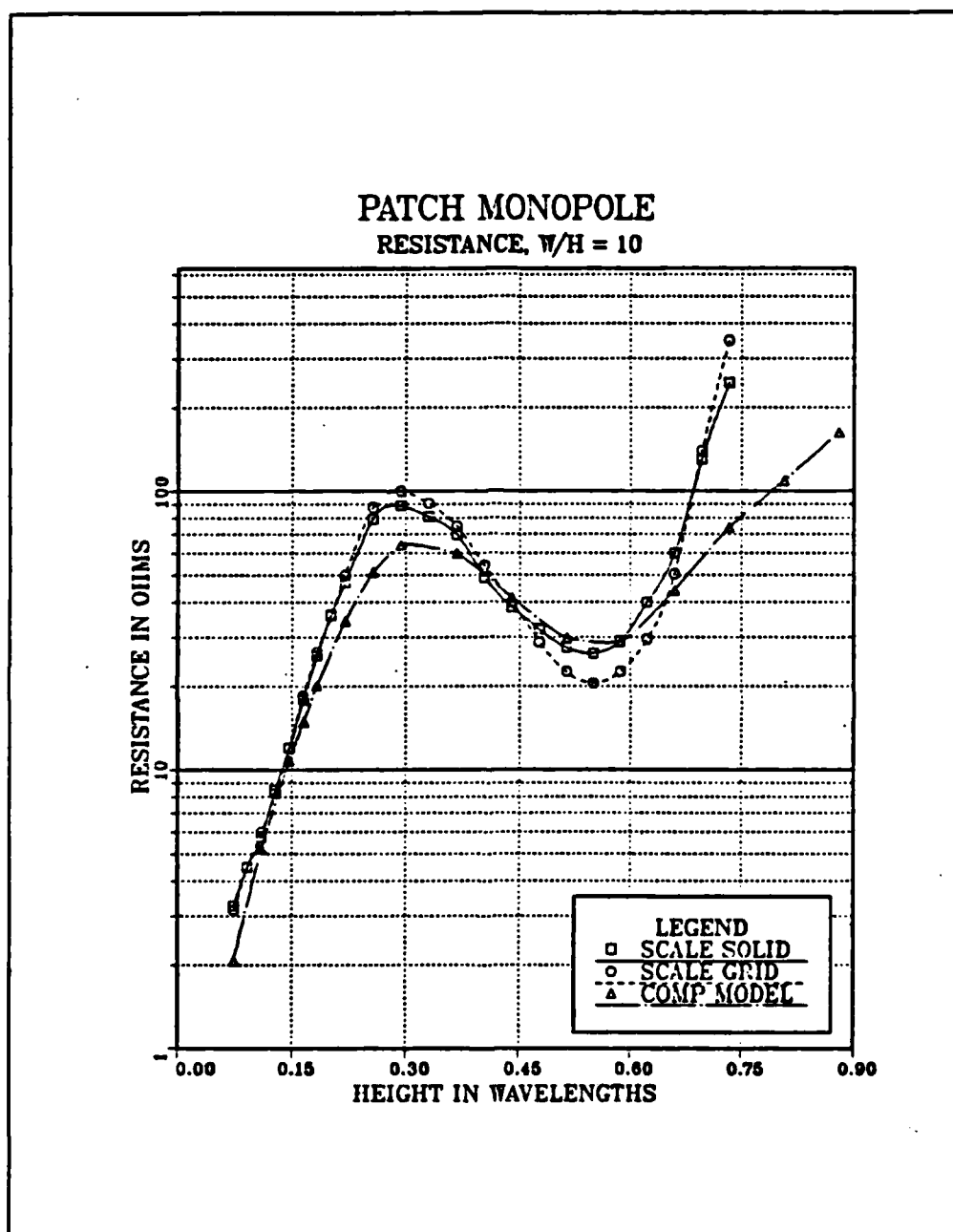
Figure 7.5.   W/H = 10 Computer and Scale Model Resistance
              Comparisons

110
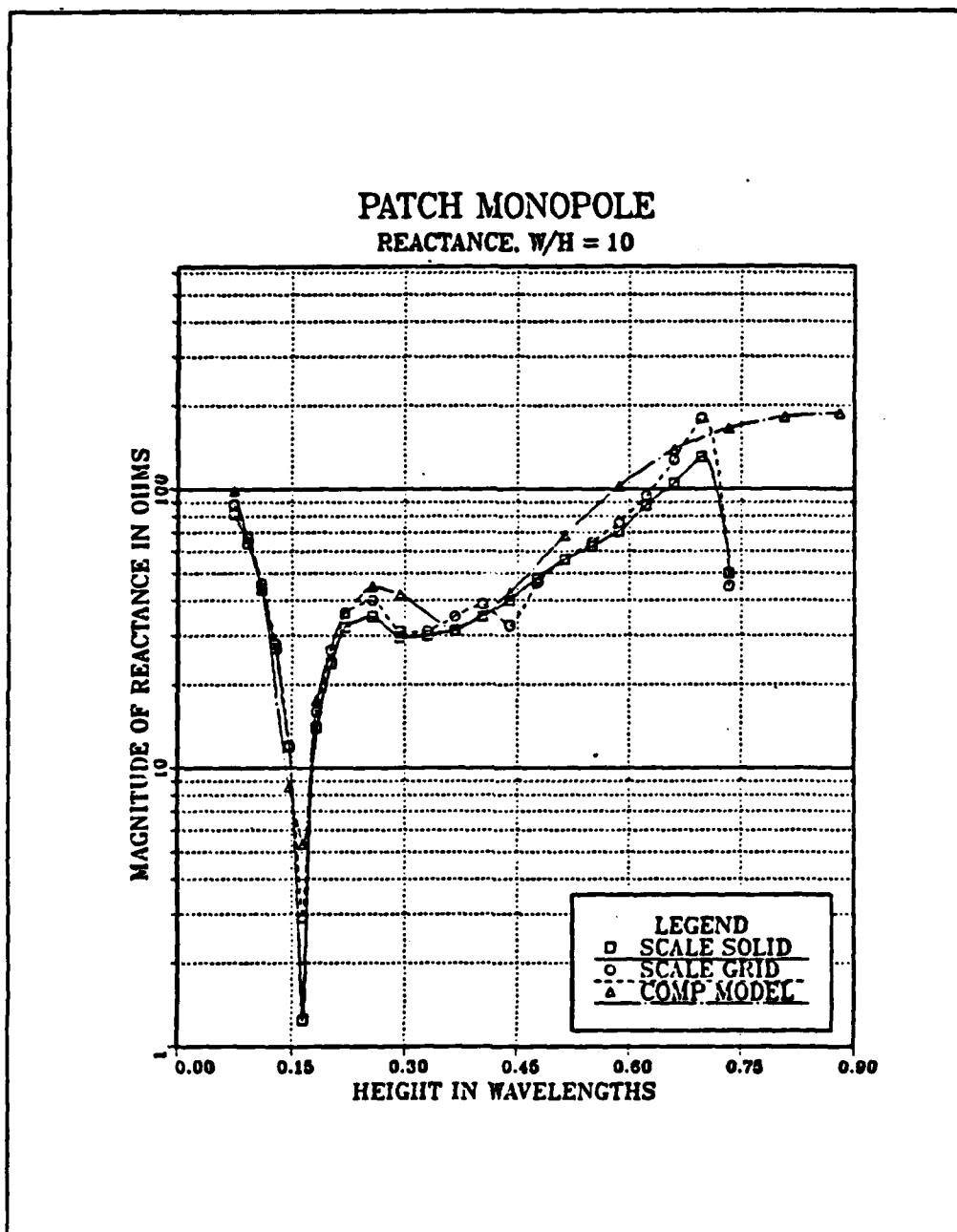
Figure 7.6.   W/H = 10 Computer and Scale Model Reactance
Comparisons

111

The resistance values of the W/H = 10 computer and scale models correlate very well up to around 20 MHZ or a scale model frequency of 900 MHZ. This correlation was expected as the questionable datapoints seen in the 315-630 MHZ range of the two smaller antennas were not present in the W/H = 10 scale models' measurements. There was some discrepancy between the physical monopole model and the theoretical monopole model at frequencies greater than 900 MHZ so the disagreement of the W/H = 10 scale and computer models above 900 MHZ was also expected.

The general result is that the computer model of the W/H = 10 is a close approximation to the real one. The computer models of the W/H = 1 and W/H = 2 antennas are good in reactance but don't agree with the measured resistance as well above 7 MHZ. Since the questionable data seems to be caused by the physical set up it is likely the computer models are also accurate above 7 MHZ.

112

VIII. <u>CONCLUSIONS AND RECOMMENDATIONS</u>

This thesis has taken a survivable antenna design and developed a computer model for the antenna which was used to determine the impedance characteristics and radiation patterns of the survivable antenna over the HF frequency range of 2-24 MHZ. In the process several computer models were looked at and compared to physical results. This lead to many conclusions concerning computer modeling and the feasibility of the survivable antenna.

A. MODELING

Wire grids can be used to model flat metal surfaces. A grid spacing of .1 wavelength is usually adequate, however, the grid density does affect the impedance of a computer model. The effect of the grid density is much more prominent in the W/H = 10 antenna than in the W/H = 1 model indicating larger structures are more sensitive to grid density. In general, models with tighter grid densities yield impedances closer to measured values.

Grid density is not the only parameter affecting the computer model's impedance. The type of voltage source, the number and size of feed segments, and the radius of the wires also affect the impedance. Since there are so many parameters affecting the impedance of the computer models, physical models should be built to determine, within experimental

113

error, the actual impedance characteristics of the antenna. The parameters of the computer model may then be varied to produce impedances comparable to the physical antenna measurements. This verified model may then be used in a more complex environment with reasonable confidence.

Sparse models, like the SPMVC one used in this study, can produce reasonably good results at low frequencies where the antenna structure is small in terms of wavelengths. Such models represent considerable savings in both computer time and storage requirements. As frequency increases sparse models tend to become inaccurate, particularly for reactance, however, this might be corrected by use of lumped loads in the computer model.

NEC may be used to model wire structures well and can be an effective antenna engineering tool when used with experience and knowledge of antenna theory. In this study the W/H = 10 antenna computer model used with NEC yielded impedances which were close to the scale model impedance measurements. The W/H = 1 and W/H = 2 antenna computer models produced reactances which agreed well with the measured reactances. There was less correlation between measured and computed resistances. This was more likely due to experimental errors than computer errors. It is also interesting that reactances correlate to the physical measurements better than the resistances in these cases, since computer modeling theory predicts greater error in reactance than in resistance.

Computer models with relatively poor average gains produced more accurate impedance values in some cases than did models with very good average gains as seen in Appendix B. In computer modeling practice it has generally been accepted that models with poor average gain are less adequate than those with good average gains. This is a guideline which needs to be investigated. It is possible that the models with poor average gain produce errors which compensate for some other deficiency in the model; this, in turn, may result in improved performance. Such a case would be a combination of errors and not necessarily desirable.

B. THE SURVIVABLE ANTENNA

The results of this thesis indicate that a rectangular volume driven by a patch monopole at an insulated or open face does possess radiation patterns and impedance characteristics which make it a feasible design.

Of the three structures investigated the W/H = 10 patch monopole at the open face of the box has the superior impedance characteristics. This antenna is matchable to a 3:1 SWR over the frequency ranges of 6-7.5 MHZ, 8.5-22 MHZ, and 24 MHZ and possesses a 3:1 SWR without the need of a matching network over the frequency range of 8.5-11 MHZ.

For small electrical heights, less than around .1 wavelengths, the radiation patterns of the three survivable antennas are similar to those of a .25 wavelength monopole. This is expected as antennas which are electrically short

115

produce similar radiation patterns almost independent of the antenna's geometry; "a small antenna is a small antenna."

The radiation patterns of all three antennas are similar below 20 MHZ, indicating the box has the dominant effect.

In the frequency range 6-14 MHZ the W/H = 10 the survivable antenna has a cardioidal horizontal pattern with vertical patterns which exhibit less lobing than those of a monopole of equal height, but they are also more directional. This directionality might be corrected by use of two patch monopoles, one on either side of the box. As the frequency increases the antenna remains directional, but to a lesser extent, and becomes more lobey. The lobing is less severe than that of a monopole of equal height and possesses better gain at higher elevation angles than does a monopole of equal height.

C. RECOMMENDATIONS

There are many aspects of this study which warrant further study.

The ground plane should be investigated and the source of impedance measurement error corrected. Impedance measurements on the scale models may then be repeated and compared to the computed values.

The current-slope-discontinuity voltage source model should be exercised over the frequency range 2-24 MHZ for comparison to the physical measurements. This model yielded promising

116

impedances and may prove to be as good as or better than the E-gap voltage source model.

To determine the antenna's response at higher frequencies, the survivable antenna impedance and radiation pattern computations should be repeated over a higher frequency range. The VHF frequency range might prove interesting.

The wire grid box models should be investigated to determine the effect of grid density and wire radius on these models. If a sparser box model could be used it would greatly reduce the computer storage and time requirements.

Finally, physical models of the survivable antenna should be built for comparison to the computer models.

APPENDIX A

EXPERIMENTAL SET UP

Figure A is a block diagram of the experimental set up used for the antenna impedance measurements. The following equipment was used for the measurements:

HP8405A Vector Voltmeter

HP8350B Sweep Oscillator

20 dB Dual Directional Coupler

Ground Plane Measurement Range
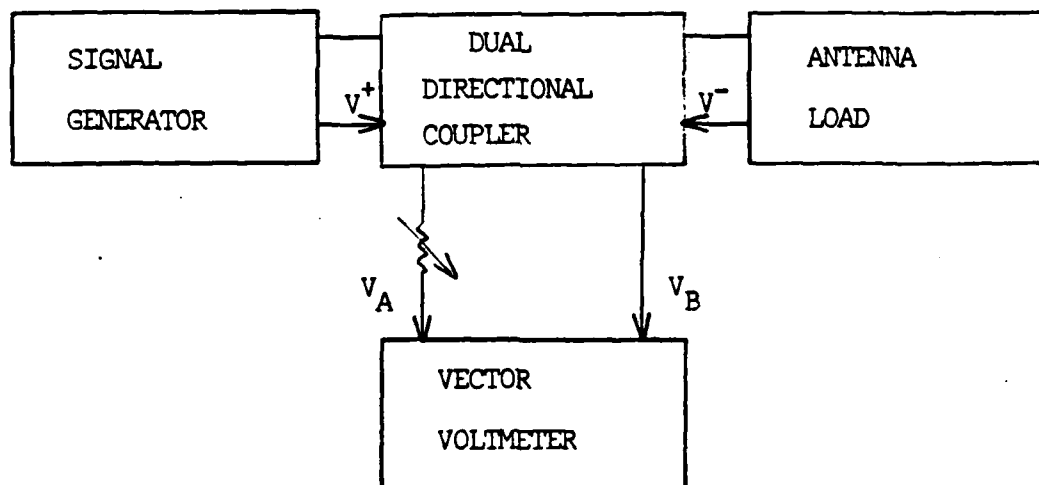
Figure A.   Equipment Arrangement for Impedance
Measurements

APPENDIX B

AVERAGE GAIN COMPARISON

An antenna radiating in a half space over a perfect ground theoretically has an average gain of 2.0. This criterion is commonly applied to antenna computer models to gauge the accuracy of the model. Table B displays representative average gains $(\overline{G})$ along with the percent change between the computer and physical scale model impedances of this study. This table reveals that some models with average gains less than 1.85 and even in the range of 1.5 produce smaller percent changes in resistance than do some models whose average gains are near 2.0. It is also true that these models with poor average gain, but good percent change in resistance, are generally worse in percent change of reactance than models with better average gains.

It is possible that the models with poor average gain produce errors which compensate for some other deficiency in the model which results in improved performance, i.e., multiple errors working to offset each other.

The data presented here is over a limited range and more investigation needs to be done before any firm conclusions may be drawn.

TABLE B

PERCENT CHANGE BETWEEN PHYSICAL IMPEDANCE MEASUREMENTS AND COMPUTER MODEL IMPEDANCES, AVERAGE GAIN OF COMPUTER MODEL FOR W/H = 10 ANTENNA MODEL

	2 MHZ			6 MHZ		
	$\Delta\%R$	$\Delta\%Xj$	$\overline{G}$	$\Delta\%R$	$\Delta\%Xj$	$\overline{G}$
Sep = 1 m 3 Seg Feed E-Gap	33.5	29.4	1.89	21.1	15.0	1.89
Sep = 2.5 m 3 Seg Feed E-Gap	17.5	76.8	1.56	7.18	64.8	1.55
Sep = 1 m 1 Seg Feed E-Gap	36.4	21.4	2.01	27.3	13.2	2.01
Sep = 2.5 m 1 Seg Feed E-Gap	27.1	52.1	1.81	10.6	48.7	1.81
Sep = 1 m 3 Seg Feed C/S Source	19.1	59.6	1.51	1.74	43.8	1.51
Sep = 2.5 m 3 Seg Feed C/S Source	.83	116	1.25	39.8	106	1.24
Sep = 1 m 1 Seg Feed C/S Source	31.7	32.3	1.82	16.9	25.3	1.82
Sep = 2.5 m 1 Seg Feed C/S Source	18.21	74.1	1.55	9.54	74.3	1.55
SPMVC	31.7	53.8	1.98	21.2	23.8	1.95
SPMV	30.1	74.4	1.84	10.0	38.5	1.82
SPMNV	24.0	74.4	1.77	9.05	83.2	1.76

LIST OF REFERENCES

1. Naval Ocean Systems Center Technical Document 116, Numerical Electromagnetics Code (NEC)--Method of Moments, by G.J. Burke and A.J. Pogio, January 1981.

2. Burke, G.J., Poggio, A.J., Logan, J.C., and Rockway, J.W., Numerical Electromagnetics Code--A Program For Antenna System Analysis, Paper presented at the EMC Symposium and Exhibition, Rotterdam, Netherlands, May 1-3, 1979.

3. Harrington, Roger F., Field Computation By Moment Methods, MacMillan Company, New York, 1968.

4. Miller, E.K. and Deadrick, F.J.: In Topics in Applied Physics, Vol. 3--Numerical and Asymptotic Techniques in Electromagnetics, ed. R. Mittra, Chpt. 4, Springer-Verlag, 1975.

5. Jasik, H., Antenna Engineering Handbook, pp. 2-51, McGraw-Hill Book Co., 1961.

6. Harrington, Roger F., Time-Harmonic Electromagnetic Fields, pp. 103-106, McGraw-Hill Book Co., 1961.

7. Balanis, Constantine A., Antenna Theory Analysis and Design, pp. 502-522, Harper and Row, Publishers, Inc., 1982.

8. Meir, A.S. and Summers, W.P., "Measured Impedance of Vertical Antennas Over Finite Ground Planes," Proceedings of the I.R.E., V. 37, pp. 609-616, June 1949.

9. King, Ronald W.P., Tables of Antenna Characteristics, pp. 46-48, IFI/Plenum, 1971.

10. Li, Shing Ted, and others, Microcomputer Tools For Communications Engineering, pp. 147-150, ARTECH House, Inc., 1983.

11. Hewlett-Packard Application Note 77-3, Measurements of Complex Impedance 1-1000 MHZ, by Engineering Staff of the Hewlett-Packard Microwave Division, pp. 7-9, 1 April 1967.

INITIAL DISTRIBUTION LIST

		No. Copies

1. Defense Technical Information Center — 2
    Cameron Station
    Alexandria, Virginia   22304-6145

2. Library, Code 0142 — 2
    Naval Postgraduate School
    Monterey, California   93943-5002

3. Lt. J.C. Tertocha — 2
    C/o Tina Boggs
    6711 Agnes St.
    N. Hollywood, California   91606

4. Dr. Richard W. Adler, Code 62Ab — 5
    Naval Postgraduate School
    Monterey, California   93943-5000

5. Dr. Stephen Jaurequi, Code 62Ja — 1
    Naval Postgraduate School
    Monterey, California   93943-5000

6. Dr. H.B. Rigas, Code 62 — 2
    Department of Electrical and
      Computer Engineering
    Naval Postgraduate School
    Monterey, California   93943-5000

7. W.F. Flanigan, Code 825 — 1
    Naval Ocean Systems Center
    271 Catalina Blvd.
    San Diego, California   92152

8. M. Selkellick, Code 1202 — 1
    David Taylor Naval Ship Research
    Development Center
    Betheseda, Maryland   20084-5000

9. D. Washburn, Code 7403 — 1
    Naval Ocean Systems Center
    271 Catalina Blvd.
    San Diego, California   92152

10. Jim Logan, Code 822 — 1
    Naval Ocean Systems Center
    271 Catalina Blvd.
    San Diego, California   92152

11. Rick Thowless, Code 822   1
    Naval Ocean Systems Center
    271 Catalina Blvd.
    San Diego, California 92152

12. Jim K. Breakall   1
    Lawrence Livermore National Laboratory
    P.O. Box 5504, 1-156
    Livermore, California 94550

13. G. Burke   1
    Lawrence Livermore National Laboratory
    P.O. Box 5504, 1-156
    Livermore, California 94550

14. E. Domning   1
    Lawrence Livermore National Laboratory
    P.O. Box 5504, 1-156
    Livermore, California 94550

15. Robert Latorre   1
    Lawrence Livermore National Laboratory
    P.O. Box 5504, 1-156
    Livermore, California 94550

16. Donn Cambell   1
    CECOM-CENCOMS
    Fort Monmouth, New Jersey 07703

17. Ron Corry   1
    USAISEA/ASBH-SET-P
    Fort Huachuca, Arizona 85613-5300

18. Bill Alvarez   1
    USAISEA/ASBH-SET-P
    Fort Huachuca, Arizona 85613-5300

19. Janet McDonald   1
    USAISEA/ASBH-SET-P
    Fort Huachuca, Arizona 85613-5300

20. Dr. Tom Tice   1
    Department of Electrical
      and Computer Engineering
    Arizona State University
    Tempe, Arizona 85287

21. Dr. Roger C. Rudduck   1
    Ohio State University
    Electrophysics Laboratory
    1320 Kinnear Rd.
    Colombus, Ohio 43212

22. Commander Naval Space and Naval
    Warfare Systems Command   1
    Attention: Dick Pride
    PDW 110-243
    Washington D.C. 20363

23. Naval Sea Systems Command   1
    Attention: P. Law
    C61X41
    Washington D.C. 20362

24. LCDR Mario Cabral Neivia   1
    Brazilian Naval Commission
    4706 Wisconsin Ave., N.W.
    Washington D.C. 20016

25. Costas Theofanopoulos   1
    355 Casa Verde Way #8
    Monterey, California 93940

26. Ioannis Vorrias   1
    1001 Funston Ave. #3
    Pacific Grove, California 93950

27. George Lynberopoulos   1
    580 Irving Ave. #D
    Monterey, California 93940

28. Director Research Administration, Code 012   1
    Naval Postgraduate School
    Monterey, California 93943-5000

END

DTIC

6 - 86